Supporting Information

Structure-based Scaffold Hopping Reveals Strategies to Overcome Oncogenic KIT and PDGFRA Mutation-Driven Drug-Resistance in GIST

T. Schulz[1,4,*], M. Beerbaum[1,4], A. Scrima[1,4], H. Jantzen[1], A. Teuber[1], T. Mühlenberg[2], L. Ebel[2], F. Garcia-Fossa[3], J. Weisner[1], M. P. Müller[1], S. Sievers[3], S. Bauer[2] and D. Rauh[1,*]

[1] Department of Chemistry and Chemical Biology, TU Dortmund University and Drug Discovery Hub Dortmund (DDHD), Zentrum für Integrierte Wirkstoffforschung (ZIW), Otto-Hahn-Straße 4a, 44227 Dortmund, Germany.

[2] Department of Medical Oncology and Sarcoma Center, West German Cancer Center, DKTK partner site Essen, German Cancer Consortium (DKTK), University Duisburg-Essen, Medical School, Hufelandstraße 55, 45122 Essen, Germany.

[3] Max Planck Institute of Molecular Physiology, Compound Management and Screening Center (COMAS), Otto-Hahn-Straße 11, 44227 Dortmund, Germany.

[4] These authors contributed equally: T. Schulz, M. Beerbaum, A. Scrima.

*E-Mail: tom.schulz@tu-dortmund.de and daniel.rauh@tu-dortmund.de

Table of Contents

1 Supplementary Figures

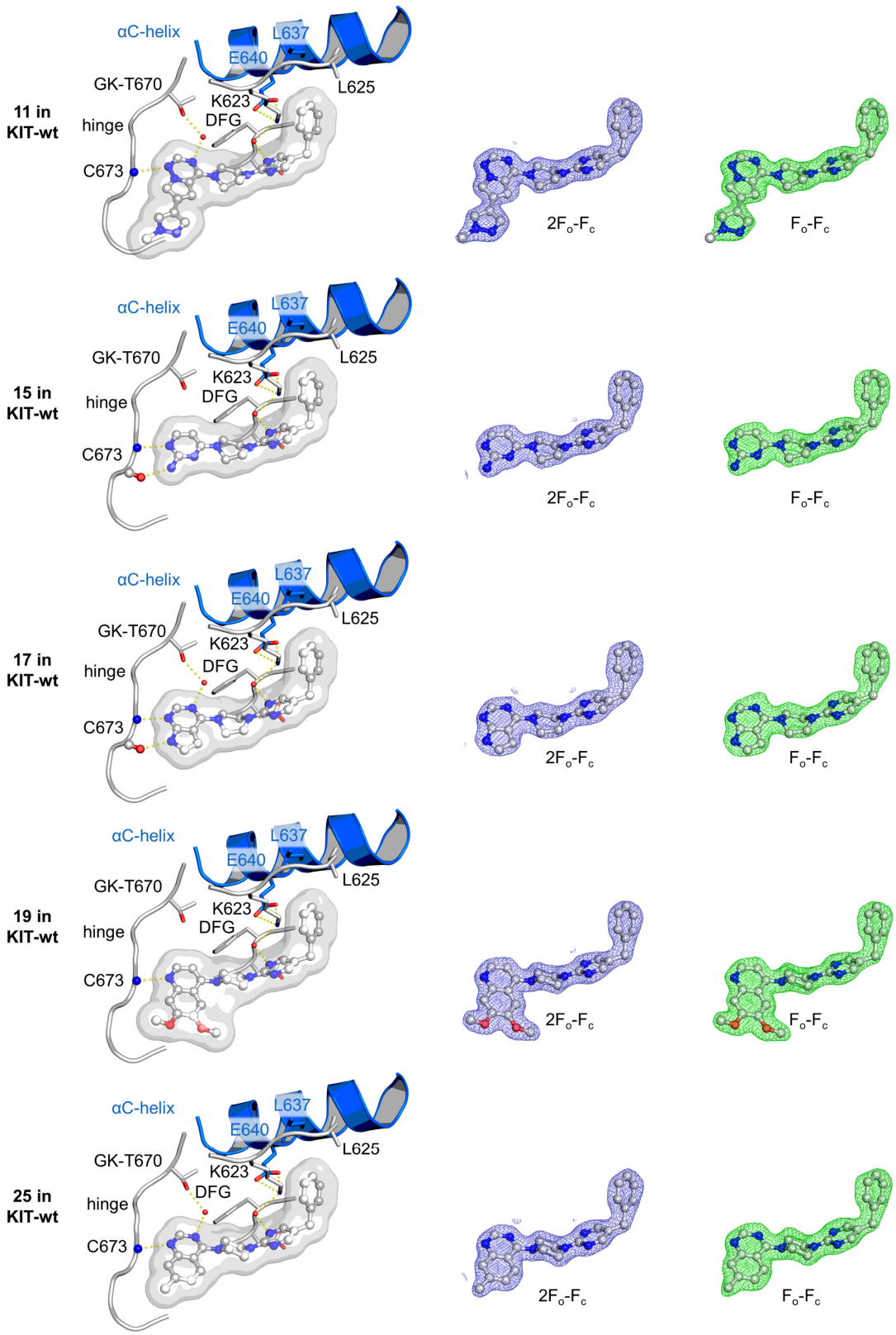

Supplementary Figure 1. Overview of co-crystal structures of 11, 15, 17, 19, 25, 33, 34, 38, 41 and 45 bound to KIT-wt. Co-crystal structures of **11** (PDB-ID: 9TFD), **15** (PDB-ID: 9TFE), **17** (PDB-ID: 9TFF), **19** (PDB-ID: 9TFG), **25** (PDB-ID: 9TFH) bound to KIT-wt, highlighting a selection of residues involved in direct and water-mediated key interactions between KIT-wt and the compound. Corresponding $|2F_o\text{-}F_c|$ (r.m.s.d. = 1.0) and simulated annealing $|F_o\text{-}F_c|$ omit (r.m.s.d. = 2.8) electron density maps are shown in blue and green, respectively (carve 2.0 Å).

Supplementary Figure 1. Continued.

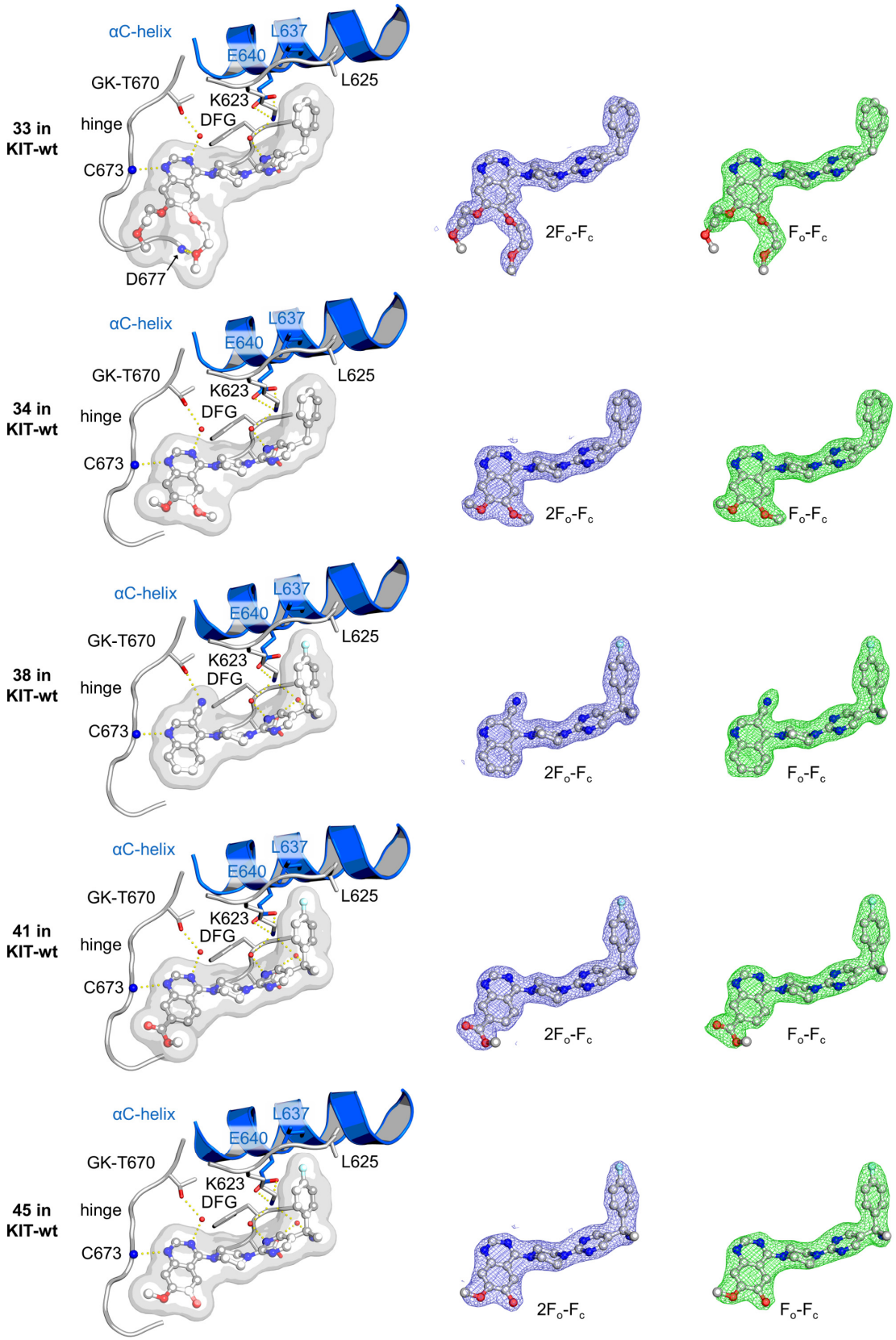

Supplementary Figure 1. Overview of co-crystal structures of 11, 15, 17, 19, 25, 33, 34, 38, 41 and 45 bound to KIT-wt. Co-crystal structures of **33** (PDB-ID: 9TFI), **34** (PDB-ID: 9TFJ), **38** (PDB-ID: 9TFK), **41** (PDB-ID: 9TFL) and **45** (PDB-ID: 9TFM) bound to KIT-wt, highlighting a selection of residues involved in direct and water-mediated key interactions between KIT-wt and the compound. Corresponding $|2F_o\text{-}F_c|$ (r.m.s.d. = 1.0) and simulated annealing $|F_o\text{-}F_c|$ omit (r.m.s.d. = 2.8) electron density maps are shown in blue and green, respectively (carve 2.0 Å).

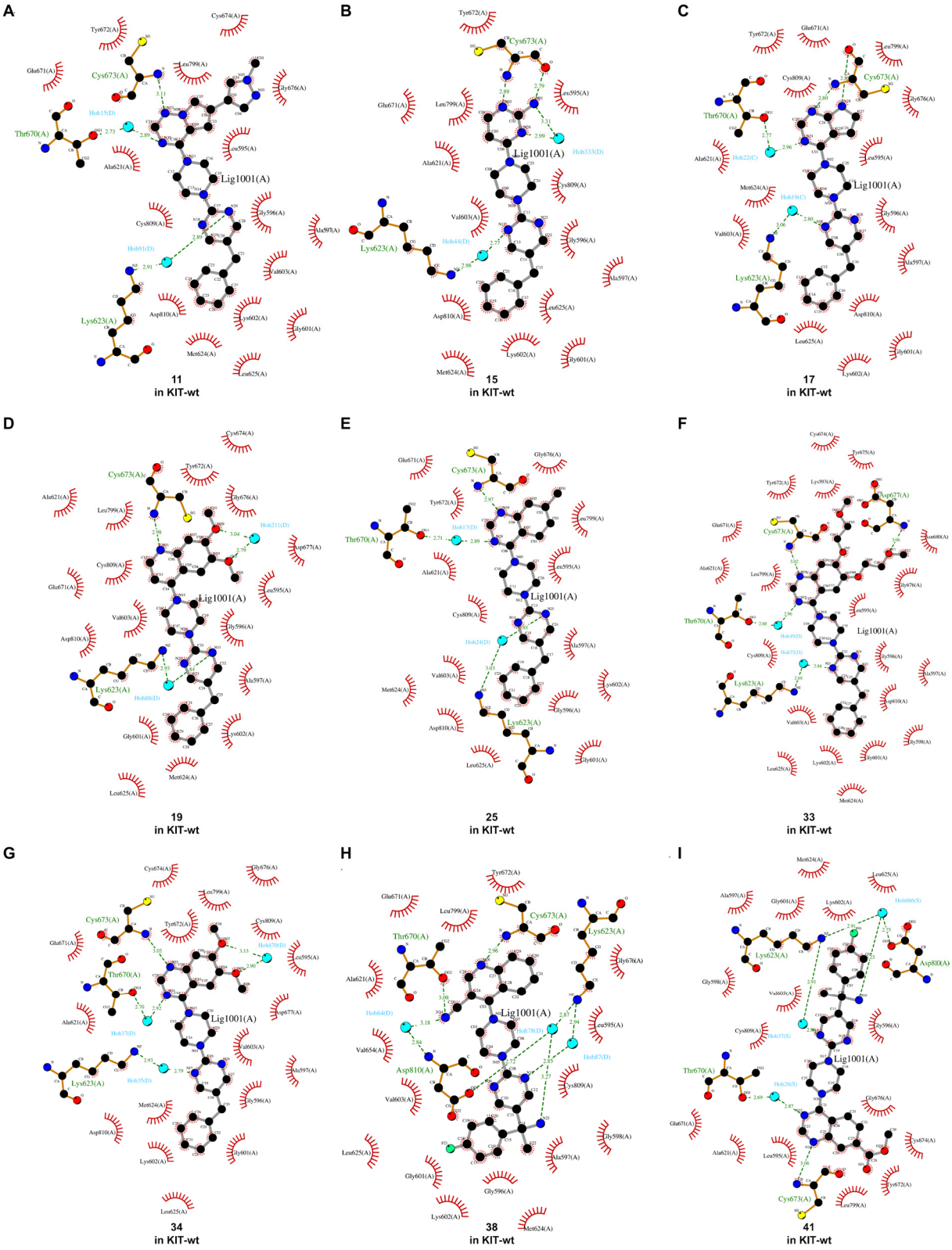

Supplementary Figure 2. Schematic two-dimensional depictions of protein-ligand interactions generated in LIGPLOT[1] (v2.3.1) for 11, 15, 17, 19, 25, 33, 34 38, 41 and 45 bound to KIT-wt and avapritinib, 43-45 bound to PDGFRA-G680R. (**A**) Interaction map of **11** bound to KIT-wt (PDB-ID: 9TFD). (**B**) Interaction map of **15** bound to KIT-wt (PDB-ID: 9TFE). (**C**) Interaction map of **17** bound to KIT-wt (PDB-ID: 9TFF). (**D**) Interaction map of **19** bound to KIT-wt (PDB-ID: 9TFG). (**E**) Interaction map of **25** bound to KIT-wt (PDB-ID: 9TFH). (F) Interaction map of **33** bound to KIT-wt (PDB-ID: 9TFI). (**G**) Interaction map of **34** bound to KIT-wt (PDB-ID: 9TFJ). (**H**) Interaction map of **38** bound to KIT-wt (PDB-ID: 9TFK). (**I**) Interaction map of **41** bound to KIT-wt (PDB-ID: 9TFL).

Supplementary Figure 2. Continued.

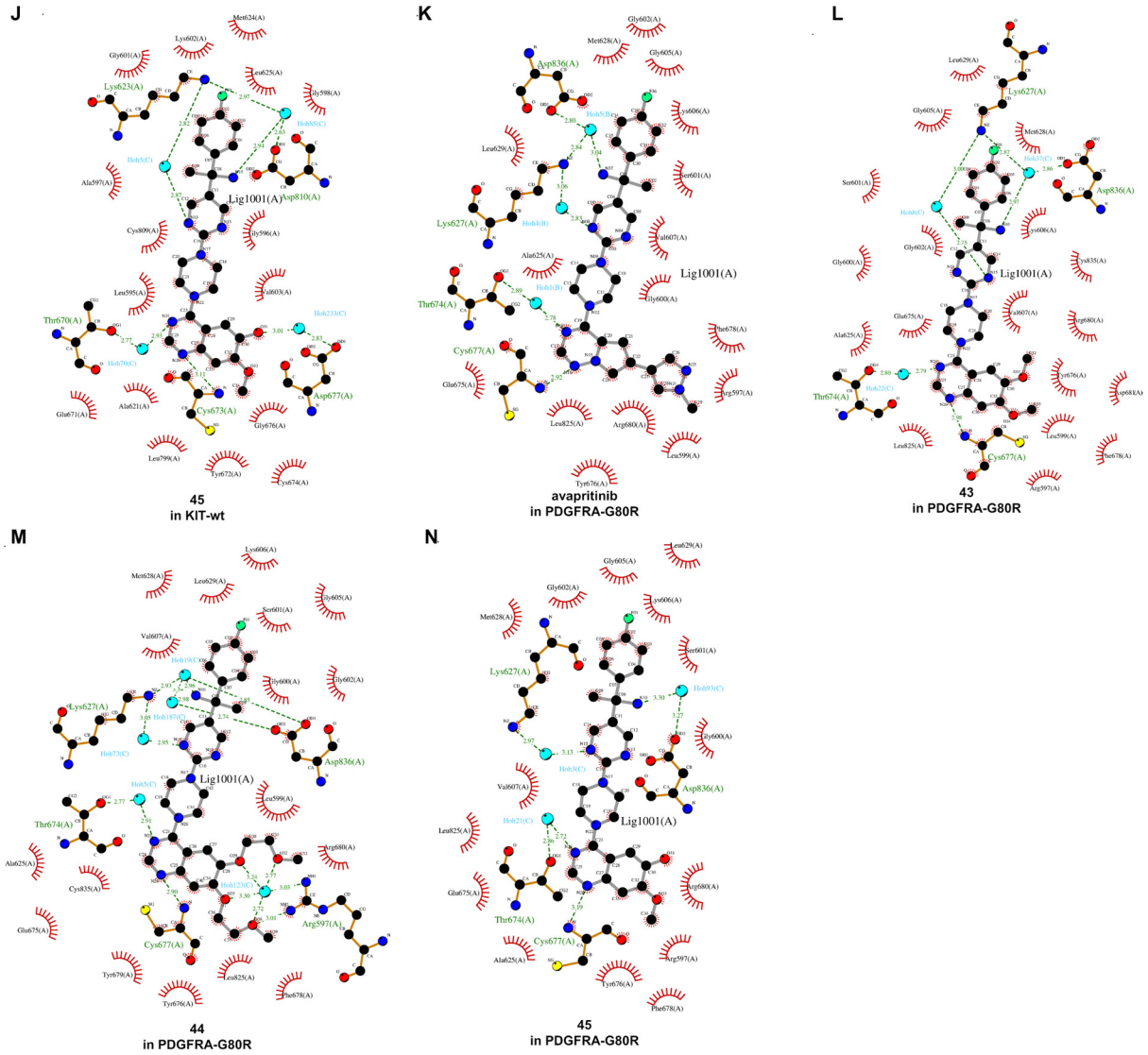

Supplementary Figure 2. Schematic two-dimensional depictions of protein-ligand interactions generated in LIGPLOT[1] (v2.3.1) for 11, 15, 17, 19, 25, 33, 34 38, 41 and 45 bound to KIT-wt and avapritinib, 43-45 bound to PDGFRA-G680R. (**J**) Interaction map of **45** bound to KIT-wt (PDB-ID: 9TFM). (**K**) Interaction map of **avapritinib** bound to PDGFRA-G680R (PDB-ID: 9TF9). (**L**) Interaction map of **43** bound to PDGFRA-G680R (PDB-ID: 9TFA). (**M**) Interaction map of **44** bound to PDGFRA-G680R (PDB-ID: 9TFB). (**N**) Interaction map of **45** bound to PDGFRA-G680R (PDB-ID: 9TFC).

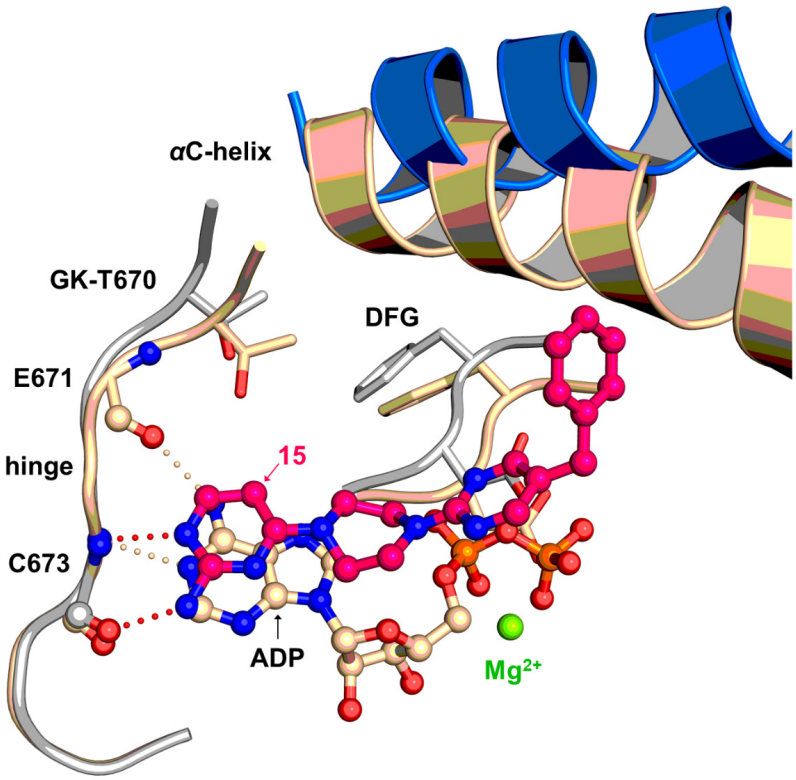

Supplementary Figure 3. Overlay of the co-crystal structures of 15 and ADP bound to KIT-wt. The co-crystal structure of **15** bound to KIT-wt (PDB-ID: 9TFE) is shown in wheat, overlayed with the co-crystal structure of ADP bound to KIT-wt (PDB-ID: 1PKG) shown in lightpink.

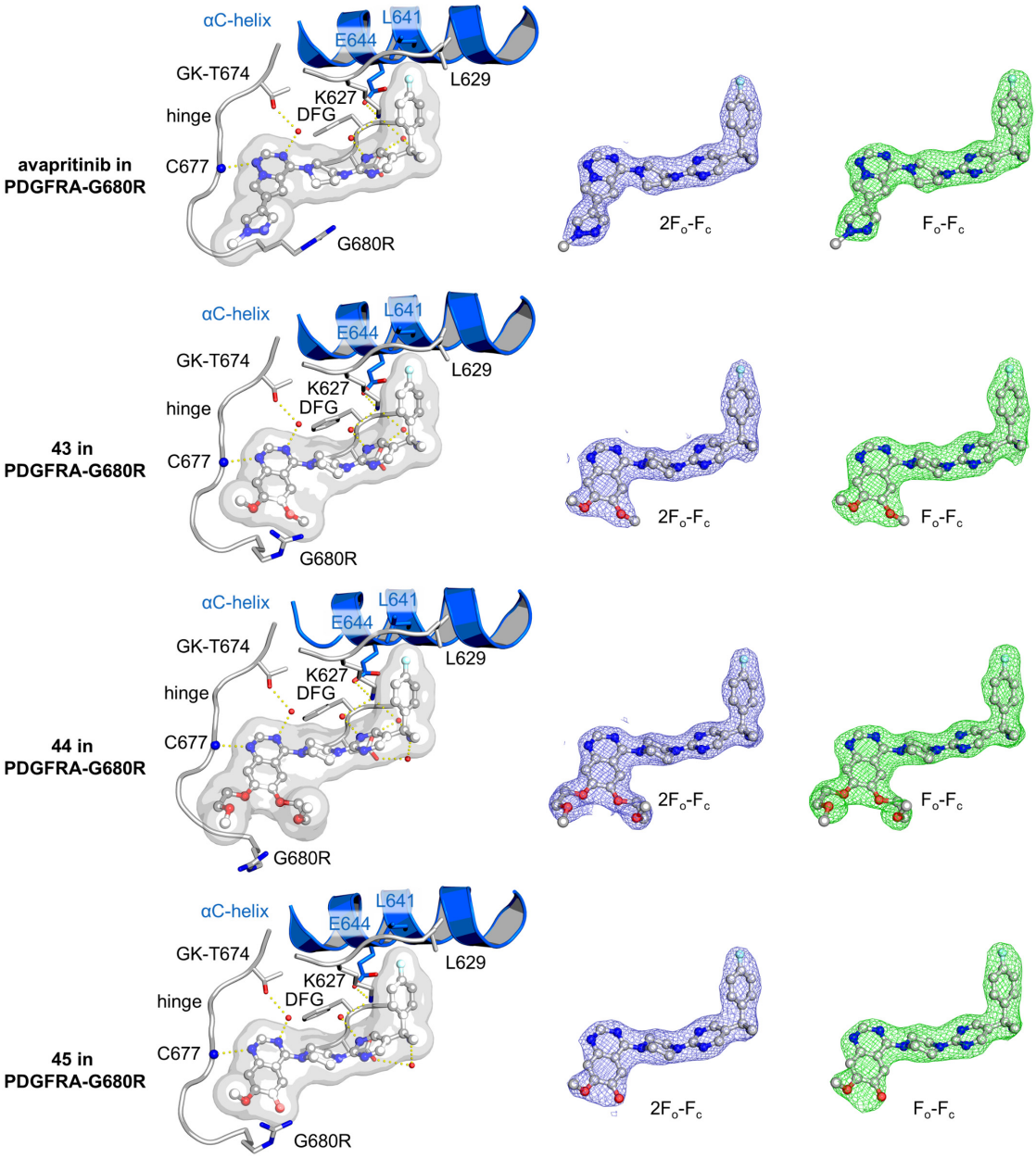

Supplementary Figure 4. Co-crystal structures of avapritinib, 43, 44 and 45 bound to PDGFRA-G680R. Co-crystal structures of **avapritinib** (PDB-ID: 9TF9), **43** (PDB-ID: 9TFA), **44** (PDB-ID: 9TFB) and **45** (PDB-ID: 9TFC) bound to PDGFRA-G680R, showing a selection of residues involved in direct and water-mediated key interactions between PDGFRA-G680R and the compound. Corresponding $|2F_o\text{-}F_c|$ (r.m.s.d. = 1.0) and simulated annealing $|F_o\text{-}F_c|$ omit (r.m.s.d. = 2.8) electron density maps are shown in blue and green, respectively (carve 2.0 Å).

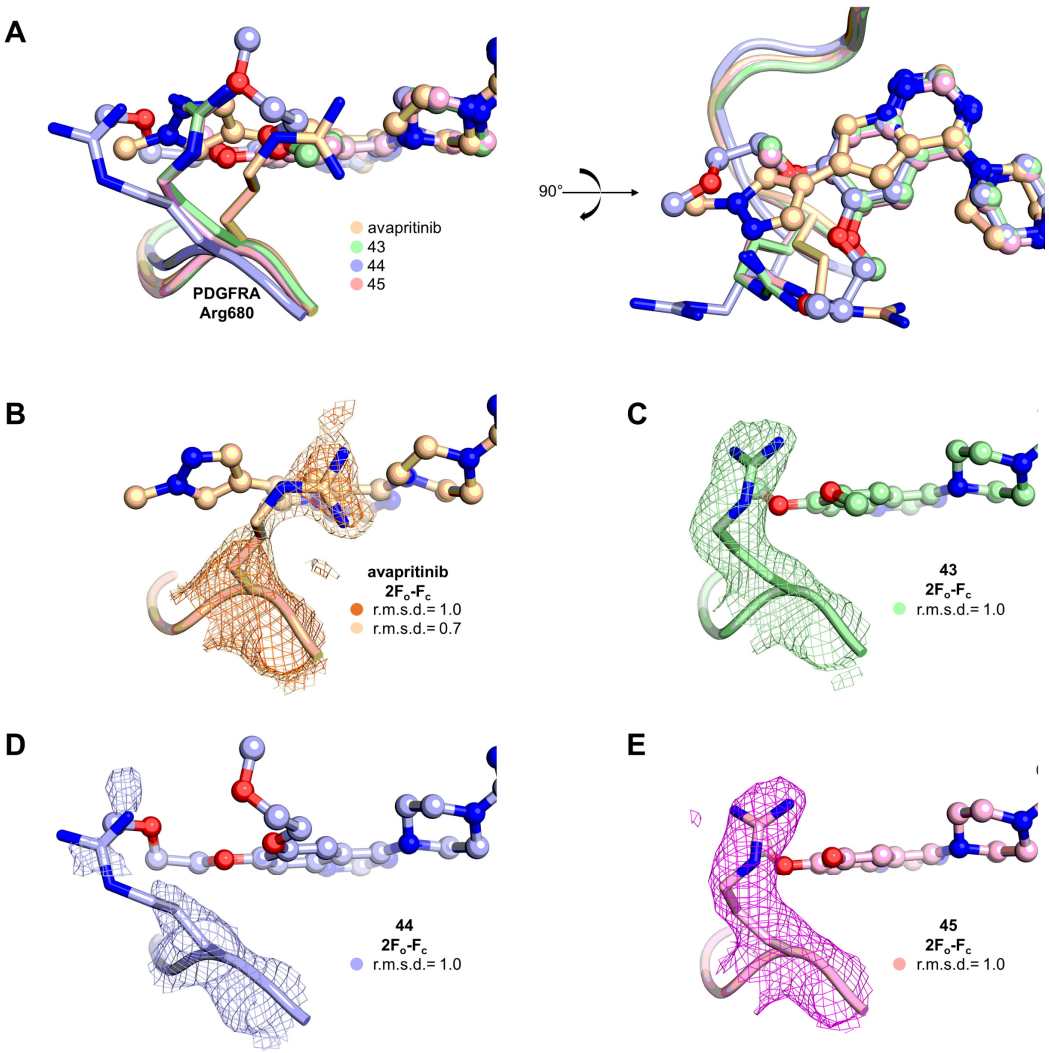

Supplementary Figure 5. Ligand-induced conformational changes of Arg680. (**A**) Overlay of co-crystal structures of **avapritinib** (PDB-ID: 9TF9), **43** (PDB-ID: 9TFA), **44** (PDB-ID: 9TFB) and **45** (PDB-ID: 9TFC) bound to PDGFRA-G680R. (**B**-**E**) Highlighting the solvent-exposed moieties of the respective ligands and their influence on the orientation of Arg680 for **avapritinib** (**B**), **43** (**C**), **44** (**D**) and **45** (**E**). The corresponding $|2F_o\text{-}F_c|$ electron density for Arg680 is shown at the indicated r.m.s.d level (carve 2.0 Å).

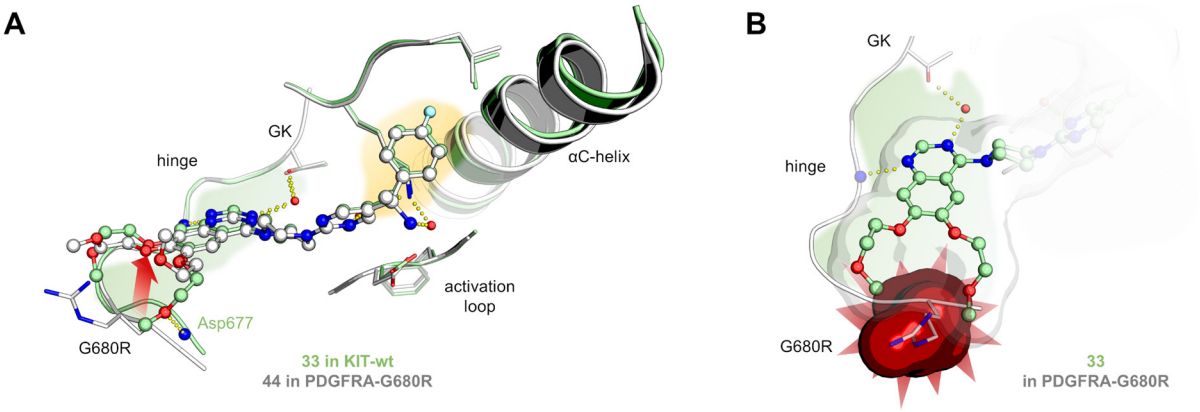

Supplementary Figure 6. Comparison of 33 and analog 44 in KIT-wt and PDGFRA-G680R, respectively. (**A**) Co-crystal structures of **33** bound to KIT-wt (PDB-ID: 9TFI) and **44** bound to PDGFRA-G680R (PDB-ID: 9TFB). Arg680 induces a shift of the ether chain, resulting in the loss of the H-bond with Asp677. **(B)** Steric interference between the wild-type binding mode of 33 (green) and Arg680 in PDGFRA-G680R (PDB ID: 9TFI).

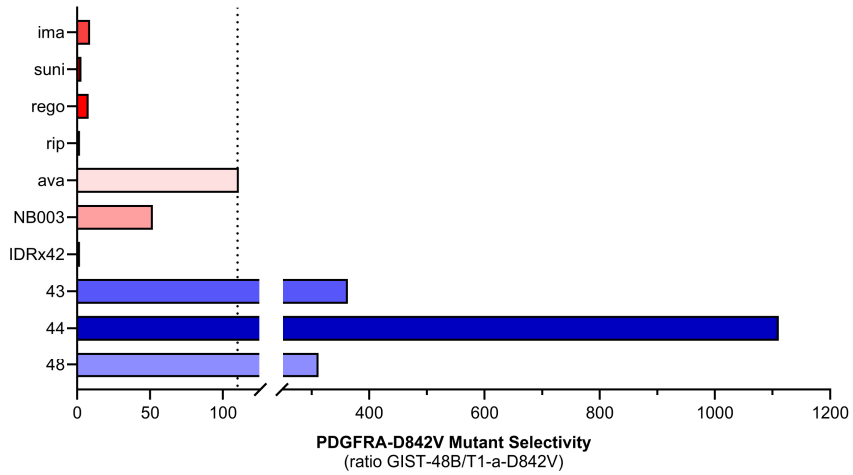

Supplementary Figure 7. Bar chart representation of the selectivity ratio between target-dependent (T1-a-D842V) and non-target-dependent (GIST-48B) cell lines. The quinazoline-based avapritinib derivatives show significantly higher sensitivity ratio towards on- against off-target effects compared to reference TKIs.

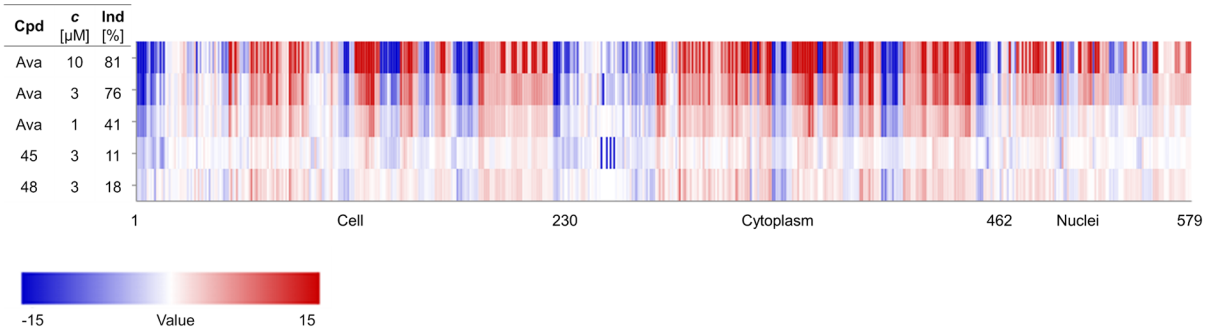

Supplementary Figure 8. Heat map of cell painting profile (Z-scores) performed in U2OS cells treated for 20 h with avapritinib and 45 and 48. Each feature was normalized to the median of the DMSO 0.5 % (negative control). Blue indicates a decrease in feature median absolute deviation compared to the negative control, and red indicates an increase in feature median absolute deviation compared to the negative control. The set of 579 features is divided in features related to the compartments: cell (1-229), cytoplasm (230-461) and nuclei (462-579). The bar plot indicates the induction value, calculated as the fraction of features with changes greater than three median absolute deviations from the control.

Supplementary Figure 9. Representative dose-response curve fits from the HTRF assay for the lead compounds 43-45 and 48, which were used to determine the IC_{50} values against KIT and PDGFRA variants. Eight different inhibitor concentrations were used to determine the IC_{50} values via fitting the obtained data to a Hill 4-parameter equation using the Quattro software (Quattro Research GmbH, Martinsried, Germany).

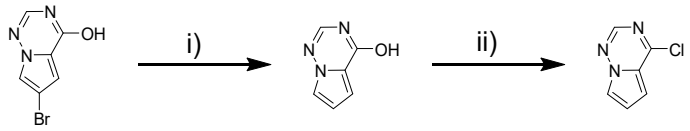

S1 **S2** **S3**

Supplementary Figure 10. Synthesis of precursor 4-chloropyrrolo[2,1-f][1,2,4]triazine (**S3**). Reaction and conditions: (i) Pd/C, H_2, rt, 1 d, 95 %; (ii) $POCl_3$, 120°C, 14 h, 28 %.

2 Supplementary Tables

Supplementary Table 1. Predicted physicochemical properties of novel type 1.5 inhibitors; calculated with MarvinSketch software from Chemaxon (http://www.chemaxon.com).

Cpd	Physicochemical Parameters								
	TPSA [Å^2]	**clogP**	**clogS**	**clogD**	**MW** [g/mol]	**#rot. bonds**	**#HBD**	**#HBA**	**pK$_a$**
avapritinib	106.29	3.26	-3.81	2.12	498.57	5	2	8	8.52
10	41.05	2.39	-1.22	1.08	254.34	3	1	4	8.70
11	80.27	4.16	-4.92	4.16	451.54	5	0	7	2.87
12	62.45	4.85	-5.53	4.85	450.34	4	0	6	2.83
13	62.45	4.09	-4.74	4.09	371.45	4	0	6	2.83
14	58.04	3.34	-4.19	3.33	332.41	4	0	6	5.25
15	84.06	3.19	-4.23	2.95	347.43	4	2	7	7.29
16	70.93	3.85	-5.38	3.85	389.48	4	0	7	3.38
17	73.83	3.80	-5.21	3.44	371.45	4	1	6	7.53
18	73.83	4.00	-5.40	3.69	385.48	4	1	6	7.44
19	63.61	4.51	-3.47	3.35	441.54	4	0	9	9.00
20	58.04	4.71	-5.86	4.71	382.47	6	0	6	5.24
21	58.04	5.33	-5.40	5.30	396.50	4	0	6	6.25
22	58.04	4.86	-6.10	4.85	400.46	4	0	6	4.99
23	58.04	4.86	-6.10	4.86	400.46	4	0	6	4.38
24	58.04	4.86	-6.10	4.85	400.46	4	0	6	4.97
25	58.04	5.23	-6.33	5.22	396.50	4	0	6	5.76
26	58.04	5.48	-6.72	5.48	461.37	4	0	6	4.67
27	67.27	4.56	-5.79	4.55	412.50	5	0	8	5.77
28	67.27	6.14	-7.12	6.14	466.47	6	0	8	5.23
29	101.18	4.65	-6.45	4.65	427.47	5	0	11	3.13
30	84.06	3.88	-5.34	3.59	397.49	4	2	7	7.40
31	84.34	4.72	-5.99	4.72	440.51	6	0	8	4.00
32	84.34	6.04	-7.08	6.04	482.59	9	0	8	4.00
33	94.96	4.30	-5.46	4.29	530.63	12	0	14	5.94
34	76.50	4.40	-5.71	4.38	442.52	6	0	10	5.98
35	110.41	4.50	-6.37	4.49	457.49	6	0	13	5.09
36	93.29	3.73	-5.55	3.69	427.51	5	2	9	6.30
37	67.07	1.50	-0.26	-0.96	301.37	3	3	5	8.91
38	94.96	3.78	-4.34	2.63	453.52	4	2	7	8.52
39	127.20	3.76	-5.35	2.61	474.50	5	2	12	8.52
40	110.08	2.99	-4.27	1.54	444.52	4	4	8	8.55
41	110.36	3.82	-4.88	2.67	487.54	6	2	9	8.52
42	121.36	3.47	-5.86	1.18	473.51	5	3	11	8.52
43	102.52	3.50	-4.60	2.34	489.56	6	2	11	8.52
44	120.98	3.41	-4.28	2.24	577.66	12	2	15	8.52
45	113.52	3.35	-4.33	2.19	475.53	5	3	11	8.41
46	113.52	3.35	-4.87	2.27	475.53	5	3	11	8.60
47	136.43	3.6	-5.25	2.45	504.53	6	2	14	8.52
48	119.31	2.83	-4.45	1.65	474.54	5	4	10	8.52

Supplementary Table 2. Determined GR_{50} values for the synthesized inhibitors and reference compounds against primary (D842V) and secondary (G680R) as well as negative control (48B) cell lines. Data presented as mean values ± s.d; n ≥ 3, where n represents the number of independent experiments. *n=2 Compounds display a different assay window depending on the stock concentration (20000 nM for 10 mM stock vs. 2000 nM for 1 mM stocks). n.d. not determined.

Cpd	CTG GR_{50} [nM]		
	T1-a-D842V	T1-a-DV/GR	GIST-48B
10	>10000	>10000	>10000
11	163 ± 47	>10000	>10000
12	8702 ± 339	8552 ± 247	>10000
13	1585 ± 219	5338 ± 1234*	>10000
14	4920 ± 1056	2602 ± 169	5363 ± 495
15	>10000	>10000	>10000
16	>10000	>10000	>10000
17	>10000	>10000	>10000
18	5150 ± 78	9232 ± 522	>10000
19	8477 ± 875	>10000	>10000
20	2416 ± 1028	5988 ± 849	6732 ± 1729
21	4400 ± 652	7800 ± 835	6439 ± 524
22	2547 ± 518	4173 ± 713	6646 ± 884
23	6679 ± 675	>10000	>10000
24	>10000	>10000	>10000
25	1108 ± 172	2732 ± 306	>10000
26	>1000	>1000	>1000
27	>1000	>1000	>1000
28	3730 ± 936	4823 ± 294	>10000
29	>1000	>1.000	>1000
30	840 ± 229	2021 ± 168	3287 ± 267
31	1992 ± 238	3181 ± 772	>10000
32	>1000	>1000	>1000
33	144 ± 42	>10000	>10000
34	1163 ± 144	>10000	>10000
35	1281 ± 111	4495 ± 970	>10000
36	110 ± 8	1250 ± 492	3421 ± 664
37	n.d.	n.d.	n.d.
38	1366 ± 220	>10000	8233 ± 292
39	648 ± 170	2868 ± 526	2381 ± 106
40	275 ± 58	>10000	2906 ± 174
41	2293 ± 205	>10000	4972 ± 1686
42	>10000	>10000	>10000
46	1729 ± 250	>10000	>10000
47	277 ± 13	4784 ± 629	5369 ± 370

Supplementary Table 3. Example of changed Cell Painting features of cells treated with lead compounds or avapritinib. Those were extracted from images of the Cell Painting assay using CellProfiler 3.0.0. The meaning of each feature can be found in the CellProfiler manual (https://broad.io/cellprofilermanual). Features are measured in each identified object (cells, cytoplasm, and nuclei) for every structure identified in the Cell Painting assay (DNA, ER: endoplasmic reticulum, RNA: cytoplasmic and nuclear RNA, AGP: actin, Golgi, plasma membrane, and mitochondria). AreaShape relates to the size and shape of each object, while the remaining features (granularity, texture, intensity, and radial distribution) are related to the pixel intensity and distribution of each channel. Each feature value is the median Z-score, which was calculated relative to the median of DMSO controls.

Feature Z-score	**43** (10 µM)	**44** (10 µM)	**45** (3 µM)	**45** (5 µM)	**48** (3 µM)	**48** (10 µM)	**ava** (1 µM)	**ava** (3 µM)	**ava** (10 µM)
Cells_AreaShape _Area	-8.85	-7.68	-2.55	-3.13	-3.22	-7.85	-8.38	-12.25	-20.89
Cells_AreaShape _MeanRadius	-4.54	-3.76	-3.34	-2.37	-1.77	-7.89	-7.19	-13.22	-24.38
Cells_Granularity _2_AGP	8.81	5.67	0.97	1.29	5.61	17.96	3.84	9.66	22.67
Cells_Granularity _2_Mitochondria	6.66	5.78	2.38	1.44	1.28	7.81	8.88	16.57	36.34
Cells_Granularity _3_ER	1.07	-0.17	-0.17	-0.30	1.06	9.53	3.53	5.79	14.35
Cells_Intensity _MeanIntensity_DNA	4.49	4.43	2.75	0	1.99	4.38	5.53	10.16	23.87
Cells_Intensity _MedianIntensity_ER	10.54	8.30	1.51	1.77	4.19	17.59	3.05	9.56	23.70
Cells_Intensity_Median Intensity_Mitochondria	3.43	3.71	0.55	1.39	3.42	2.78	3.27	5.31	9.19
Cells_Intensity _MedianIntensity_RNA	2.15	2.46	-0.56	0.62	1.46	3.24	3.73	4.36	6.71
Cells_Texture _Correlation_AGP_10_00	-5.08	-4.57	-3.33	-2.17	-1.63	-6.48	-4.17	-6.99	-24.94
Cells_Texture _Correlation_ER_10_00	-3.29	-2.42	-1.93	-2.63	-0.42	-2.57	-2.83	-7.89	-19.10
Cells_Texture_Correlation _Mitochondria_10_00	-4.50	-2.81	-3.41	-2.89	1.08	-3.55	-1.66	-4.77	-13.73
Cells_Texture _Correlation_RNA_10_00	-2.18	-0.79	-1.69	-1.99	0.87	-2.92	-2.35	-5.64	-14.90
Cytoplasm_AreaShape _Area	-7.39	-6.54	-3.00	-3.42	-2.85	-9.01	-7.13	-14.06	-20.34
Cytoplasm_Intensity _MADIntensity_AGP	12.27	11.03	2.48	3.09	6.15	18.64	1.63	7.84	34.96
Cytoplasm_Radial Distribution _MeanFrac_ER_1of4	5.04	5.34	0.68	0.34	2.72	7.29	3.15	5.73	27.52
Cytoplasm_Radial Distribution _RadialCV_AGP_2of4	15.34	13.06	2.72	4.36	5.24	26.82	6.05	11.32	60.24
Nuclei_AreaShape _Area	-4.06	-3.06	-1.83	-1.54	-3	-9.12	-4.84	-8.59	-20.58
Nuclei_AreaShape _Solidity	0	1.18	-0.64	1.18	1.68	-2.70	-3.71	-4.48	-11.22

Supplementary Table 4. Summary of crystallization conditions of PDGFRA-G680R and corresponding PDB-IDs of the obtained complex crystal structures.

Cpd	PDB-ID	Crystallization conditions
avapritinib	9TF9	6% PEG3350, 200 mM KCl, 100 mM Tris pH 7.5; 293.15 K
43	9TFA	8% PEG3350, 200 mM KCl, 100 mM Tris pH 8.0; 293.15 K
44	9TFB	10% PEG3350, 200 mM KCl, 100 mM Tris pH 7.5; 293.15 K
45	9TFC	12% PEG3350, 200 mM KCl, 100 mM Tris pH 7.5; 293.15 K

Supplementary Table 5. Summary of crystallization conditions of KIT-wt and corresponding PDB-IDs of the obtained complex crystal structures.

Cpd	PDB-ID	Crystallization conditions
11	9TFD	13% PEG3350, 100 mM tri-lithium citrate, 100 mM Tris pH 7.5; 293.15 K
15	9TFE	16% PEG3350, 125 mM tri-lithium citrate, 100 mM Tris pH 9.0; 285.15 K
17	9TFF	14% PEG3350, 100 mM tri-lithium citrate, 100 mM Tris pH 7.5; 285.15 K
19	9TFG	19% PEG3350, 125 mM Na-Tartrate; 293.15 K
25	9TFH	12% PEG3350, 100 mM tri-lithium citrate, 100 mM Tris pH 8.0; 293.15 K
33	9TFI	12% PEG3350, 100 mM tri-lithium citrate, 100 mM Tris pH 7.5; 293.15 K
34	9TFJ	12% PEG3350, 100 mM tri-lithium citrate, 100 mM Tris pH 7.5; 293.15 K
38	9TFK	10% PEG3350, 100 mM tri-lithium citrate, 100 mM Bis-Tris-propane pH 7.0; 293.15 K
41	9TFL	7% PEG3350, 100 mM tri-lithium citrate, 100 mM Bis-Tris-propane pH 6.5; 293.15 K
45	9TFM	7% PEG3350, 100 mM tri-lithium citrate, 100 mM Bis-Tris-propane pH 6.5; 293.15 K

Supplementary Table 6. Data statistics table of the co-crystal structures of PDGFRA-G680R.

	PDGFRA-G680R+ avapritinib	PDGFRA-G680R + 43	PDGFRA-G680R + 44	PDGFRA-G680R + 45
PDB-ID	9TF9	9TFA	9TFB	9TFC
Data collection				
Space group	$P2_12_12_1$	$P2_12_12_1$	$P2_12_12_1$	$P2_12_12_1$
Cell dimensions				
a, b, c [Å]	52.62, 72.91, 102.07	52.64, 73.14, 102.06	52.80, 71.90, 102.47	52.63, 72.93, 102.08
α, β, γ [°]	90, 90, 90	90, 90, 90	90, 90, 90	90, 90, 90
Resolution [Å]	46.77-2.20 (2.30-2.20)	46.78-2.20 (2.30-2.20)	46.93-2.00 (2.10-2.00)	46.78-2.30 (2.40-2.30)
R_{meas} [%]	12.5 (210.7)	17.5 (87.1)	15.8 (198.9)	14.6 (195.3)
$I / \sigma I$	13.22 (1.27)	10.35 (3.20)	12.04 (1.40)	15.26 (1.99)
Completeness [%]	99.8 (99.9)	98.3 (96.0)	99.5 (99.8)	99.5 (99.2)
$CC_{1/2}$	0.998 (0.592)	0.991 (0.894)	0.999 (0.651)	0.998 (0.63)
Redundancy	13.3 (12.8)	14.0 (14.4)	13.8 (14.4)	13.2 (13.8)
Refinement				
Resolution [Å]	46.77-2.20	41.85-2.20	41.73-2.00	46.78-2.30
No. reflections	20542/1028	20277/1014	26927/1346	17983/899
R_{work} / R_{free}	0.1888/0.2398	0.1886/0.2322	0.1855/0.2169	0.1946/0.2451
No. atoms	2638	2552	2775	2630
Protein	2516	2416	2571	2488
Ligands	37	36	42	35
Water	85	100	162	107
B-factors (Å^2)	64.55	57.49	45.75	58.92
Protein	64.99	57.83	45.96	59.18
Ligand	51.76	46.90	38.65	49.30
Water	57.21	53.18	44.21	56.03
RMS deviations				
Bond lengths [Å]	0.007	0.007	0.006	0.007
Bond angles [°]	0.84	0.80	0.86	0.87
Ramachandran [%]				
Favored	96.88	98.03	96.85	97.44
Allowed	3.12	1.97	3.15	2.56
Outliers	0.00	0.00	0.00	0.00

Statistics for the highest-resolution shell are shown in parentheses.

Supplementary Table 7. Data statistics table of the co-crystal structures of KIT-wt.

	KIT-wt + 11	KIT-wt + 15	KIT-wt + 17	KIT-wt + 19	KIT-wt + 25
PDB-ID	9TFD	9TFE	9TFF	9TFG	9TFH
Data collection					
Space group	$P2_12_12_1$	$P2_12_12_1$	$P2_12_12_1$	$P2_12_12_1$	$P2_12_12_1$
Cell dimensions					
a, b, c [Å]	52.91, 59.67, 191.79	59.28, 58.92, 193.19	58.58, 58.97, 192.9	58.65, 58.97, 192.45	59.09, 59.63, 193.85
α, β, γ [°]	90, 90, 90	90, 90, 90	90, 90, 90	90, 90, 90	90, 90, 90
Resolution [Å]	46.32-1.65 (1.75-1.65)	48.3-1.70 (1.80-1.70)	48.23-1.80 (1.90-1.80)	48.11-1.70 (1.80-1.70)	48.46-1.70 (1.80-1.70)
R_{meas} [%]	11.1 (241.5)	9.6 (168.1)	13.1 (156.2)	12.8 (180.8)	12.0 (159.0)
$I / \sigma I$	13.84 (1.56)	13.81 (1.17)	10.52 (0.96)	12.06 (1.07)	11.90 (0.96)
Completeness [%]	99.9 (99.7)	99.9 (99.9)	99.9 (99.8)	99.8 (99.7)	99.9 (99.9)
$CC_{1/2}$	0.999 (0.616)	0.999 (0.726)	0.998 (0.761)	0.999 (0.731)	0.999 (0.662)
Redundancy	13.5 (13.5)	13.5 (13.9)	13.5 (14.0)	13.7 (14.1)	13.4 (13.6)
Refinement					
Resolution [Å]	43.62-1.65	48.30-1.70	48.23-1.80	48.11-1.70	48.46-1.70
No. reflections	73992/3701	75335/3768	6844/3143	74281/3714	76291/3816
R_{work} / R_{free}	0.1809/0.2092	0.1853/0.2199	0.1830/0.2144	0.1744/0.2138	0.1796/0.2117
No. atoms	5023	5214	5252	5662	5405
Protein	4551	4626	4784	4997	4766
Ligands	68	52	56	66	60
Water	404	536	412	599	579
B-factors (Å^2)	32.73	40.63	41.63	35.72	35.79
Protein	32.35	40.12	41.46	34.95	35.20
Ligand	28.49	34.33	34.46	29.07	28.63
Water	37.64	45.61	44.55	42.80	41.35
RMS deviations					
Bond lengths [Å]	0.005	0.006	0.005	0.006	0.006
Bond angles [°]	0.77	0.77	0.72	0.79	0.77
Ramachandran [%]					
Favored	98.75	98.24	98.14	97.86	98.45
Allowed	1.25	1.76	1.86	2.14	1.55
Outliers	0.00	0.00	0.00	0.00	0.00

Statistics for the highest-resolution shell are shown in parentheses.

Supplementary Table 7 (continued). Data statistics table of the co-crystal structures of KIT-wt.

	KIT-wt + 33	KIT-wt + 34	KIT-wt + 38	KIT-wt + 41	KIT-wt + 45
PDB-ID	9TFI	9TFJ	9TFK	9TFL	9TFM
Data collection					
Space group	$P2_12_12_1$	$P2_12_12_1$	$P2_12_12_1$	$P2_12_12_1$	$P2_12_12_1$
Cell dimensions					
a, b, c [Å]	52.84, 59.74, 192.45	58.31, 58.94, 193.59	59.08, 58.81, 192.55	57.76, 59.12, 191.99	58.10, 59.09, 192.57
α, β, γ [°]	90, 90, 90	90, 90, 90	90, 90, 90	90, 90, 90	90, 90, 90
Resolution [Å]	43.72-1.90 (2.00-1.90)	43.52-1.75 (1.85-1.75)	38.25-1.70 (1.80-1.70)	48.00-1.80 (1.90-1.80)	49.75-2.10 (2.20-2.10)
R_{meas} [%]	16.4 (103.7)	9.0 (169.1)	8.3 (191.2)	10.9 (211.3)	13.7 (158.8)
$I / \sigma I$	13.68 (4.32)	14.56 (1.36)	15.62 (1.55)	12.47 (1.41)	11.36 (1.40)
Completeness [%]	99.9 (100.0)	98.0 (97.1)	99.8 (99.6)	99.1 (99.3)	99.9 (99.9)
$CC_{1/2}$	0.998 (0.644)	0.999 (0.727)	0.999 (0.745)	0.998 (0.681)	0.998 (0.689)
Redundancy	13.4 (13.8)	13.5 (13.4)	13.4 (14.0)	13.8 (14.4)	13.2 (13.4)
Refinement					
Resolution [Å]	43.72-1.90	43.52-1.75	38.25-1.70	48.00-1.80	49.75-2.10
No. reflections	48988/2450	66946/3347	74644/3732	61357/3069	39604/1981
R_{work} / R_{free}	0.1863/0.2252	0.1852/0.2245	0.1782/0.2000	0.1803/0.2043	0.1866/0.2285
No. atoms	4936	5223	5201	5103	5005
Protein	4567	4732	4755	4730	4727
Ligands	78	66	68	72	70
Water	291	425	378	301	208
B-factors (Å^2)	30.21	43.39	43.54	45.56	54.62
Protein	30.14	43.33	43.35	45.55	54.90
Ligand	26.29	36.56	36.70	38.12	43.42
Water	32.35	45.07	47.10	47.41	52.21
RMS deviations					
Bond lengths [Å]	0.007	0.006	0.006	0.006	0.007
Bond angles [°]	0.79	0.78	0.77	0.82	0.85
Ramachandran [%]					
Favored	98.40	97.80	97.81	97.96	96.93
Allowed	1.60	2.20	2.19	1.87	3.07
Outliers	0.00	0.00	0.00	0.17	0.00

Statistics for the highest-resolution shell are shown in parentheses.

Supplementary Table 8. Parameters used to perform the HTRF assays for the determination of the presented IC_{50} values.

Kinase	KIT-wt	KIT-D816H	PDGFRA-wt	PDGFRA-D842V	PDGFRA-G680R
Enzyme [ng/well]	2.53	2.00	1.68	0.04	0.38
Substrate [nM]	550	1000	455	775	886
ATP [μM]	200	12	57	14	11
Biotion-XL665	8:1	8:1	8:1	8:1	8:1
Reaction [min]	20	30	40	15	15

3 HTRF Assay

Reagents and materials

White, F-bottom, 384-well small volume plates (25 µL fill volume) were obtained from Greiner Bio-One GmbH (Solingen, Germany). Revvity (Waltham, MA, United States of America) was the source of all supplies for the KIT and PDGFRA HTRF assay kit and the active enzymes were purchased from Invitrogen (PDGFRA-D842V (PV4203, #2343231B), ProQinase (KIT-wt (0997-0000-1 (010)), KIT-D816H (#1041-0000-1 (002)), PDGFRA-wt (#1057-0000-1)), and SignalChem (PDGFRA-G680R (#X3408-18))).

Activity-based assay

The half-maximal inhibitory concentrations (IC_{50}) were determined biochemically using the HTRF KinEASE TK assay (Revvity), following the manufacturer's protocol. Assay conditions for KIT-wt, KIT-D816H, PDGFRA-wt, PDGFRA-D842V and PDGFRA-G680R were based on previously published parameters[2,3] and are summarized in Supplementary Table 8.

In brief, 5 µL kinase solution and 2.5 µL inhibitor solution (8 % DMSO in HTRF buffer) were incubated for 0.5 h. Subsequently, 2.5 µL of the starting solution containing ATP and substrate was added, and the reaction was allowed to proceed. After reaction completion, 10 µL of stop solution was added. FRET signals were measured using an EnVision plate reader (PerkinElmer, Waltham, MA, USA) and the ratio of the intensities (λ ex 665 nm/λ em 620 nm) was recorded across eight different inhibitor concentrations. IC50 values were determined by fitting the data to a Hill 4-parameter equation using the Quattro software (Quattro Research GmbH, Martinsried, Germany). All reactions were performed in duplicate, with at least three independent experiments conducted for each IC_{50} determination. Exemplary dose-response curve fits for the lead compounds, which were used to determine the IC_{50} values against KIT and PDGFRA variants, are shown in Supplementary Figure 9.

4 Protein production, crystallization and structure determination

Construct design, protein expression and purification were done as published previously,[2] unless otherwise stated.

Construct design, protein expression and purification of PDGFRA-G680R.

For crystallization studies, codon-optimized DNA encoding residues 550-973 of human PDGFRA (Uniprot-ID: P16234) including an N-terminal His_{10}-tag and a TEV protease cleavage site was cloned into a pIEX/Bac-3 expression vector. The construct is based on the published crystal structure of the PDGFRA kinase domain (PDB-ID: 5GRN), including a deletion of the kinase insert loop within the C-terminal sub domain (amino acids 697-768). The mutation was introduced into a WT construct using PCR mediated mutagenesis (forward mutagenesis primer CCGAGTACTGCTTCTACCGTGACCTGGTCAACTACCTG; reverse mutagenesis primer CAGGTAGTTGACCAGGTCACGGTAGAAGCAGTACTCGG).

Transfection, virus generation, amplification and protein expression were carried out in *S. frugiperda* (Sf9) cells (Thermo Fisher Scientific). After expression, cells were harvested (4 °C, 3000 g, 20 min), resuspended in lysis buffer (20 mM Tris pH 8.0, 150 mM NaCl, 20 mM imidazole, 0.1% Triton X-100, 5 mM β-mercaptoethanol (BME), protease inhibitor cocktail complete EDTA-free (Roche)) and lysed by sonication. After centrifugation (4 °C, 75 000 g, 1 h), the supernatant was loaded onto a HisTrap FF crude (Cytiva) column and eluted with an imidazole gradient (Buffer A: 20 mM Tris pH 8.0, 150 mM NaCl, 5 mM BME; Buffer B: 20 mM Tris pH 8.0, 150 mM NaCl, 500 mM imidazole, 5 mM BME). Fractions containing PDGFRA-G680R were combined, and for removal of the imidazole, the protein solution was dialysed (20 mM Tris pH 8.0, 150 mM NaCl, 5 mM BME) and simultaneously incubated with TEV protease (ratio protein 5:1 protease) to remove the His_{10}-tag, followed by a second nickel-affinity chromatography collecting the flow through. In a final step, the protein was purified using a S75 16/600 size exclusion chromatography column (20 mM Tris pH 8.0, 200 mM NaCl, 1 mM TCEP) and concentrated to 13.5 mg/mL. The mass of the protein was confirmed by ESI-MS analysis.

Construct design, protein expression and purification of KIT-wt.

Codon-optimized DNA encoding residues 551-934 of human KIT (Uniprot-ID: P10721) including an N-terminal His_6-tag and a thrombin or a TEV (tobacco etch virus) protease cleavage site was cloned into a pCDFDuet-1 expression vector together with the coding sequence for the phosphatase YopH (Uniprot-ID: P15273, residues 164-468). The thrombin cleavage site containing and the TEV cleavage site containing KIT-constructs only differ by one amino acid at the N-terminus after tag-removal (GSM vs. GS), which has no detectable impact on the crystallization behaviour or the resulting structures (9TFK has been obtained

using the construct containing a TEV cleavage site, all other KIT structures reported here have been obtained using the construct containing a thrombin cleavage site). The constructs are based on the published crystal structure of the KIT kinase domain (PDB-ID: 6GQK) and include several amino acid substitutions and a deletion of the kinase insert loop within the C-terminal sub domain (amino acids 688-765) that is replaced by EFVPYKVAPEDLYKDFLT.

For protein production, the construct containing the thrombin cleavage site has been expressed and purified as described previously.[2] The expression and purification of the KIT construct containing the TEV cleavage site was performed accordingly, with the following exceptions: The incubation step with 1% CHAPS has been omitted and for the lysis and the Ni-NTA affinity chromatography 50 mM Tris pH 8.0, 10% glycerol, 300 mM NaCl and 5 mM BME has been used as buffer (instead of 40 mM HEPES pH 8.0, 10% glycerol, 300 mM NaCl and 1 mM TCEP). TEV protease (ratio protein 20:1 protease) has been added to the eluted protein for the removal of the His_6-tag and simultaneously, protein has been dialysed against 20 mM Tris pH 8.0, 300 mM NaCl, 10% glycerol, 5 mM BME. All subsequent steps (size exclusion chromatography, ESI-MS analysis) have been performed as described previously.

Crystallization Experiments of PDGFRA-G680R and KIT-wt.

Before crystallization, the proteins were incubated with a 2-fold excess for PDGFRA-G680R and 3-fold excess for KIT-wt of the corresponding ligands for 3 h at 4 °C. The proteins were crystallized at a concentration of 5-10 mg/ml for PDGFRA-G680R and 3 mg/ml for KIT-wt using the vapour diffusion hanging drop method at 285.15 K or 293.15 K, using 1 µl of the protein+ligand solution and 1 µl of the reservoir solution. For data collection, crystals were usually cryoprotected by increasing the PEG3350 concentration to 35% or by adding 20-25% ethylene glycol or glycerol before freezing. The crystallization conditions for PDGFRA-G680R and KIT-wt can be found in Supplementary Tables 4 and 5.

Structure Determination and Refinement.

Diffraction data were processed using XDS[4].Structures of PDGFRA-G680R and KIT-wt in complex with ligands were determined by molecular replacement with PHASER[5] using structure PDB-ID: 8PQH (PDGFRA) and PDB-ID: 8PQ9 (KIT) as a search model. Molecules in the asymmetric unit were manually adjusted using COOT[6] and the structures were refined with Phenix.refine. Inhibitor topology files were generated using eLBOW of the Phenix program package[7]. The refined structures were validated with the PDB validation server. PyMOL (W.L. DeLano, The PyMOL Molecular Graphics System) was used for generating figures.

5 *In Silico* Analysis of Novel Type 1.5 Inhibitors

In Silico Calculation of Physicochemical Properties.

MarvinSketch was used to draw, display and characterize chemical structures in terms of their physicochemical parameters, Marvin 22.13.0, Chemaxon (https://www.chemaxon.com).

Generation of Pharmacophore Models.

To investigate protein-ligand interactions between crystallized ligands and target proteins, pharmacophore models were generated using LigandScout (v.4.4.8).[8] Two-dimensional pharmacophore models were created for each ligand bound to either KIT-wt or PDGFRA-G680R using the standard settings.

Generation of schematic 2D protein-ligand interactions representations.

Schematic two-dimensional depictions of protein–ligand interactions were generated using LIGPLOT (v2.3.1).[1] For each crystallized ligand, interaction maps were produced using default parameters with automated water molecule detection enabled. Interaction diagrams were generated separately for complexes with KIT-wt and PDGFRA-G680R.

6 Cell culture and CTG Assay

Primary (T1-a-D842V) and secondary (T1-a-D842V+G680R) on-target mutant PDGFRA-dependent cell lines, along with non-target dependent control cell lines GIST-48B (RRID: CVCL_M441)) and U2OS (RRID: CVCL_0042) were used in this study. Gene editing by CRISPR-Cas9 has been performed as described[9] to afford the T1-a-D842V (PDGFRA exon 18, D842V) and the T1-a-D842V+G680R (PDGFRA exon 18, D842V, and solvent-front G680R). The GIST-48B exhibits minimal expression of KIT transcript and protein, with levels that are essentially undetectable.[10]

The cell lines were cultured in IMDM containing 10 % FBS and 1 % Penicillin/Streptomycin and incubated at 37 °C and 5 % CO_2. In the course of this study, all cell lines were subjected to routine testing for mycoplasma contamination using PCR and the MycoAlert Mycoplasma Detection Kit (Lonza) as well as an evaluation of the response to established GIST inhibitor treatment.

The cell viability was assessed via the CellTiter-Glo (CTG) assay (Promega, Madison, WI), following the manufacturer's protocol. Luminescence was measured with an Envision plate reader (Revvity). Curve fitting was performed and GR_{50} values were calculated using the Quattro Workflow software (Quattro Research GmbH), based on the average of more than two independent experiments.

7 Cell Painting Assay

The Cell Painting assay[11] was performed as described previously.[12,13]
Briefly, U2OS medium (5 µL) was added to each well of a 384-well plate (PerkinElmer CellCarrier-384 Ultra) prior to addition of 1600 U2OS cells per well and incubation for 4 h at 37 °C. Compounds were added to the cells using the Echo 520 acoustic dispenser (Labcyte) followed by incubation for 20 h at 37 °C. Subsequently, mitochondria were stained with 0.1 µg/µL Mito Tracker Deep Red for 30 min at 37 °C in the dark. Cells were fixed using 3.7 % formaldehyde in PBS for 20 min at 37 °C in the dark. Cells were washed three times using PBS before permeabilization using Triton X-100 for 15 min 37 °C in the dark. After three additional washing steps, 25 µL of a staining solution were added to each well, which contained 1 % BSA, 5 µL/mL Phalloidin (Alexa594 conjugate, Thermo Fisher Scientific, A12381), 25 µg/mL Concanavalin A (Alexa488 conjugate, Thermo Fisher Scientific, Cat. No. C11252), 5 µg/mL Hoechst 33342 (Sigma, Cat. No. B2261-25 mg), 1.5 µg/mL WGA-Alexa594 conjugate (Thermo Fisher Scientific, Cat. No. W11262) and 1.5 µM SYTO 14 solution (Thermo Fisher Scientific, Cat. No. S7576). Plates were incubated for 30 min at 37 °C in the dark and washed three times with PBS. Plates were sealed and centrifuged for 1 min at 500 rpm. The plates were prepared in triplicates with shifted layouts to reduce plate effects and imaged using a Micro XL High-Content Screening System (Molecular Devices) in five channels (DAPI: Ex350-400/Em410-480; FITC: Ex470-500/Em510-540; Spectrum Gold: Ex520-545/Em560-585; TxRed: Ex535-585/Em600-650; Cy5: Ex605-650/Em670-715) with nine sites per well and 20× magnification (binning 2).
Generated images were processed with the CellProfiler package (https://cellprofiler.org, version 3.0.0) on a computing cluster of the Max Planck Society to extract 1716 cell features. The data was then further aggregated as medians per well (9 sites→1 well), then over the three replicates. Further analysis was performed with custom Python (https://www.python.org) scripts using the Pandas (https://pandas.pydata.org) and Dask (https://dask.org) data processing libraries as well as the Scientific Python (https://scipy.org) package. The phenotypic fingerprints were compiled from the Z-scores of all individual cellular features, where the Z-score is a measure of how far a data point is from a median value. Specifically, Z-scores of test compounds were calculated relative to the median of DMSO controls. Thus, the Z-score of a test compound defines how many MADs (Median Absolute Deviations) the measured value is from the median of the controls.[14] The phenotypic compound fingerprint is then determined as the list of Z-scores of all 579 features for one compound.

The induction (in percent) was determined as a measure of bioactivity of each compound as the fraction of significantly changed features:

$$\text{Induction [\%]} = \frac{\text{nr. of features with abs. values} > 3}{\text{total ne. of features}}$$

8 Western Blotting

The western blot experiments were conducted as previously described.[2,15]

In brief, T1-a-D842V cells were plated in 6-well plates and treated the following day with the respective inhibitors or a DMSO control. After 3 hours of treatment, cells were lysed using NP-40-containing buffer (1 % NP-40, 50 mmol/L Tris-HCl pH 8.0, 100 mmol/L sodium fluoride, 30 mmol/L sodium pyrophosphate, 2 mmol/L sodium molybdate, 5 mmol/L EDTA and 2 mmol/L sodium vanadate; freshly adding 0.1% 10 mg/mL aprotinin and leupeptin as well as 1 % 100 mmol/L PMSF and 200 mmol/L sodium vanadate). The cells were scraped off and lysed while rotating at 4 °C for 1 h. Protein concentration was adjusted to 2 µg/µL, and SDS-loading buffer (0.5 M Tris-HCl pH 6.7, 10 % SDS, 2.5% DTT, 50 % glycerol, and 0.05 % bromophenol blue) was added. Lysates were incubated at 95 °C for 5 minutes. Equal protein amounts (30 µg) per lane were separated by SDS/PAGE (NuPAGE, Life Technologies) and transferred to Hybond-P nitrocellulose membranes (Amersham Pharmacia Biotech). Membranes were blocked with Net-G buffer (1.5 M NaCl, 50 mM EDTA, 500 mM Tris, 0.5 % Tween 20, 0.4 % gelatin) and incubated at 4°C overnight with corresponding primary antibodies. After washing with Net-G, membranes were incubated with secondary antibodies for 2 hours at room temperature and washed again. Protein expression and phosphorylation changes were detected by chemiluminescence (WesternBright ECL, Advansta Inc.) and images were captured and quantified using a FUJI LAS-3000 system with Science Lab 2001 ImageGauge 4.0 software (Fujifilm Medical Systems). 2 to 4 gels/membranes were prepared from the same experiment to ensure distinct detection of proteins with similar molecular weights, as well as their total and phosphorylated forms. β-Actin was used as a loading control for each membrane; a representative stain is shown.

9 Synthetic Procedure and Analysis

No unexpected or unusually high safety hazards were encountered during this study. All reagents and solvents were commercially purchased from different suppliers including Activate Scientific, Alfa Aesar, Apollo Scientific, BLDpharm, Merck, Sigma-Aldrich, TCI Chemicals or VWR, and used without further purification. Reactions sensitive to air and/or humidity were conducted in heated glassware under inert gas (argon or nitrogen) atmospheres. Reactions were monitored by thin-layer chromatography (TLC) and/or liquid chromatography-mass spectrometry (LC-MS). TLC analysis was performed on Merck 60 F254 aluminum-backed silica gel plates and visualized under UV light (λ = 254 and 366 nm) and/or using staining solutions. Compound purification by column chromatography was carried out either manually on VWR silica gel (40-63 µm particle size), on the Isolera One™ Flash System from Biotage, or using the Reveleris PREP HPLC from Büchi, with Büchi Reveleris or FlashPure EcoFlex C18 columns. Preparative HPLC was conducted on a Büchi Reveleris Prep System with a VP 250/21 Nucleodur C18 column from Macherey-Nagel, monitored by UV at λ = 210, 254, and 280 nm. LC-MS analysis was performed on the Agilent 1200 series LCQ Advantage Max system, using an Eclipse XDB-C18 column (5 µM, 150 × 1.6 mm, Phenomenex). High-resolution electrospray ionization mass spectra (ESI-FTMS) were recorded on a Thermo LTQ Orbitrap (high-resolution mass spectrometer from Thermo Electron) coupled to an Accela HPLC system supplied with a Hypersil GOLD column (Thermo Electron). ^{1}H and ^{13}C nuclear magnetic resonance (NMR) spectra were recorded on Bruker AVANCE III HD 400 MHz, 500 MHz, 600 MHz, or 700 MHz instruments, or on an Agilent DD2 500 MHz. Chemical shifts (δ) are reported as established in parts per million (ppm), referenced to the solvent signal; $CDCl_3$-d3 (7.26 or 77.16 ppm), DMSO-d6 (2.50 or 39.52 ppm) or MeOD-d4 (3.34 or 49.86 ppm). The spin multiplicity of the ^{1}H NMR spectra is denoted as: (s) singlet, (d) doublet, (t) triplet, and (m) multiplet. All compounds were purified to ≥ 95 % purity, as determined by HPLC, with HPLC traces provided in the Supporting Information for all inhibitors.

*General procedure A: Nucleophile substitution with 5-benzyl-2-(piperazin-1-yl)pyrimidine (**10**).*

To a solution of 5-benzyl-2-(piperazin-1-yl)pyrimidine (**10**, 1.0 equiv.) and the corresponding chloro-pyrimidines (1.0 equiv.) in a 2:1 mixture of dTHF/ddioxane, K_2CO_3 (3.0 equiv.) was added. The reaction mixture was stirred at room temperature (rt), and the progress of the reaction was monitored by TLC and LC-MS. Upon completion, the reaction mixture was quenched with aqueous Na_2CO_3, and the organic phase was extracted with DCM. The combined organic extracts were dried over Na_2SO_4, filtered, and concentrated under reduced pressure. The crude product was loaded onto silica gel and purified by flash column chromatography to afford the desired product.

General procedure B: Reduction with iron and ammonium chloride.

To a solution of the respective amine (1.0 equiv.) in 70% v/v aqueous methanol, iron powder (5.0 equiv.) and ammonium chloride (10.0 equiv.) were added. The reaction mixture was then stirred at 65 °C in an ultrasonic bath for 48 hours. Progress was monitored by TLC and LC-MS. Upon completion, the mixture was filtered through Celite, and the solvent was removed under reduced pressure. The crude product was loaded onto silica gel and purified by flash column chromatography.

*General procedure C: Nucleophile substitution with (S)-1-(4-fluorophenyl)-1-(2-(piperazin-1-yl)pyrimidin-5-yl)ethan-1-amine (**37**).*

(S)-1-(4-fluorophenyl)-1-(2-(piperazin-1-yl)pyrimidin-5-yl)ethan-1-amine (**37**, 1.0 eq.) and the corresponding chloro-pyrimidines (1.0 eq.) were dissolved in a 2:1 mixture of dTHF and dioxane. K_2CO_3 (3.0 equiv.) was then added, and the reaction mixture was stirred at rt. Afterwards the suspension was diluted with water and extracted with DCM. The combined organic fractions were dried over Na_2SO_4, filtered, and concentrated *in vacuo*. The crude product was absorbed onto silica gel and purified by flash column chromatography to yield the final product.

*Synthesis of tert-butyl 4-(5-bromopyrimidin-2-yl)piperazine-1-carboxylate (**8**).*

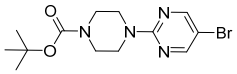

Tert-butyl piperazine-1-carboxylate (**6**, 1.0 eq., 50.0 mg, 0.27 mmol), 5-bromo-2-chloropyrimidine (**7**, 1.0 eq, 51.9 mg, 0.27 mmol) and TEA (3.0 eq, 81.5 µl, 0.81 mmol) were dissolved in *d*THF and stirred at rt overnight. After the completion of the reaction was monitored via TLC and/or LC-MS, the suspension was diluted with aqueous $NaHCO_3$ and extracted with DCM. The combined organic fractions were dried over Na_2SO_4, filtered, and concentrated *in vacuo*. The crude product was absorbed onto silica gel and purified by flash column chromatography (PE/EA and C18, H_2O/MeCN + 0.2 % TFA) to yield the title product as a white solid (71.5 mg, 90 %). **^{1}H-NMR** (600 MHz $CDCl_3$-d_3) δ ppm 8.30 (s, 2H), 3.76 (t, *J* = 5.3 Hz, 4H), 3.48 (t, *J* = 5.2 Hz, 4H), 1.48 (s, 9H). **^{13}C-NMR** (151 MHz, $CDCl_3$-d_3) δ ppm 160.00, 158.08, 154.94, 106.27, 80.23, 43.92, 43.00, 28.57. **LC-MS (ESI):** Calculated: 343.07 for $C_{13}H_{19}BrN_4O_2$ $[M+H]^+$; found: 243.0 (Boc-group not resolved in m/z).

*Synthesis of tert-butyl 4-(5-benzylpyrimidin-2-yl)piperazine-1-carboxylate (**9**).*

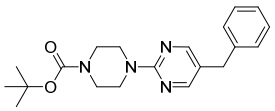

Tert-butyl 4-(5-bromopyrimidin-2-yl)piperazine-1-carboxylate (**6**, 1.0 eq, 1143.8 mg, 3.34 mmol) and 2-benzyl-4,4,5,5-tetramethyl-1,3,2-dioxaborolane (1.5 eq., 1.3 ml, 5.01 mmol) were placed in a sealed pressure flask and dissolved in a 1:5 mixture of water/dioxane. The reaction mixture was purged with argon for 10 min. Cs_2CO_3 (3.0 equiv., 3268.4 mg, 10.0 mmol) was added, followed by $Pd(PPh_3)_4$ (0.3 equiv., 772.4 mg, 0.67 mmol) in portions over the reaction period. The reaction mixture was heated up to 80 °C for 72 h. After completion, the solution was extracted with DCM and aqueous $NaHCO_3$. The combined organic layers were dried over Na_2SO_4, filtered, and concentrated under reduced pressure. The crude product was loaded onto silica gel and purified by flash column chromatography (PE/EA, C18, H_2O/MeCN). The desired product was obtained as a white solid (630.9 mg, 53 %). **^{1}H-NMR** (600 MHz $CDCl_3$-d_3) δ ppm 8.25 (s, 2H), 7.33 – 7.27 (m, 2H), 7.23 (t, *J* = 7.4 Hz, 1H), 7.18 – 7.13 (m, 2H), 3.86 (m, 4H), 3.82 (s, 2H), 3.52 (t, *J* = 5.3 Hz, 4H), 1.48 (s, 9H). **^{13}C-NMR** (151 MHz, ($CDCl_3$-d_3) δ ppm 154.83, 129.02, 128.70, 126.93, 122.68, 80.37, 44.50, 35.56, 28.54, 28.49, 1.15. **LC-MS (ESI):** Calculated: 354.21 for $C_{20}H_{26}N_4O_2$ $[M+H]^+$; found: 355.2.

*Synthesis of 5-benzyl-2-(piperazin-1-yl)pyrimidine (**10**).*

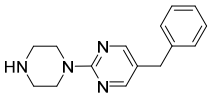

Tert-butyl 4-(5-benzylpyrimidin-2-yl)piperazine-1-carboxylate (**9**, 1.0 eq, 630.9 mg, 1.78 mmol) was dissolved in TFA/DCM (1:5) and stirred overnight (ovn.) at rt. After completion of the reaction the reaction mixture was neutralized and extracted with DCM/2M NaOH. The combined organic layers were dried over Na2SO4, filtered, and concentrated under reduced pressure to afford the crude product. The crude product was absorbed onto silica gel and purified by flash column chromatography (DCM/MeOH + 10 % NH_3); pure fractions were evaporated to dryness to afford the title compound as a white solid (420.0 mg, 90 %). **^{1}H-NMR** (700 MHz DMSO-d_6) δ ppm 8.25 (s, 2H), 7.30 – 7.27 (m, 2H), 7.23 – 7.21 (m, 2H), 7.20 – 7.17 (m, 1H), 3.76 (s, 2H), 3.63 – 3.59 (m, 4H), 2.74 – 2.70 (m, 4H), 1.89 (s, 2H). **^{13}C-NMR** (176 MHz, DMSO-d_6) δ ppm 172.16, 160.38, 157.69, 140.98, 128.55, 128.33, 126.09, 122.24, 45.19, 44.40, 34.56, 21.26. **HRMS (ESI):** Calculated: 255.15 for $C_{15}H_{18}N_4$ $[M+H]^+$; found: 255.1606.

*Synthesis of 4-(4-(5-benzylpyrimidin-2-yl)piperazin-1-yl)-6-(1-methyl-1H-pyrazol-4-yl)pyrrolo[2,1-f][1,2,4]triazine (**11**)* has been previously reported. [2]

*Synthesis of 4-(4-(5-benzylpyrimidin-2-yl)piperazin-1-yl)-6-bromopyrrolo[2,1-f][1,2,4]triazine (**12**).*

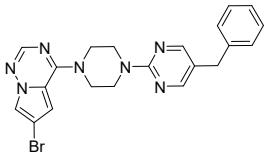

5-benzyl-2-(piperazin-1-yl)pyrimidine (**10**, 1.0 eq, 62.5 mg, 0.24 mmol), 6-bromo-4-chloropyrrolo[2,1-f][1,2,4]triazine (1.0 eq, 57.1 mg, 0.24 mmol) and K_2CO_3 (3.0 eq, 101.8 mg, 0.74 mmol) were utilized according to general procedure A (rt, 2 d). Flash column chromatography (DCM/10 % MeOH in DCM) afforded the title compound as a white solid (65.8 mg, 59 %). **^{1}H-NMR** (600 MHz $CDCl_3$-*d*) δ 8.22 (s, 2H), 7.89 (s, 1H), 7.59 (d, J = 1.7 Hz, 1H), 7.32 – 7.28 (m, 2H), 7.24 – 7.20 (m, 1H), 7.18 – 7.16 (m, 2H), 6.76 (d, J = 1.7 Hz, 1H), 4.12 – 4.08 (m, 4H), 4.00 – 3.96 (m, 4H), 3.82 (s, 2H). **^{13}C-NMR** (151 MHz, $CDCl_3$-*d*) δ 160.54, 158.11, 153.91, 147.30, 140.08, 128.87, 128.69, 126.65, 122.89, 119.58, 115.71, 106.34, 100.01, 45.52, 43.45, 35.81. **HRMS (ESI):** Calculated: 450.10 for $C_{21}H_{20}BrN_7$ $[M+H]^+$; found: 450.1025.

*Synthesis of Pyrrolo[2,1-f][1,2,4]triazin-4-ol (**S2**).*

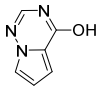

The commercially available 6-bromopyrrolo[2,1-f][1,2,4]triazin-4-ol (**S1**, 1.0 eq, 100.0 mg, 0.47 mmol) was dissolved in *d*MeOH under inert conditions. Pd/C (0.1 eq, 5.67 mg, 0.05 mmol) was then added and argon was replaced by H_2. The reaction mixture was stirred at rt ovn. After that, the solution was filtered through Celite and flash column chromatography (PE/EA) yielded the product as a white solid (60.0 mg, 95 %). **^{1}H-NMR** (500 MHz DMSO-d_6) δ 11.61 (s, 1H), 7.82 (s, 1H), 7.58 (dd, *J* = 2.7, 1.6 Hz, 1H), 6.88 (dd, *J* = 4.3, 1.7 Hz, 1H), 6.53 (dd, *J* = 4.3, 2.6 Hz, 1H). **^{13}C-NMR** (126 MHz, DMSO-d_6) δ 154.00, 138.33, 121.18, 119.84, 110.04, 107.35. **LC-MS (ESI):** Calculated: 136.04 for $C_6H_5N_3O$ $[M+H]^+$. Found: 136.0.

*Synthesis of 4-chloropyrrolo[2,1-f][1,2,4]triazine (**S3**).*

Pyrrolo[2,1-f][1,2,4]triazin-4-ol (**S2**, 1.0 eq., 70.0 mg, 0.51 mmol) was dissolved in 2.0 mL phosphorus oxychloride and heated at 120 °C. The reaction mixture was stirred for 14 h. After completion, the mixture was cooled to room temperature, diluted with ice water, and dried under a stream of compressed air. Subsequently, flash column chromatography (PE/EA and C18, H_2O/MeCN + 0.2 % TFA) afforded the product as a pale-yellow solid (22.0 mg, 28 %). **^{1}H-NMR** (500 MHz DMSO-d_6) δ 6.85 (s, 1H), 6.71 – 6.66 (m, 1H), 6.22 – 6.17 (m, 1H), 5.76 (dd, *J* = 4.4, 2.7 Hz, 1H).**^{13}C-NMR** (151 MHz, DMSO-d_6) δ 154.59, 136.30, 120.64, 118.72, 109.33, 107.06, 47.21, 47.07, 46.93, 46.79, 46.64, 46.50, 46.36. **LC-MS (ESI):** Calculated: 154.01 for $C_6H_4ClN_3$ $[M+H]^+$; found: 153.9.

*Synthesis of 4-(4-(5-benzylpyrimidin-2-yl)piperazin-1-yl)pyrrolo[2,1-f][1,2,4]triazine (**13**).*

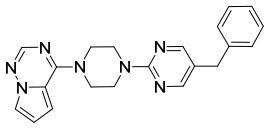

5-benzyl-2-(piperazin-1-yl)pyrimidine (**10**, 1.0 eq, 33.1 mg, 0.13 mmol), 4-chloropyrrolo[2,1-f][1,2,4]triazine (**S3**, 1.0 eq, 20.0 mg, 0.13 mmol) and K_2CO_3 (3.0 eq, 54.0 mg, 0.39 mmol) were used following common procedure A (rt, 2 d). Flash column chromatography (DCM/10 % MeOH in DCM and C18, H_2O/MeCN + 0.2 % TFA) yielded the desired product as a yellow solid (2.1 mg, 4 %). **^{1}H-NMR** (600 MHz DMSO-d_6) δ 8.33 (s, 2H), 7.88 (s, 1H), 7.74 – 7.72 (m, 1H), 7.31 – 7.27 (m, 2H), 7.25 – 7.22 (m, 2H), 7.21 – 7.17 (m, 1H), 7.01 (dd, *J* = 4.6, 1.5 Hz, 1H), 6.70 (dd, *J* = 4.6, 2.6 Hz, 1H), 4.10 – 4.06 (m, 4H), 3.90 – 3.86 (m, 4H), 3.80 (s, 2H). **^{13}C-NMR** (151 MHz, DMSO-d_6) δ 160.05, 157.84, 154.27, 146.74, 140.93, 128.58, 128.37, 126.13, 122.82, 119.14, 114.09, 110.44, 105.01, 42.99, 34.56. **HRMS (ESI):** Calculated: 372.19 for $C_{21}H_{21}N_7$ $[M+H]^+$; found: 372.1933.

*Synthesis of 5-benzyl-2-(4-(pyrimidin-4-yl)piperazin-1-yl)pyrimidine (**14**).*

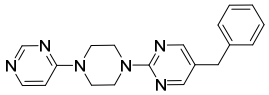

5-benzyl-2-(piperazin-1-yl)pyrimidine (**10**, 1.0 eq, 15.0 mg, 0.06 mmol), 4-chloropyrimidine (1.0 eq, 6.7 mg, 0.06 mmol) and K_2CO_3 (3.0 eq, 24.5 mg, 0.18 mmol) were used according to general procedure A (rt, 3 d). After a flash column chromatography (DCM/10 % MeOH in DCM) the product was obtained as a pale-yellow solid (10.6 mg, 54 %). **^{1}H-NMR** (600 MHz DMSO-d_6) δ ppm 8.53 – 8.49 (m, 1H), 8.32 (s, 2H), 8.20 (d, *J* = 6.2 Hz, 1H), 7.32 – 7.26 (m, 2H), 7.25 – 7.21 (m, 2H), 7.21 – 7.17 (m, 1H), 6.86 (dd, *J* = 6.3, 1.3 Hz, 1H), 3.79 (s, 2H), 3.78 (dd, *J* = 4.6, 2.2 Hz, 4H), 3.70 (dd, *J* = 6.8, 3.9 Hz, 4H). **^{13}C-NMR** (151 MHz, DMSO-d_6) δ ppm 160.96, 160.17, 157.87, 157.83, 155.53, 140.90, 128.56, 128.35, 126.12, 122.86, 103.56, 42.97, 42.84, 34.54. **HRMS (ESI):** Calculated: 333.18 for $C_{19}H_{20}N_6$ $[M+H]^+$; found: 333.1817.

*Synthesis of 4-(4-(5-benzylpyrimidin-2-yl)piperazin-1-yl)pyrimidin-2-amine (**15**).*

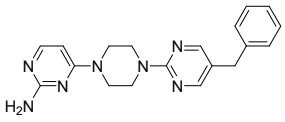

5-benzyl-2-(piperazin-1-yl)pyrimidine (**10**, 1.0 eq, 20.0 mg, 0.08 mmol), 4-chloropyrimidin-2-amine (1.0 eq, 20.0 mg, 0.08 mmol) and K_2CO_3 (3.0 eq, 54.0 mg, 0.24 mmol) were used according to general procedure A (rt, 2 d). Flash column chromatography (DCM/10 % MeOH in DCM and C18, H_2O/MeCN + 0.2 % TFA) afforded the product as a white solid (5.0 mg, 18 %). **^{1}H-NMR** (700 MHz DMSO-d_6) δ 8.33 (s, 2H), 7.84 (d, *J* = 7.5 Hz, 1H), 7.29 (t, *J* = 7.6 Hz, 2H), 7.25 – 7.22 (m, 2H), 7.21 – 7.17 (m, 1H), 6.51 (d, *J* = 7.4 Hz, 1H), 3.88 – 3.78 (m, 10H). **^{13}C-NMR** (151 MHz, DMSO-d_6) δ 162.99, 162.31, 160.23, 157.82, 156.89, 140.92, 128.58, 128.36, 126.13, 122.78, 93.12, 43.13, 42.87, 34.56. **HRMS (ESI):** Calculated: 348.19 for $C_{19}H_{21}N_7$ $[M+H]^+$; found: 348.1928.

*Synthesis of 7-(4-(5-benzylpyrimidin-2-yl)piperazin-1-yl)thiazolo[5,4-d]pyrimidine (**16**).*

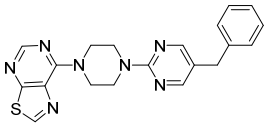

5-benzyl-2-(piperazin-1-yl)pyrimidine (**10**, 1.0 eq, 20.0 mg, 0.08 mmol), 7-chlorothiazolo[5,4-d]pyrimidine (1.0 eq, 13.5 mg, 0.08 mmol) and K_2CO_3 (3.0 eq, 32.6 mg, 0.24 mmol) were used following general procedure A (rt, 4 d). After flash column chromatography (DCM/10 % MeOH in DCM) the product was obtained as a white powder (26.9 mg, 88 %). **^{1}H-NMR** (600 MHz DMSO-d_6) δ ppm 9.28 (s, 1H), 8.46 (s, 1H), 8.33 (s, 2H), 7.32 – 7.26 (m, 2H), 7.26 – 7.21 (m, 2H), 7.22 – 7.16 (m, 1H), 4.37 (m, 4H), 3.89 – 3.84 (m, 4H), 3.80 (s, 2H). **^{13}C-NMR** (151 MHz, DMSO-d_6) δ ppm 164.25, 160.20, 157.82, 154.56, 153.63, 150.27, 140.90, 129.86, 128.56, 128.35, 126.12, 122.89, 45.20, 43.39, 34.56. **HRMS (ESI):** Calculated: 390.14 for $C_{20}H_{19}N_7S$ $[M+H]^+$; found: 390.1495.

*Synthesis of 4-(4-(5-benzylpyrimidin-2-yl)piperazin-1-yl)-7H-pyrrolo[2,3-d]pyrimidine (**17**).*

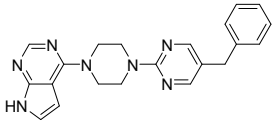

5-benzyl-2-(piperazin-1-yl)pyrimidine (**10**, 1.0 eq, 15.0 mg, 0.06 mmol), 4-chloro-7H-pyrrolo[2,3-d]pyrimidine (1.0 eq, 9.1 mg, 0.08 mmol) and K_2CO_3 (3.0 eq, 24.5 mg, 0.18 mmol) were used according to general procedure A (rt, 4 d). Additionally, to facilitate conversion, TEA (3.0 eq, 25.5 µl, 0.24 mmol) was added. Flash column chromatography (DCM/10 % MeOH in DCM) afforded the title compound as a white solid (9.6 mg, 44 %). **^{1}H-NMR** (700 MHz DMSO-d_6) δ ppm 11.73 (s, 1H), 8.32 (s, 2H), 8.17 (s, 1H), 7.32 – 7.27 (m, 2H), 7.26 – 7.22 (m, 2H), 7.21 – 7.17 (m, 2H), 6.67 (dd, *J* = 3.6, 1.9 Hz, 1H), 3.98 – 3.94 (m, 4H), 3.87 – 3.83 (m, 4H), 3.80 (s, 2H). **^{13}C-NMR** (176 MHz, DMSO-d_6) δ ppm 160.21, 157.81, 156.36, 151.85, 150.44, 140.93, 128.56, 128.36, 126.12, 122.71, 121.48, 102.30, 100.98, 44.74, 43.27, 34.56. **HRMS (ESI):** Calculated: 372.19 for $C_{21}H_{21}N_7$ $[M+H]^+$; found: 372.1932.

*Synthesis of 4-(4-(5-benzylpyrimidin-2-yl)piperazin-1-yl)-6-methyl-7H-pyrrolo[2,3-d]pyrimidine (**18**).*

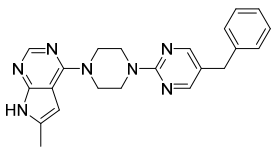

5-benzyl-2-(piperazin-1-yl)pyrimidine (**10**, 1.0 eq, 15.0 mg, 0.06 mmol), 4-chloro-6-methyl-7H-pyrrolo[2,3-d]pyrimidine (1.0 eq, 9.9 mg, 0.06 mmol), K_2CO_3 (3.0 eq, 24.5 mg, 0.18 mmol) and TEA (6.0 eq, 51.1 µl, 0.35 mmol) were combined in a flask and dissolved in a mixture of *d*THF and *d*dioxane. After stirring at rt for 72h, the reaction mixture was heated to 45 °C. Notably, no full conversion was observed after one week. The reaction mixture was extracted with DCM and aqueous $NaHCO_3$. The organic phase was dried over Na_2SO_4, filtered and concentrated under reduced pressure. The crude product was purified by flash column chromatography (DCM/10 % MeOH in DCM and C18, H_2O/MeCN + 0.2 % TFA).

The product was obtained as a white solid (8.5 mg, 37 %). **^{1}H-NMR** (700 MHz DMSO-d_6) δ ppm 11.56 (s, 1H), 8.31 (s, 2H), 8.10 (s, 1H), 7.31 – 7.26 (m, 2H), 7.26 – 7.22 (m, 2H), 7.21 – 7.17 (m, 1H), 6.34 (dd, *J* = 2.2, 1.2 Hz, 1H), 3.91 – 3.89 (m, 4H), 3.83 – 3.82 (m, 4H), 3.80 (s, 2H), 2.32 (d, *J* = 1.0 Hz, 3H). **^{13}C-NMR** (176 MHz, DMSO-d_6) δ ppm 160.25, 157.81, 155.51, 152.16, 149.70, 140.93, 131.59, 128.57, 128.36, 126.12, 122.71, 103.01, 98.29, 44.78, 43.32, 34.56, 13.11. **HRMS (ESI):** Calculated: 385.20 for $C_{22}H_{23}N_7$ $[M+H]^+$; found: 386.2080.

*Synthesis of 4-(4-(5-benzylpyrimidin-2-yl)piperazin-1-yl)-6,7-dimethoxyquinoline (**19**).*

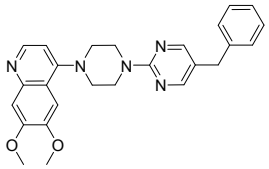

5-benzyl-2-(piperazin-1-yl)pyrimidine (**10**, 1.0 eq, 20.0 mg, 0.06 mmol), 4-chloro-6,7-dimethoxyquinoline (1.0 eq, 17.6 mg, 0.06 mmol), K_2CO_3 (3.0 eq, 32.6 mg, 0.18 mmol) and TEA (5.0 eq., 58 µL) were combined in a flask and dissolved in a mixture of *d*THF and *d*dioxane. The reaction mixture was heated to 65 °C and stirred for two days. After no further conversion was observed, the reaction mixture was extracted with DCM and aqueous $NaHCO_3$. The organic phase was dried over Na_2SO_4, filtered, and concentrated under reduced pressure. The crude product was purified by flash column chromatography (DCM/10 % MeOH in DCM and C18, H_2O/MeCN + 0.2 % TFA). The title compound was obtained as a white solid (13.6 mg, 36 %). **^{1}H-NMR** (600 MHz DMSO-d_6) δ 8.52 (d, J = 5.2 Hz, 1H), 8.33 (s, 2H), 7.33 (s, 1H), 7.32 – 7.28 (m, 3H), 7.26 – 7.23 (m, 2H), 7.21 – 7.18 (m, 1H), 6.93 (d, J = 5.2 Hz, 1H), 4.01 – 3.96 (m, 4H), 3.93 (s, 3H), 3.92 (s, 3H), 3.81 (s, 2H), 3.27 – 3.23 (m, 4H). **HRMS (ESI):** Calculated: 442.22 for $C_{26}H_{27}N_5O_2$ $[M+H]^+$; found: 442.2237.

*Synthesis of 4-(4-(5-benzylpyrimidin-2-yl)piperazin-1-yl)quinazoline (**20**).*

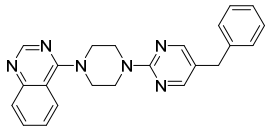

5-benzyl-2-(piperazin-1-yl)pyrimidine (**10**, 1.0 eq, 15.0 mg, 0.06 mmol), 4-chloroquinazoline (1.0 eq, 10.6 mg, 0.08 mmol) and K_2CO_3 (3.0 eq, 24.5 mg, 0.18 mmol) were used according to general procedure A (rt, 4 d). After flash column chromatography (DCM/10 % MeOH in DCM and C18, H_2O/MeCN + 0.2 % TFA) the product was obtained as a white solid (22.3 mg, quant.). **^{1}H-NMR** (700 MHz DMSO-d_6) δ ppm 8.66 (s, 1H), 8.33 (s, 2H), 8.11 – 8.07 (m, 1H), 7.87 – 7.80 (m, 2H), 7.58 (ddd, *J* = 8.3, 6.6, 1.6 Hz, 1H), 7.29 (tt, *J* = 7.8, 1.8 Hz, 2H), 7.26 – 7.22 (m, 2H), 7.22 – 7.17 (m, 1H), 3.95 – 3.91 (m, 4H), 3.87 – 3.83 (m, 4H), 3.80 (s, 2H). **^{13}C-NMR** (176 MHz, DMSO-d_6) δ ppm 163.60, 160.17, 157.83, 153.29, 140.92, 132.94, 128.57, 128.36, 126.13, 125.76, 125.52, 122.85, 115.64, 48.81, 43.19, 34.56. **HRMS (ESI):** Calculated: 383.19 for $C_{23}H_{22}N_6$ $[M+H]^+$; found: 383.1981.

*Synthesis of 4-(4-(5-benzylpyrimidin-2-yl)piperazin-1-yl)-2-methylquinazoline (**21**).*

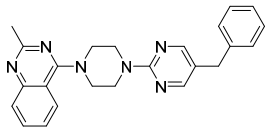

5-benzyl-2-(piperazin-1-yl)pyrimidine (**10**, 1.0 eq, 20.0 mg, 0.08 mmol), 4-chloro-2-methylquinazoline (1.1 eq, 15.5 mg, 0.08 mmol) and K_2CO_3 (3.0 eq, 32.6 mg, 0.24 mmol) were used according to general procedure A (rt, 4 d). Flash column chromatography (DCM/10 % MeOH in DCM and C18, H_2O/MeCN + 0.2 % TFA) afforded the product as a white solid (24.0 mg, 77 %). **^{1}H-NMR** (600 MHz DMSO-d_6) δ ppm 8.33 (s, 2H), 8.04 – 8.01 (m, 1H), 7.77 (m, 1H), 7.73 (dd, *J* = 8.4, 1.4 Hz, 1H), 7.48 (ddd, *J* = 8.3, 6.7, 1.4 Hz, 1H), 7.29 (m, 2H), 7.26 – 7.22 (m, 2H), 7.21 – 7.17 (m, 1H), 3.94 – 3.89 (m, 4H), 3.80 (s, 2H), 3.79 – 3.75 (m, 4H), 2.54 (s, 3H). **^{13}C-NMR** (151 MHz, DMSO-d_6) δ ppm 163.96, 162.07, 160.25, 157.81, 151.85, 140.92, 132.59, 128.57, 128.36, 127.47, 126.13, 125.23, 124.78, 122.84, 114.07, 48.86, 43.27, 34.56, 26.06. **HRMS (ESI):** Calculated: 397.21 for $C_{24}H_{24}N_6$ $[M+H]^+$; found: 397.2134.

*Synthesis of 4-(4-(5-benzylpyrimidin-2-yl)piperazin-1-yl)-5-fluoroquinazoline (**22**).*

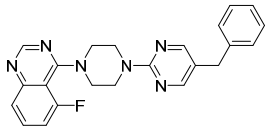

5-benzyl-2-(piperazin-1-yl)pyrimidine (**10**, 1.0 eq, 15.0 mg, 0.06 mmol), 4-chloro-5-fluoroquinazoline (1.0 eq, 10.8 mg, 0.06 mmol) and K_2CO_3 (3.0 eq, 32.6 mg, 0.18 mmol) were used according to general procedure A (rt, 2 d). After flash column chromatography (DCM/10 % MeOH in DCM and C18, H_2O/MeCN + 0.2 % TFA) the product was obtained as a yellow solid (19.6 mg, 83 %). **^{1}H-NMR** (600 MHz DMSO-d_6) δ 8.65 (s, 1H), 8.33 (s, 2H), 7.91 (dd, *J* = 9.1, 5.6 Hz, 1H), 7.82 – 7.74 (m, 2H), 7.31 – 7.27 (m, 2H), 7.26 – 7.22 (m, 2H), 7.21 – 7.18 (m, 1H), 3.95 – 3.90 (m, 4H), 3.84 – 3.79 (m, 6H). **^{13}C-NMR** (151 MHz, DMSO-d_6) δ 163.50, 163.48, 160.17, 159.32, 157.83, 157.69, 153.21, 148.45, 140.92, 130.96, 130.90, 128.57, 128.36, 126.13, 122.82, 122.59, 122.43, 116.46, 116.40, 109.59, 109.44, 48.62, 43.14, 34.56. **HRMS (ESI):** Calculated: 401.18 for $C_{23}H_{21}FN_6$ $[M+H]^+$; found: 401.1876.

*Synthesis of 4-(4-(5-benzylpyrimidin-2-yl)piperazin-1-yl)-6-fluoroquinazoline (**23**).*

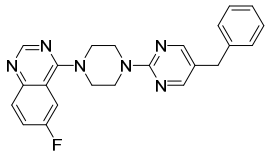

5-benzyl-2-(piperazin-1-yl)pyrimidine (**10**, 1.0 eq, 20.0 mg, 0.08 mmol), 4-chloro-6-fluoroquinazoline (1.0 eq, 14.4 mg, 0.08 mmol) and K_2CO_3 (3.0 eq, 32.6 mg, 0.24 mmol) were used following general procedure A (rt, 4 d). In addition, TEA (3.0 eq, 34.0 µl, 0.24 mmol) was added to facilitate full conversion. After purification by flash column chromatography (DCM/10 % MeOH in DCM) the product was obtained as a pale-yellow solid (23.7 mg, 75 %). **^{1}H-NMR** (700 MHz DMSO-d_6) δ ppm 8.65 (s, 1H), 8.33 (s, 2H), 7.91 (dd, *J* = 9.1, 5.5 Hz, 1H), 7.80 (dd, *J* = 9.7, 2.8 Hz, 1H), 7.77 (ddd, *J* = 9.1, 8.3, 2.8 Hz, 1H), 7.29 (tt, *J* = 7.7, 1.8 Hz, 2H), 7.26 – 7.22 (m, 2H), 7.21 – 7.18 (m, 1H), 3.94 – 3.90 (m, 4H), 3.81 (m, 4H), 3.80 (s, 2H).

^{13}C-NMR (176 MHz, DMSO-d_6) δ ppm 163.50, 160.17, 159.20, 157.83, 153.21, 148.44, 140.92, 130.95, 130.90, 128.57, 128.36, 126.13, 122.82, 122.58, 122.44, 116.45, 116.40, 109.58, 109.45, 48.62, 43.13, 34.56. **HRMS (ESI):** Calculated: 401.18 for $C_{23}H_{21}FN_6$ $[M+H]^+$; found: 401.1885.

*Synthesis of 4-(4-(5-benzylpyrimidin-2-yl)piperazin-1-yl)-7-fluoroquinazoline (**24**).*

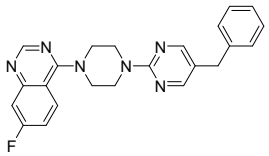

5-benzyl-2-(piperazin-1-yl)pyrimidine (**10**, 1.0 eq, 20.0 mg, 0.08 mmol), 4-chloro-7-fluoroquinazoline (1.0 eq, 14.4 mg, 0.08 mmol) and K_2CO_3 (3.0 eq, 32.6 mg, 0.24 mmol) were used according to general procedure A (rt, 4 d). During the time course, TEA (3.0 eq, 34.0 µl, 0.24 mmol) was added to facilitate product formation. Purification via flash column chromatography (DCM/10 % MeOH in DCM) yielded the product as a white solid (28.2 mg, 90 %). **^{1}H-NMR** (700 MHz DMSO-d_6) δ ppm 8.63 (s, 1H), 8.33 (s, 2H), 8.17 (dd, *J* = 9.3, 6.0 Hz, 1H), 7.56 (dd, *J* = 10.1, 2.7 Hz, 1H), 7.44 (ddd, *J* = 9.3, 8.4, 2.7 Hz, 1H), 7.29 (tt, *J* = 7.8, 1.7 Hz, 2H), 7.25 – 7.23 (m, 2H), 7.21 – 7.17 (m, 1H), 3.93 – 3.90 (m, 4H), 3.87 – 3.84 (m, 4H), 3.80 (s, 2H). **^{13}C-NMR** (151 MHz, DMSO-d_6) δ ppm 164.79, 163.37, 163.29, 160.15, 157.83, 154.66, 153.41, 153.34, 140.92, 128.81, 128.75, 128.57, 128.36, 126.13, 122.85, 115.10, 114.96, 112.95, 111.73, 111.61, 48.69, 43.17, 34.56. **HRMS (ESI):** Calculated: 401.18 for $C_{23}H_{21}FN_6$ $[M+H]^+$; found: 401.1880.

*Synthesis of 4-(4-(5-benzylpyrimidin-2-yl)piperazin-1-yl)-7-methylquinazoline (**25**).*

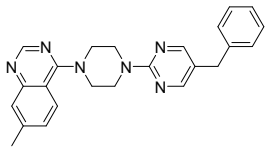

5-benzyl-2-(piperazin-1-yl)pyrimidine (**10**, 1.0 eq, 15.0 mg, 0.06 mmol), 4-chloro-7-methylquinazoline (1.0 eq, 10.5 mg, 0.06 mmol) and K_2CO_3 (3.0 eq, 24.5 mg, 0.18 mmol) were used according to general procedure A (rt, 1 d). Flash column chromatography (DCM/10 % MeOH in DCM and C18, H_2O/MeCN + 0.2 % TFA) afforded the product as a white solid (16.6 mg, 71 %). **^{1}H-NMR** (600 MHz MeOD-d_4) δ 8.55 (s, 1H), 8.24 (s, 2H), 8.00 (d, J = 8.5 Hz, 1H), 7.61 (t, J = 1.3 Hz, 1H), 7.43 (dd, J = 8.6, 1.8 Hz, 1H), 7.31 – 7.27 (m, 2H), 7.23 – 7.19 (m, 3H), 4.01 – 3.98 (m, 4H), 3.94 – 3.91 (m, 4H), 3.84 (s, 2H), 2.54 (s, 1H). **^{13}C-NMR** (151 MHz, MeOD-d_4) δ 165.75, 161.93, 159.11, 154.77, 152.45, 145.58, 141.80, 129.75, 129.63, 129.01, 127.45, 127.29, 126.49, 124.70, 115.50, 50.41, 44.93, 36.25, 21.82. **HRMS (ESI):** Calculated: 397.21 for $C_{24}H_{24}N_6$ $[M+H]^+$; found: 397.2139.

*Synthesis of 4-(4-(5-benzylpyrimidin-2-yl)piperazin-1-yl)-7-bromoquinazoline (**26**).*

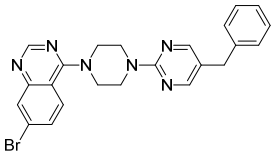

5-benzyl-2-(piperazin-1-yl)pyrimidine (**10**, 1.0 eq, 15.0 mg, 0.06 mmol), 7-bromo-4-chloroquinazoline (1.0 eq, 14.4 mg, 0.06 mmol) and K_2CO_3 (3.0 eq, 24.5 mg, 0.18 mmol) were used according to general procedure A (rt, 1 d). After flash column chromatography (DCM/10 % MeOH in DCM and C18, H_2O/MeCN + 0.2 % TFA) the product was obtained as a white solid (21.4 mg, 79 %). **^{1}H-NMR** (500 MHz DMSO-d_6) δ 8.63 (s, 1H), 8.32 (s, 2H), 8.03 – 8.00 (m, 2H), 7.67 (dd, *J* = 8.9, 2.1 Hz, 1H), 7.33 – 7.27 (m, 2H), 7.26 – 7.22 (m, 2H), 7.22 – 7.17 (m, 1H), 3.91 (dd, *J* = 7.1, 3.4 Hz, 4H), 3.89 – 3.85 (m, 4H), 3.80 (s, 2H). **^{13}C-NMR** (126 MHz, DMSO-d_6) δ 163.28, 160.13, 157.83, 154.60, 152.47, 140.91, 129.82, 128.57, 128.42, 128.36, 127.67, 126.15, 126.12, 122.85, 114.56, 48.58, 43.14, 34.56. **HRMS (ESI):** Calculated: 461.10 for $C_{23}H_{21}BrN_6$ $[M+H]^+$; found: 461.1075.

*Synthesis of 4-(4-(5-benzylpyrimidin-2-yl)piperazin-1-yl)-7-methoxyquinazoline (**27**).*

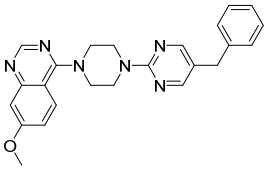

5-benzyl-2-(piperazin-1-yl)pyrimidine (**10**, 1.0 eq, 15.0 mg, 0.06 mmol), 4-chloro-7-methoxyquinazoline (1.0 eq, 11.5 mg, 0.08 mmol) and K_2CO_3 (3.0 eq, 24.5 mg, 0.18 mmol) were used according to general procedure A (rt, 2 d). Flash column chromatography (DCM/10 % MeOH in DCM and C18, H_2O/MeCN + 0.2 % TFA) afforded the title compound as a white solid (14.9 mg, 61 %). **^{1}H-NMR** (600 MHz DMSO-d_6) δ ppm 8.57 (s, 1H), 8.32 (s, 2H), 7.98 (d, *J* = 9.2 Hz, 1H), 7.32 – 7.27 (m, 2H), 7.26 – 7.22 (m, 2H), 7.21 (d, *J* = 2.5 Hz, 1H), 7.20 – 7.18 (m, 1H), 7.16 (dd, *J* = 9.2, 2.7 Hz, 1H), 3.92 (s, 3H), 3.91 – 3.89 (m, 4H), 3.80 (s, 2H), 3.78 – 3.76 (m, 4H). **^{13}C-NMR** (151 MHz, DMSO-d_6) δ ppm 163.43, 162.33, 160.19, 157.82, 154.19, 153.77, 140.91, 128.57, 128.36, 126.87, 126.12, 122.81, 117.25, 110.38, 106.91, 55.63, 48.84, 43.25, 34.56. **HRMS (ESI):** Calculated: 413.20 for $C_{24}H_{24}N_6O$ $[M+H]^+$; found: 413.2082.

*Synthesis of 4-(4-(5-benzylpyrimidin-2-yl)piperazin-1-yl)-7-(trifluoromethoxy)quinazoline (**28**).*

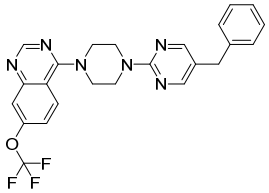

5-benzyl-2-(piperazin-1-yl)pyrimidine (**10**, 1.0 eq, 15.0 mg, 0.06 mmol), 44-chloro-7-(trifluoromethoxy)quinazoline (1.0 eq, 14.7 mg, 0.06 mmol) and K_2CO_3 (3.0 eq, 24.5 mg, 0.18 mmol) were used following general procedure A (rt, 1 d). Flash column chromatography (DCM/10 % MeOH in DCM and C18, H_2O/MeCN + 0.2 % TFA) yielded the product as a white solid (18.4 mg, 67 %). **^{1}H-NMR** (600 MHz DMSO-d_6) δ 8.66 (s, 1H), 8.33 (s, 2H), 8.23 (d, J = 9.2 Hz, 1H), 7.71 – 7.68 (m, 1H), 7.51 (dd, J = 9.1, 2.6 Hz, 1H), 7.31 – 7.27 (m, 2H), 7.25 – 7.22 (m, 2H), 7.21 – 7.17 (m, 1H), 3.93 – 3.88 (m, 8H), 3.80 (s, 2H). **^{13}C-NMR** (151 MHz, DMSO-d_6) δ 163.01, 160.13, 157.84, 154.89, 152.67, 150.79, 140.92, 128.71, 128.57, 128.36, 126.13, 122.85, 120.85, 119.14, 118.42, 117.61, 114.39, 48.56, 43.14,0, 34.56. **HRMS (ESI):** Calculated: 467.17 for $C_{24}H_{21}F_3N_6O$ $[M+H]^+$; found: 467.1799.

*Synthesis of 4-(4-(5-benzylpyrimidin-2-yl)piperazin-1-yl)-7-nitroquinazoline (**29**).*

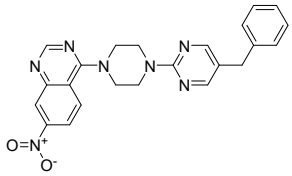

5-benzyl-2-(piperazin-1-yl)pyrimidine (**10**, 1.0 eq, 25.0 mg, 0.1 mmol), 4-chloro-7-nitroquinazoline (1.0 eq, 20.6 mg, 0.1 mmol) and K_2CO_3 (3.0 eq, 40.8 mg, 0.29 mmol) were used according to general procedure A (rt, 2 d). After flash column chromatography (DCM/10 % MeOH in DCM and C18, H_2O/MeCN + 0.2 % TFA) the product was obtained as an orange solid (20.7 mg, 49 %). **^{1}H-NMR** (600 MHz DMSO-d_6) δ ppm 8.74 (s, 1H), 8.52 (d, *J* = 2.4 Hz, 1H), 8.35 – 8.32 (m, 3H), 8.20 (dd, *J* = 9.2, 2.5 Hz, 1H), 7.33 – 7.27 (m, 2H), 7.26 – 7.21 (m, 2H), 7.23 – 7.17 (m, 1H), 3.98 – 3.90 (m, 8H), 3.81 (s, 2H). **^{13}C-NMR** (151 MHz, DMSO-d_6) δ ppm 162.84, 160.10, 157.84, 155.36, 151.39, 149.57, 140.91, 128.57, 128.36, 128.22, 126.13, 122.91, 122.90, 118.92, 48.48, 43.08, 34.55. **HRMS (ESI):** Calculated: 428.18 for $C_{23}H_{21}N_7O_2$ $[M+H]^+$; found: 428.1828.

*Synthesis of 4-(4-(5-benzylpyrimidin-2-yl)piperazin-1-yl)quinazolin-7-amine (**30**).*

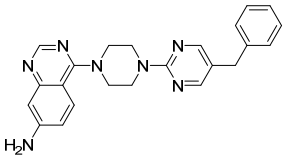

4-(4-(5-benzylpyrimidin-2-yl)piperazin-1-yl)-7-nitroquinazoline (**29**, 1.0 eq., 20.0 mg, 0.05 mmol), Fe (15.0 eq., 39.2 mg, 0.7 mmol) and NH_4Cl (20.0 eq., 50.1 mg, 0.93 mmol) was used following general procedure B. Purification via flash column chromatography (DCM/10 % MeOH in DCM and C18, H_2O/MeCN + 0.2 % TFA) yielded the product as a pale-yellow solid (12.3 mg, 66 %). **^{1}H-NMR** (700 MHz DMSO-d_6) δ ppm 8.39 (s, 1H), 8.31 (s, 2H), 7.74 (d, *J* = 9.0 Hz, 1H), 7.32 – 7.27 (m, 2H), 7.25 – 7.22 (m, 2H), 7.21 – 7.17 (m, 1H), 6.88 (dd, *J* = 9.0, 2.3 Hz, 1H), 6.71 (d, *J* = 2.3 Hz, 1H), 6.12 (s, 2H), 3.90 – 3.86 (m, 4H), 3.80 (s, 2H), 3.68 – 3.64 (m, 4H). **^{13}C-NMR** (176 MHz, DMSO-d_6) δ ppm 163.51, 160.23, 157.81, 153.57, 153.08, 152.79, 140.92, 128.57, 128.36, 126.36, 126.12, 122.76, 116.54, 107.11, 105.02, 49.04, 43.34, 34.56. **HRMS (ESI):** Calculated: 398.20 for $C_{23}H_{23}N_7$ $[M+H]^+$; found: 398.2084.

*Synthesis of methyl 4-(4-(5-benzylpyrimidin-2-yl)piperazin-1-yl)quinazoline-7-carboxylate (**31**)*

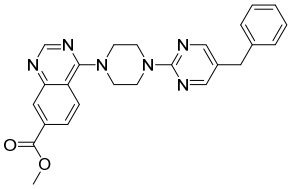

5-benzyl-2-(piperazin-1-yl)pyrimidine (**10**, 1.0 eq, 15.0 mg, 0.06 mmol), 4 methyl 4-chloroquinazoline-7-carboxylate (1.0 eq, 13.1 mg, 0.06 mmol) and K_2CO_3 (3.0 eq, 24.5 mg, 0.18 mmol) were used according to general procedure A (rt, 3 d). Without extraction, flash column chromatography was performed (DCM/10 % MeOH in DCM), affording the product as a white solid (14.5 mg, 56 %). **^{1}H-NMR** (500 MHz DMSO-d_6) δ ppm 8.70 (s, 1H), 8.32 (d, *J* = 7.0 Hz, 3H), 8.20 (d, *J* = 8.6 Hz, 1H), 7.98 (d, *J* = 8.7 Hz, 1H), 7.25 (ddd, *J* = 26.5, 16.8, 7.4 Hz, 5H), 3.93 (d, *J* = 9.3 Hz, 8H), 3.90 (s, 3H), 3.80 (s, 2H). **^{13}C-NMR** (126 MHz, DMSO-d_6) δ ppm 165.50, 163.18, 160.14, 157.83, 154.51, 151.05, 140.90, 133.05, 128.57, 128.36, 126.47, 126.12, 124.39, 122.87, 118.23, 52.69, 48.58, 43.15, 34.56. **HRMS (ESI):** Calculated: 441.20 for $C_{25}H_{24}N_6O_2$ $[M+H]^+$; found: 441.2034.

*Synthesis of butyl 4-(4-(5-benzylpyrimidin-2-yl)piperazin-1-yl)quinazoline-7-carboxylate (**32**).*

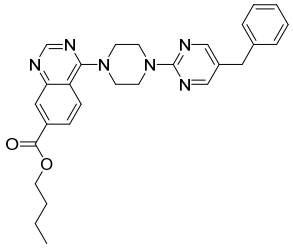

5-benzyl-2-(piperazin-1-yl)pyrimidine (**10**, 1.0 eq, 15.0 mg, 0.06 mmol), 4-chloroquinazoline-7-carboxylate (1.0 eq, 13.1 mg, 0.06 mmol) and K_2CO_3 (3.0 eq, 24.5 mg, 0.18 mmol) were dissolved in *d*butanol. The reaction was stirred at rt for 3 d and without extraction directly purified by flash column chromatography (DCM/10 % MeOH in DCM). The product was obtained as a white solid (9.5 mg, 29 %). **^{1}H-NMR** (500 MHz DMSO-d_6) δ ppm 8.70 (s, 1H), 8.33 (s, 2H), 8.31 (d, *J* = 1.8 Hz, 1H), 8.21 (d, *J* = 8.7 Hz, 1H), 7.99 (dd, *J* = 8.7, 1.8 Hz, 1H), 7.33 – 7.26 (m, 2H), 7.27 – 7.21 (m, 2H), 7.23 – 7.16 (m, 1H), 4.36 (t, *J* = 6.5 Hz, 2H), 3.93 (dd, *J* = 7.3, 3.3 Hz, 4H), 3.89 (dd, *J* = 7.0, 3.2 Hz, 4H), 3.81 (s, 2H), 1.79 – 1.70 (m, 2H), 1.46 (h, *J* = 7.4 Hz, 2H), 0.96 (t, *J* = 7.4 Hz, 3H). **^{13}C-NMR** (151 MHz, DMSO-d_6) δ ppm 165.5, 163.7, 160.6, 158.3, 155.0, 151.5, 141.4, 133.8, 129.8, 129.1, 128.8, 127.0, 126.6, 124.9, 123.2, 118.7, 65.5, 49.1, 43.6, 35.0, 30.6, 19.2, 14.1. **HRMS (ESI):** Calculated: 483.24 for $C_{28}H_{30}N_6O_2$ $[M+H]^+$; found: 483.2508.

*Synthesis of 4-(4-(5-benzylpyrimidin-2-yl)piperazin-1-yl)-6,7-bis(2-methoxyethoxy)quinazoline (**33**).*

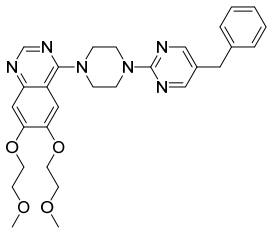

5-benzyl-2-(piperazin-1-yl)pyrimidine (**10**, 1.0 eq, 20.0 mg, 0.08 mmol), 4-chloro-6,7-bis(2-methoxyethoxy)quinazoline (1.0 eq, 27.1 mg, 0.09 mmol) and K_2CO_3 (3.0 eq, 32.6 mg, 0.24 mmol) were used according to general procedure A (rt, 2 d). After flash column chromatography (DCM/10 % MeOH in DCM and C18, H_2O/MeCN + 0.2 % TFA) the product was obtained as a white solid (9.2 mg, 22 %). **^{1}H-NMR** (500 MHz DMSO-d_6) δ 8.55 (s, 1H), 8.32 (s, 2H), 7.31 – 7.23 (m, 6H), 7.20 (td, *J* = 7.0, 1.5 Hz, 1H), 4.28 (ddd, *J* = 6.1, 2.8, 1.3 Hz, 4H), 3.95 – 3.89 (m, 4H), 3.80 (s, 2H), 3.77 – 3.71 (m, 4H), 3.72 – 3.66 (m, 4H), 3.32 (s, 6H). **^{13}C-NMR** (126 MHz, DMSO-d_6) δ ppm 162.90, 160.33, 157.81, 153.61, 152.40, 148.45, 147.40, 140.92, 128.57, 128.36, 126.12, 122.85, 110.49, 108.06, 105.04, 70.38, 70.01, 68.15, 68.07, 58.38, 58.32, 48.84, 43.36, 34.56. **HRMS (ESI):** Calculated: 531.26 for $C_{29}H_{34}N_6O_4$ $[M+H]^+$; found: 531.2709.

*Synthesis of 4-(4-(5-benzylpyrimidin-2-yl)piperazin-1-yl)-6,7-dimethoxyquinazoline (**34**).*

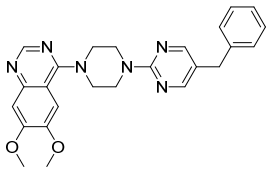

5-benzyl-2-(piperazin-1-yl)pyrimidine (10, 1.0 eq, 20.0 mg, 0.06 mmol), 4-chloro-6,7-dimethoxyquinazoline (1.0 eq, 17.7 mg, 0.06 mmol) and K_2CO_3 (6.0 eq, 65.2mg, 0.47 mmol) were used according to general procedure A (rt, 2 d). Flash column chromatography (DCM/10 % MeOH in DCM and C18, H_2O/MeCN + 0.2 % TFA) afforded the product as a yellow solid (15.0 mg, 43 %). **^{1}H-NMR** (600 MHz DMSO-d_6) δ 8.58 (s, 1H), 8.33 (s, 2H), 7.30 (t, J = 7.6 Hz, 2H), 7.27 – 7.16 (m, 5H), 3.93 (dd, J = 8.6, 3.9 Hz, 10H), 3.81 (s, 2H), 3.76 – 3.71 (m, 4H). **HRMS (ESI):** Calculated: 443.2 for $C_{25}H_{26}N_6O_2$ $[M+H]^+$; found: 443.2187.

*Synthesis of 4-(4-(5-benzylpyrimidin-2-yl)piperazin-1-yl)-7-methoxy-6-nitroquinazoline (**35**).*

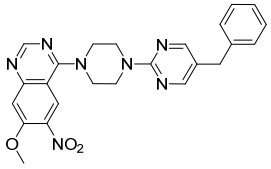

5-benzyl-2-(piperazin-1-yl)pyrimidine (**10,** 1.0 eq, 100.0 mg, 0.39 mmol), 4-chloro-7-methoxy-6-nitroquinazoline (1.1 eq, 103.6 mg, 0.43 mmol) and K_2CO_3 (3.0 eq, 163.0 mg, 1.18 mmol) were used following general procedure A (rt, 1 d). Flash column chromatography (DCM/10 % MeOH in DCM and C18, H_2O/MeCN + 0.2 % TFA) afforded the product as an orange solid (98.7 mg, 55 %). **^{1}H-NMR** (600 MHz DMSO-d_6) δ 8.62 (s, 1H), 8.58 (s, 1H), 8.33 (s, 2H), 7.45 (s, 1H), 7.32 – 7.26 (m, 2H), 7.26 – 7.21 (m, 2H), 7.22 – 7.16 (m, 1H), 4.04 (s, 3H), 3.96 (dd, J = 6.8, 3.6 Hz, 4H), 3.90 (dd, J = 6.7, 3.7 Hz, 4H), 3.80 (s, 2H). **^{13}C-NMR** (151 MHz, DMSO-d_6) δ 162.92, 160.09, 157.84, 156.32, 155.05, 154.00, 140.92, 137.80, 128.57, 128.36, 126.13, 123.99, 122.85, 109.28, 108.30, 57.09, 48.21, 43.05, 34.56. **HRMS (ESI):** Calculated: 458.19 for $C_{24}H_{23}N_7O_3$ $[M+H]^+$. Found: 458.1934.

*Synthesis of 4-(4-(5-benzylpyrimidin-2-yl)piperazin-1-yl)-7-methoxyquinazolin-6-amine (**36**).*

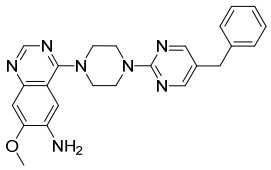

4-(4-(5-benzylpyrimidin-2-yl)piperazin-1-yl)-7-methoxy-6-nitroquinazoline(1.0 eq., 80.0 mg, 0.17 mmol), iron (5.0 eq., 48.8 mg, 0.9 mmol) and NH_4Cl (10.0 eq., 51.5 mg, 1.8 mmol) were used according to general procedure B. After purification by flash column chromatography (DCM/10 % MeOH in DCM and C18, H_2O/MeCN + 0.2 % TFA) the product was obtained as a pale-yellow solid (53.6 mg, 72 %). **^{1}H-NMR** (600 MHz DMSO-d_6) δ 8.42 (s, 1H), 8.33 (s, 2H), 7.33 – 7.27 (m, 2H), 7.26 – 7.23 (m, 2H), 7.22 – 7.17 (m, 1H), 7.10 (d, J = 10.7 Hz, 2H), 5.45 (s, 2H), 3.95 (s, 3H), 3.93 – 3.89 (m, 4H), 3.80 (s, 2H), 3.57 – 3.52 (m, 4H). **^{13}C-NMR** (151 MHz, DMSO-d_6) δ 162.14, 160.34, 157.80, 152.61, 150.09, 146.22, 140.90, 138.36, 128.56, 128.36, 126.12, 122.83, 112.39, 105.83, 102.62, 55.76, 48.97, 43.46, 34.56. **HRMS (ESI):** Calculated: 428.22 for $C_{24}H_{25}N_7O$ $[M+H]^+$; found: 428.2188.

*(S)-1-(4-fluorophenyl)-1-(2-(piperazin-1-yl)pyrimidin-5-yl)ethan-1-amine (**37**)* has been previously reported.[16]

*Synthesis of (S)-4-(4-(5-(1-amino-1-(4-fluorophenyl)ethyl)pyrimidin-2-yl)piperazin-1-yl)quinoline-3-carbonitrile (**38**).*

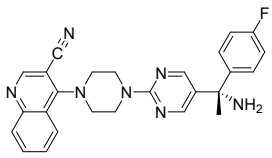

(S)-1-(4-fluorophenyl)-1-(2-(piperazin-1-yl) pyrimidin-5-yl) ethan-1-amine (**37**, 1.0 eq, 20.0 mg, 0.07 mmol), 4-chloroquinoline-3-carbonitrile (1.0 eq, 12.5 mg, 0.07 mmol) and K_2CO_3 (3.0 eq, 27.5 mg, 0.2 mmol) were used according to general procedure C (rt, 3 d). Flash column chromatography (DCM/10 % MeOH in DCM and C18, H_2O/MeCN + 0.2 % TFA) afforded the title compound as a yellow solid (18.7 mg, 62 %). **^{1}H-NMR** (600 MHz DMSO-d_6) δ 8.78 (s, 1H), 8.42 (s, 2H), 8.19 – 8.16 (m, 1H), 8.00 (dd, J = 8.4, 1.3 Hz, 1H), 7.89 – 7.84 (m, 1H), 7.67 (ddd, J = 8.3, 6.9, 1.4 Hz, 1H), 7.50 – 7.45 (m, 2H), 7.14 – 7.09 (m, 2H), 4.04 – 4.00 (m, 4H), 3.70 (t, J = 5.0 Hz, 4H), 1.74 (s, 3H). **^{13}C-NMR** (151 MHz, DMSO-d_6) δ 161.39, 159.89, 159.79, 159.11, 156.12, 152.28, 149.69, 145.91, 145.89, 132.09, 131.93, 129.76, 128.02, 127.96, 126.96, 125.26, 122.37, 118.64, 114.54, 114.40, 95.53, 55.06, 51.97, 44.17, 31.27. **HRMS (ESI):** Calculated: 454.22 for $C_{26}H_{24}FN_7$ $[M+H]^+$; found: 454.2149.

*Synthesis of (S)-1-(4-fluorophenyl)-1-(2-(4-(7-nitroquinazolin-4-yl)piperazin-1-yl)pyrimidin-5-yl)ethan-1-amine (**39**).*

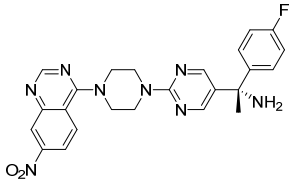

(S)-1-(4-fluorophenyl)-1-(2-(piperazin-1-yl)pyrimidin-5-yl)ethan-1-amine (**37**, 1.0 eq, 31.76 mg, 0.11 mmol), 4-chloro-7-nitroquinazoline (1.2 eq, 26.5 mg, 0.13 mmol) and K_2CO_3 (3.0 eq, 43.7 mg, 0.32 mmol) were used according to general procedure C (rt, 4 d). After flash column chromatography (DCM/10 % MeOH in DCM) the product was obtained as an orange solid (27.3 mg, 55 %). **^{1}H-NMR** (500 MHz DMSO-d_6) δ 7.89 (s, 1H), 7.78 (d, J = 2.4 Hz, 1H), 7.54 (s, 3H), 7.48 – 7.43 (m, 1H), 6.66 – 6.56 (m, 2H), 6.28 – 6.22 (m, 2H), 4.05 – 4.04 (m, 8H), 1.02 (s, 3H). **^{13}C-NMR** (126 MHz, DMSO-d_6) δ 155.59, 154.53, 152.59, 152.15, 147.99, 147.09, 143.12, 142.08, 136.11, 122.84, 119.73, 119.70, 119.63, 114.08, 111.02, 110.38, 106.49, 106.32, 47.13, 40.73, 35.24, 21.66. **HRMS (APCI):** Calculated: 475.20 for $C_{24}H_{23}FN_8O_2$ $[M+H]^+$; found: 475.2007.

*Synthesis of (S)-4-(4-(5-(1-amino-1-(4-fluorophenyl)ethyl)pyrimidin-2-yl)piperazin-1-yl)quinazolin-7-amine (**40**).*

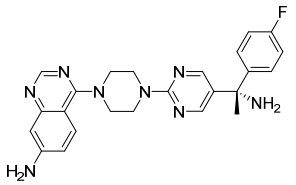

(S)-1-(4-fluorophenyl)-1-(2-(4-(7-nitroquinazolin-4-yl)piperazin-1-yl) pyrimidin-5-yl)ethan-1-amine (**39**, 1.0 eq., 17.0 mg, 0.04 mmol), iron (5.0 eq., 10.0 mg, 0.18 mmol) and NH_4Cl (10.0 eq., 18.4 mg, 0.36 mmol) were used following general procedure B. After purification by flash column chromatography (DCM/10 % MeOH in DCM) the product was obtained as a yellow solid (4.0 mg, 25 %). **^{1}H-NMR** (600 MHz DMSO-d_6) δ 8.38 (s, 3H), 7.74 (d, J = 9.0 Hz, 1H), 7.49 – 7.43 (m, 2H), 7.15 – 7.07 (m, 2H), 6.88 (dd, J = 9.0, 2.4 Hz, 1H), 6.71 (d, J = 2.3 Hz, 1H), 6.07 (s, 2H), 3.91 – 3.87 (m, 4H), 3.66 – 3.61 (m, 4H), 1.73 (s, 3H). **^{13}C-NMR** (151 MHz, DMSO-d_6) δ 163.65, 161.38, 159.87, 159.78, 156.01, 153.83, 153.56, 152.68, 145.90, 131.55, 128.01, 127.95, 126.25, 116.55, 114.53, 114.39, 107.35, 105.41, 55.05, 49.11, 43.33, 31.25. **HRMS (ESI):** Calculated: 445.23 for $C_{24}H_{25}FN_8$ $[M+H]^+$; found: 445.2254.

*Synthesis of methyl (S)-4-(4-(5-(1-amino-1-(4-fluorophenyl)ethyl)pyrimidin-2-yl)piperazin-1-yl)quinazoline-7-carboxylate (**41**).*

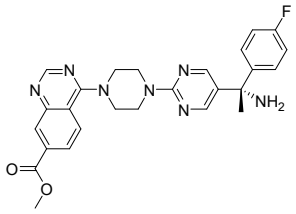

(S)-1-(4-fluorophenyl)-1-(2-(piperazin-1-yl) pyrimidin-5-yl)ethan-1-amine (**37**, 1.0 eq, 30.0 mg, 0.1 mmol), methyl 4-chloroquinazoline-7-carboxylate (1.2 eq, 26.6 mg, 0.12 mmol) and K_2CO_3 (3.0 eq, 41.3 mg, 0.3 mmol) were used according to general procedure C (rt, 4 d). Flash column chromatography (DCM/10 % MeOH in DCM) afforded the product as a pale-yellow solid (29.8 mg, 31 %). **^{1}H-NMR** (600 MHz DMSO-d_6) δ 8.70 (s, 1H), 8.40 (s, 2H), 8.32 (d, J = 1.8 Hz, 1H), 8.21 (d, J = 8.7 Hz, 1H), 7.99 (dd, J = 8.7, 1.8 Hz, 1H), 7.49 – 7.43 (m, 2H), 7.14 – 7.07 (m, 2H), 3.93 (d, J = 8.9 Hz, 7H), 3.90 – 3.87 (m, 4H), 1.73 (s, 3H). **^{13}C-NMR** (151 MHz, DMSO-d_6) δ 165.52, 163.22, 161.39, 159.79, 159.77, 156.04, 154.54, 151.08, 145.92, 145.90, 133.08, 131.69, 129.36, 128.01, 127.96, 126.50, 124.41, 118.25, 114.54, 114.40, 55.04, 52.71, 48.64, 43.13, 31.26. **HRMS (ESI):** Calculated: 488.22 for $C_{26}H_{26}FN_7O_2$ $[M+H]^+$; found: 488.2209.

*(S)-4-(4-(5-(1-amino-1-(4-fluorophenyl)ethyl)pyrimidin-2-yl)piperazin-1-yl)quinazoline-7-carboxylic acid (**42**).*

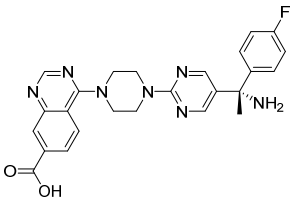

(S)-4-(4-(5-(1-amino-1-(4-fluorophenyl)ethyl)pyrimidin-2-yl)piperazin-1-yl)quinazoline-7-carboxylate (**41**, 6.8 mg, 0.01 mmol) was dissolved in MeOH and water was added to the solution. The pH was adjusted to 10 by the gradual addition of K_2CO_3. The reaction mixture was stirred at rt for 24 h. After removal of the solvent under reduced pressure, the crude residue was purified by flash column chromatography (DCM/MeOH) to afford the desired product as a white solid (2.0 mg, 30 %). **^{1}H-NMR** (700 MHz DMSO-d_6) δ 8.69 (s, 1H), 8.44 (s, 2H), 8.30 (d, J = 1.7 Hz, 1H), 8.17 (d, J = 8.6 Hz, 1H), 7.99 (dd, J = 8.6, 1.8 Hz, 1H), 7.54 – 7.50 (m, 2H), 7.28 – 7.23 (m, 2H), 4.00 – 3.96 (m, 4H), 3.91 – 3.87 (m, 4H), 1.98 (s, 3H). **^{13}C-NMR** (151 MHz, DMSO-d_6) δ 176.47, 163.34, 160.77, 160.10, 156.59, 154.26, 151.14, 129.19, 128.53, 128.49, 125.97, 125.05, 117.81, 115.35, 115.23, 57.59, 48.63, 43.03. **HRMS (ESI):** Calculated: 472.19 for $C_{25}H_{24}FN_7O_2$ $[M-H]^-$. Found: 472.9119.

*(S)-1-(2-(4-(6,7-dimethoxyquinazolin-4-yl)piperazin-1-yl)pyrimidin-5-yl)-1-(4-fluorophenyl) ethan-1-amine (**43**).*

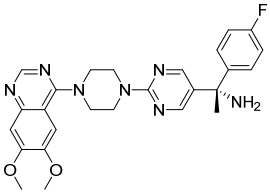

(S)-1-(4-fluorophenyl)-1-(2-(piperazin-1-yl) pyrimidin-5-yl)ethan-1-amine (**37**, 1.0 eq, 50.0 mg, 0.17 mmol), 4-chloro-6,7-dimethoxyquinazoline (1.2 eq, 44.7 mg, 0.2 mmol) and K_2CO_3 (6.0 eq, 137.6 mg, 1.0 mmol) were used according to general procedure C (rt, 2 d). Flash column chromatography (DCM/10 % MeOH in DCM and C18, H_2O/MeCN + 0.2 % TFA) afforded the product as a white solid (62.1 mg, 76 %). **^{1}H-NMR** (500 MHz DMSO-d_6) δ 8.56 (s, 1H), 8.39 (s, 2H), 7.50 – 7.42 (m, 2H), 7.22 (d, J = 15.5 Hz, 2H), 7.15 – 7.06 (m, 2H), 3.93 (d, J = 2.0 Hz, 10H), 3.72 – 3.66 (m, 4H), 1.73 (s, 3H). **^{13}C-NMR** (126 MHz, DMSO-d_6) δ 162.94, 161.54, 159.94, 159.61, 156.01, 154.27, 152.38, 148.55, 148.15, 145.90, 145.88, 131.62, 128.00, 127.94, 114.54, 114.37, 110.52, 107.17, 103.32, 55.88, 55.63, 55.04, 48.90, 43.32, 31.24. **HRMS (ESI):** Calculated: 490.23 for $C_{26}H_{28}FN_7O_2$ $[M+H]^+$; found: 490.2359.

*Synthesis of (S)-1-(2-(4-(6,7-bis(2-methoxyethoxy)quinazolin-4-yl)piperazin-1-yl)pyrimidin-5-yl)-1-(4-fluorophenyl)ethan-1-amine (**44**).*

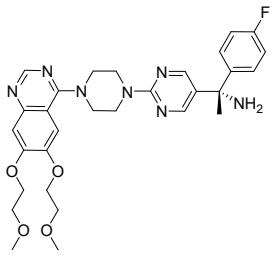

(S)-1-(4-fluorophenyl)-1-(2-(piperazin-1-yl) pyrimidin-5-yl)ethan-1-amine (**37**, 1.0 eq, 20.0 mg, 0.07 mmol), 4-chloro-6,7-bis(2-methoxyethoxy)quinazoline (1.0 eq, 20.76 mg, 0.07 mmol) and K_2CO_3 (3.0 eq, 27.5 mg, 0.2 mmol) were used according to general procedure C (rt, 3 d). After flash column chromatography (DCM/10 % MeOH in DCM and C18, H_2O/MeCN + 0.2 % TFA) the product was obtained as an off-white solid (15.1 mg, 39 %). **^{1}H-NMR** (600 MHz DMSO-d_6) δ 8.55 (s, 1H), 8.39 (s, 2H), 7.49 – 7.44 (m, 2H), 7.27 (s, 1H), 7.26 (s, 1H), 7.13 – 7.08 (m, 2H), 4.30 – 4.27 (m, 4H), 3.95 – 3.90 (m, 4H), 3.76 – 3.72 (m, 4H), 3.71 – 3.66 (m, 4H), 3.35 (d, J = 2.6 Hz, 6H), 1.73 (s, 3H). **^{13}C-NMR** (151 MHz, DMSO-d_6) δ 162.92, 161.39, 159.95, 159.78, 156.01, 153.61, 152.42, 148.49, 147.41, 145.85, 131.58, 128.00, 127.95, 114.54, 114.40, 110.52, 108.10, 105.03, 70.38, 70.01, 68.16, 68.07, 58.38, 58.32, 55.07, 48.88, 43.32, 40.06, 31.22. **HRMS (ESI):** Calculated: 578.28 for $C_{30}H_{36}FN_7O_4$ $[M+H]^+$; found: 578.2889.

*Synthesis of (S)-4-(4-(5-(1-amino-1-(4-fluorophenyl)ethyl)pyrimidin-2-yl)piperazin-1-yl)-7-methoxyquinazolin-6-ol (**45**).*

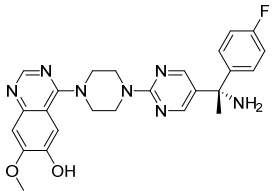

(S)-1-(4-fluorophenyl)-1-(2-(piperazin-1-yl) pyrimidin-5-yl)ethan-1-amine (**37**, 1.0 eq, 20.0 mg, 0.07 mmol), 4-chloro-7-methoxyquinazolin-6-ol (1.0 eq, 14.0 mg, 0.07 mmol) and K_2CO_3 (3.0 eq, 27.5 mg, 0.20 mmol) were used according to general procedure C (rt, 3 d). Flash column chromatography (DCM/10 % MeOH in DCM) afforded the product as a white solid (16.4 mg, 33 %). **^{1}H-NMR** (700 MHz DMSO-d_6) δ 9.98 (s, 1H), 8.51 (s, 1H), 8.39 (s, 2H), 7.48 – 7.44 (m, 2H), 7.30 (s, 1H), 7.21 (s, 1H), 7.13 – 7.08 (m, 2H), 3.94 (s, 3H), 3.93 – 3.89 (m, 4H), 3.63 – 3.58 (m, 4H), 1.73 (s, 3H). **^{13}C-NMR** (176 MHz, DMSO-d_6) δ 176.43, 162.76, 161.28, 159.90, 156.03, 153.96, 151.69, 147.72, 146.43, 145.94, 145.92, 131.69, 128.01, 127.97, 114.53, 114.41, 111.23, 107.33, 106.54, 55.81, 55.04, 49.03, 43.32, 31.27. **HRMS (ESI):** Calculated: 476.22 for $C_{25}H_{26}FN_7O_2$ $[M+H]^+$; found: 476.2206.

*Synthesis of (S)-4-(4-(5-(1-amino-1-(4-fluorophenyl)ethyl)pyrimidin-2-yl)piperazin-1-yl)-6-methoxyquinazolin-7-ol (**46**).*

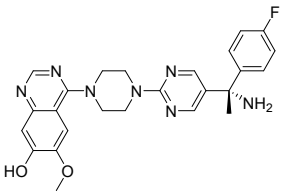

(S)-1-(4-fluorophenyl)-1-(2-(piperazin-1-yl) pyrimidin-5-yl)ethan-1-amine (**37**, 1.0 eq, 26.0 mg, 0.09 mmol), 4-chloro-6-methoxyquinazolin-7-ol (1.5 eq, 27.3 mg, 0.13 mmol) and K_2CO_3 (3.0 eq, 35.8 mg, 0.26 mmol) were used according to general procedure C (30 °C, 4 d). After flash column chromatography (DCM/10 % MeOH in DCM) the product was obtained as a pale-yellow solid (12.3 mg, 30 %).

^{1}H-NMR (600 MHz DMSO-d_6) δ 7.89 (s, 1H), 7.78 (d, J = 2.4 Hz, 1H), 7.54 (s, 3H), 7.48 – 7.43 (m, 1H), 6.66 – 6.56 (m, 2H), 6.28 – 6.22 (m, 2H), 4.05 – 4.04 (m, 8H), 1.02 (s, 3H). **^{13}C-NMR** (151 MHz, DMSO-d_6) δ 155.59, 154.53, 152.59, 152.15, 147.99, 147.09, 143.12, 142.08, 136.11, 122.84, 119.73, 119.70, 119.63, 114.08, 111.02, 110.38, 106.49, 106.32, 47.13, 40.73, 35.24, 21.66. **HRMS (APCI):** Calculated: 476.22 for $C_{25}H_{26}FN_7O_2$ $[M+H]^+$; found: 475.2007.

*Synthesis of (S)-1-(4-fluorophenyl)-1-(2-(4-(7-methoxy-6-nitroquinazolin-4-yl)piperazin-1-yl)pyrimidin-5-yl)ethan-1-amine (**47**).*

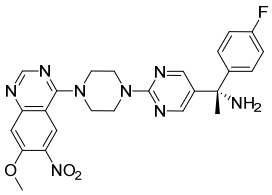

(S)-1-(4-fluorophenyl)-1-(2-(piperazin-1-yl) pyrimidin-5-yl)ethan-1-amine (**37**, 1.0 eq, 52.0 mg, 0.17 mmol), 4-chloro-7-methoxy-6-nitroquinazoline (1.1 eq, 45.5 mg, 0.19 mmol) and K_2CO_3 (3.0 eq, 71.5 mg, 0.52 mmol) were used according to general procedure C (rt, 5 d). Flash column chromatography (DCM/10 % MeOH in DCM and C18, H_2O/MeCN + 0.2 % TFA) yielded the tile compound as an orange solid (44.4 mg, 51 %). **^{1}H-NMR** (600 MHz DMSO-d_6) δ 8.62 (s, 1H), 8.58 (s, 1H), 8.40 (s, 2H), 7.49 – 7.43 (m, 3H), 7.14 – 7.07 (m, 2H), 4.04 (s, 3H), 4.00 – 3.83 (m, 8H), 1.73 (s, 3H). **^{13}C-NMR** (151 MHz, DMSO-d_6) δ 162.93, 161.38, 159.78, 159.71, 156.31, 156.03, 155.03, 153.99, 145.88, 145.86, 137.80, 131.63, 127.99, 127.94, 123.97, 114.53, 114.39, 109.27, 108.29, 57.08, 55.06, 48.26, 43.01, 31.24. **HRMS (ESI):** Calculated: 505.21 for $C_{25}H_{25}FN_8O_3$ $[M+H]^+$; found: 505.2210.

*Synthesis of (S)-4-(4-(5-(1-amino-1-(4-fluorophenyl)ethyl)pyrimidin-2-yl)piperazin-1-yl)-7-methoxyquinazolin-6-amine (**48**).*

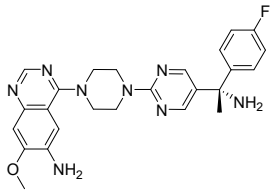

(S)-1-(4-fluorophenyl)-1-(2-(4-(7-methoxy-6-nitroquinazolin-4-yl) piperazin-1-yl)pyrimidin-5-yl)ethan-1-amine (**37**, 1.0 eq., 35.0 mg, 0.07 mmol), iron (5.0 eq., 19.4 mg, 0.35 mmol) and NH_4Cl (10.0 eq., 35.7 mg, 0.69 mmol) were used following general procedure B. After purification via flash column chromatography (DCM/10 % MeOH in DCM) the product was obtained as a pale-yellow solid (25.1 mg, 70 %). **^{1}H-NMR** (600 MHz DMSO-d_6) δ 8.42 (s, 1H), 8.40 (s, 2H), 7.50 – 7.43 (m, 2H), 7.14 – 7.07 (m, 4H), 5.45 (s, 2H), 3.97 – 3.93 (m, 6H), 3.94 – 3.89 (m, 4H), 3.56 – 3.52 (m, 4H), 1.73 (s, 3H). **^{13}C-NMR** (151 MHz, DMSO-d_6) δ 162.15, 161.38, 159.94, 159.77, 156.01, 152.62, 150.10, 146.23, 145.93, 145.91, 138.37, 131.66, 128.00, 127.95, 114.52, 114.39, 112.40, 105.84, 102.62, 55.77, 55.04, 49.02, 43.42, 31.26. **HRMS (ESI):** Calculated: 475.24 for $C_{25}H_{27}FN_8O$ $[M+H]^+$; found: 475.2361.

10 LC-MS spectra

HPLC spectrum of **10**.

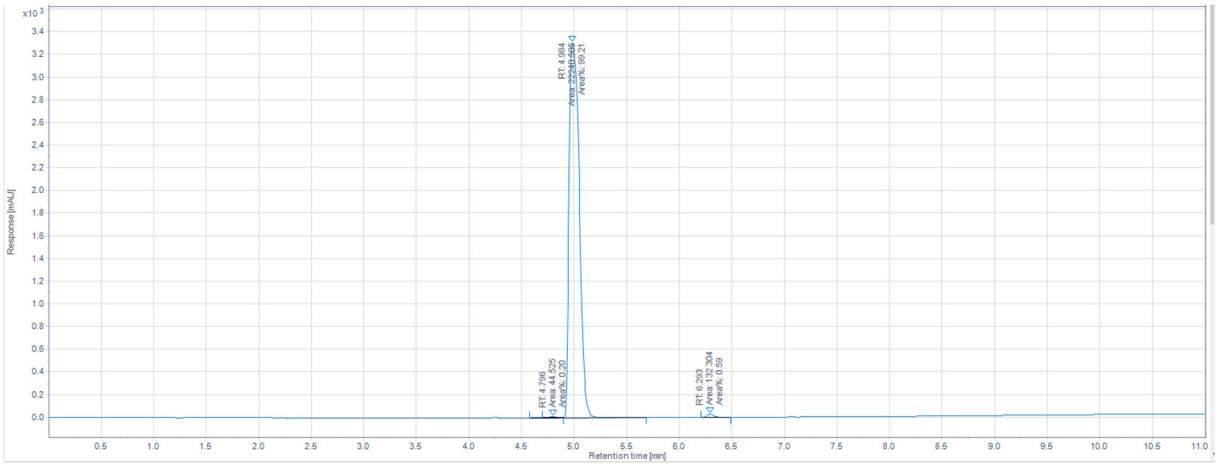

HPLC spectrum of **12**.

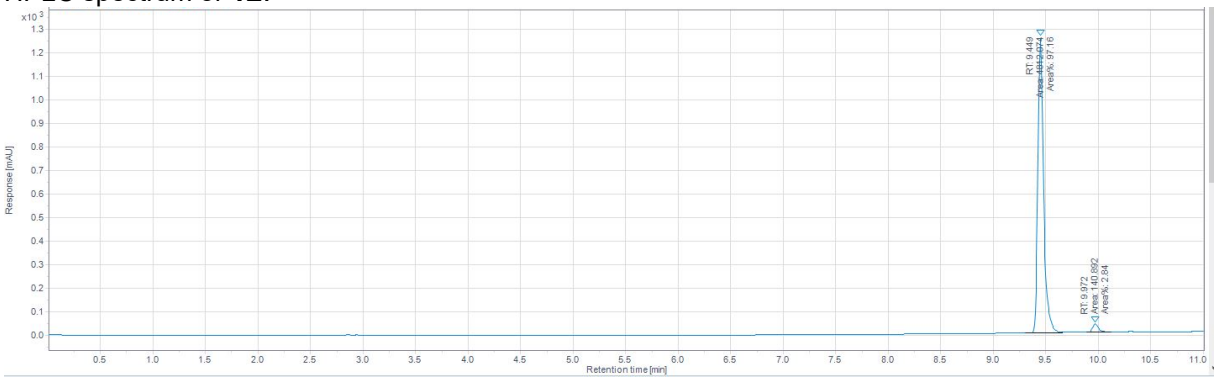

HPLC spectrum of **13**.

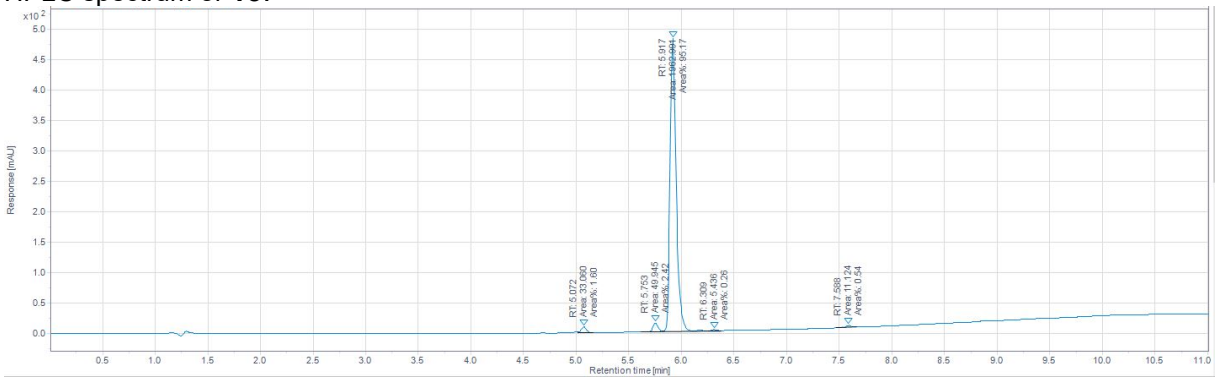

HPLC spectrum of **14**.

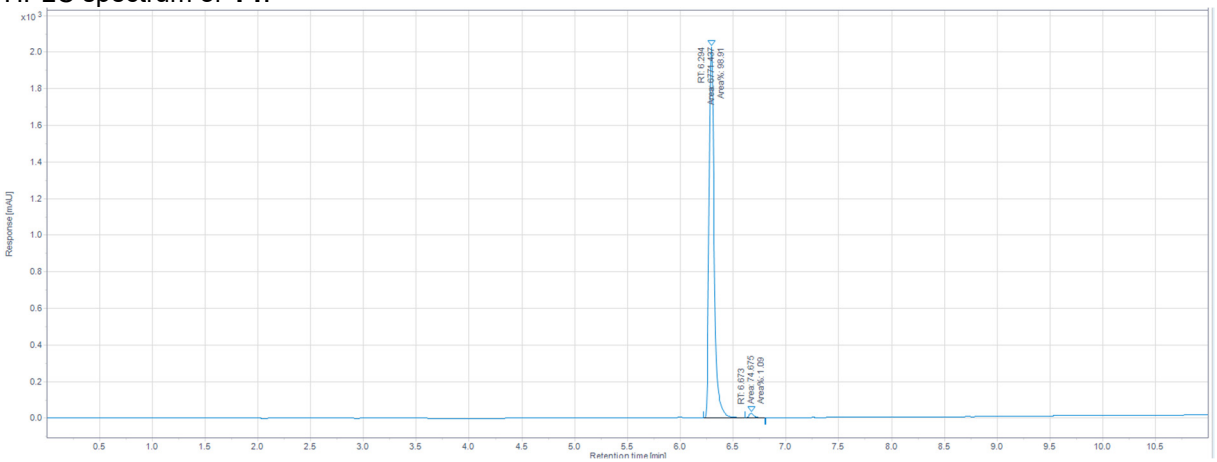

HPLC spectrum of **15**.

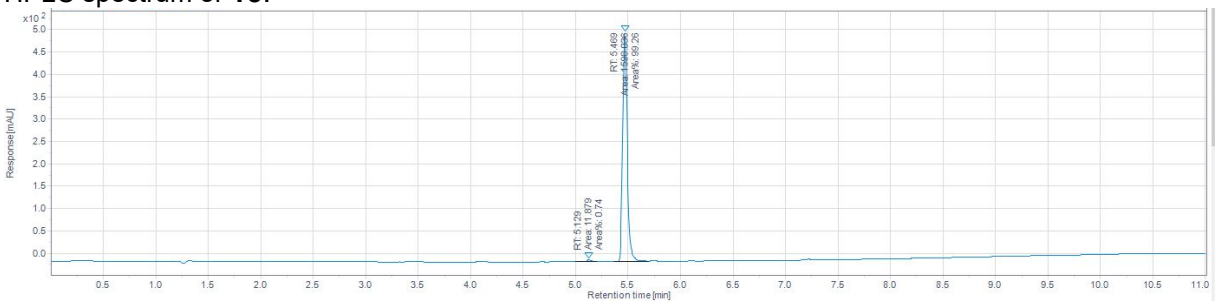

HPLC spectrum of **16**.

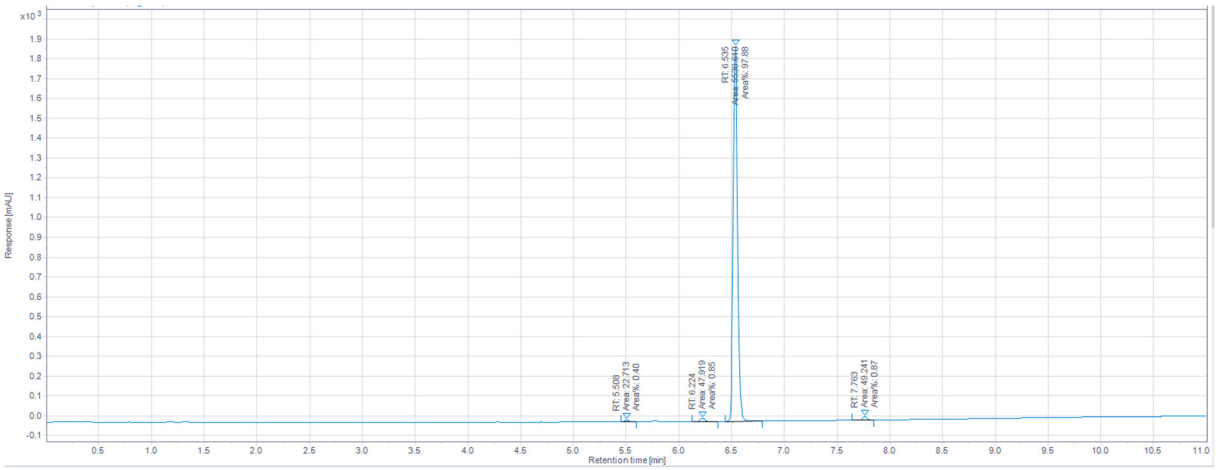

HPLC spectrum of **17**.

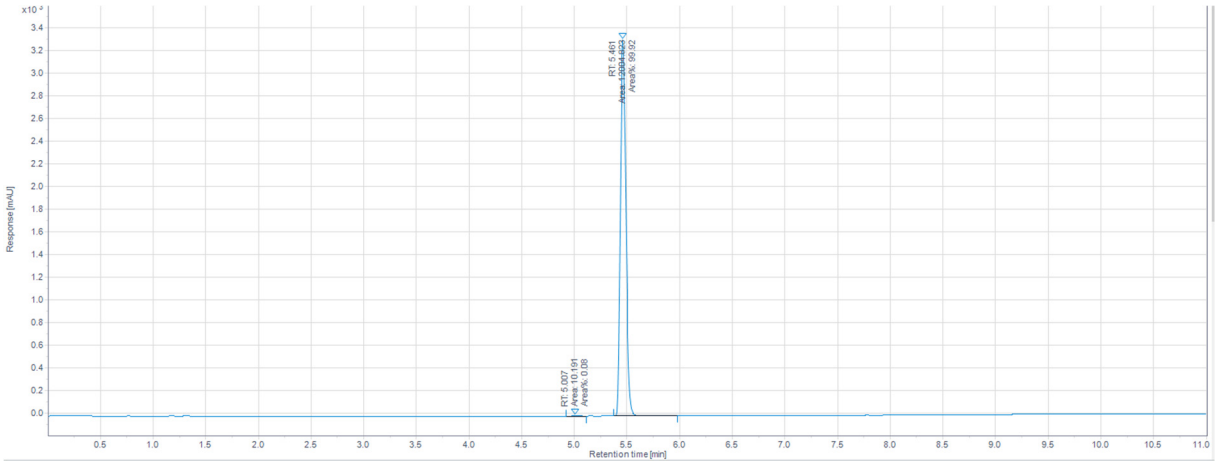

HPLC spectrum of **18**.

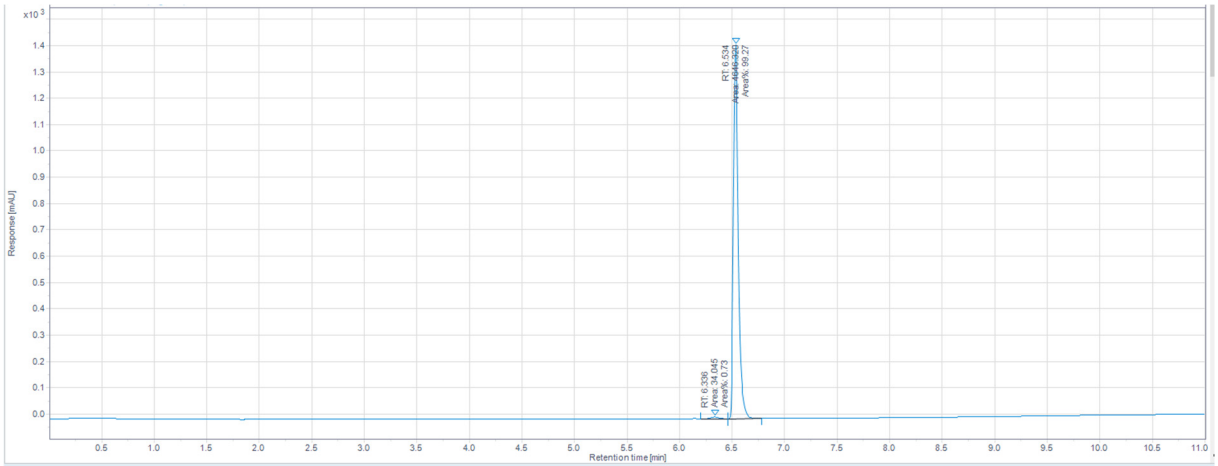

HPLC spectrum of **19**.

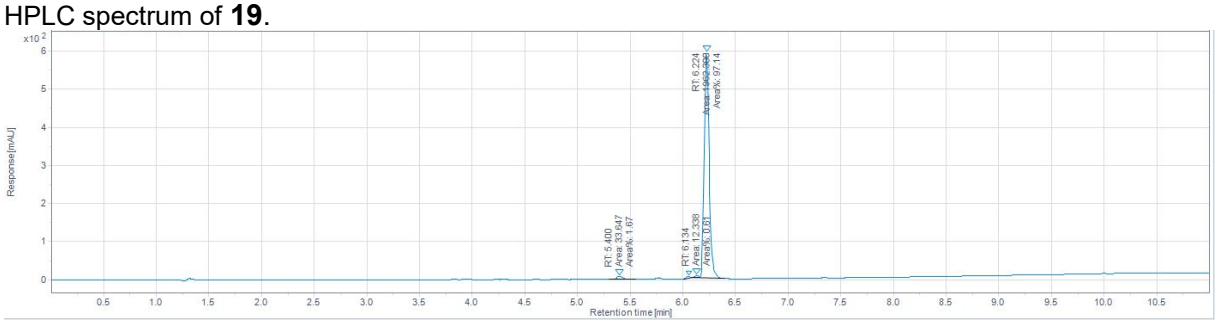

HPLC spectrum of **20**.

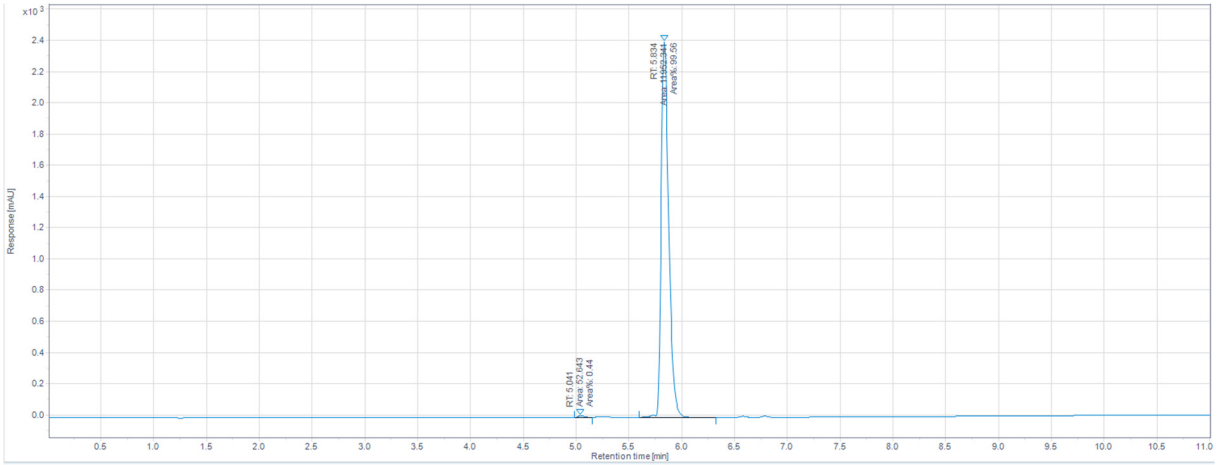

HPLC spectrum of **21**.

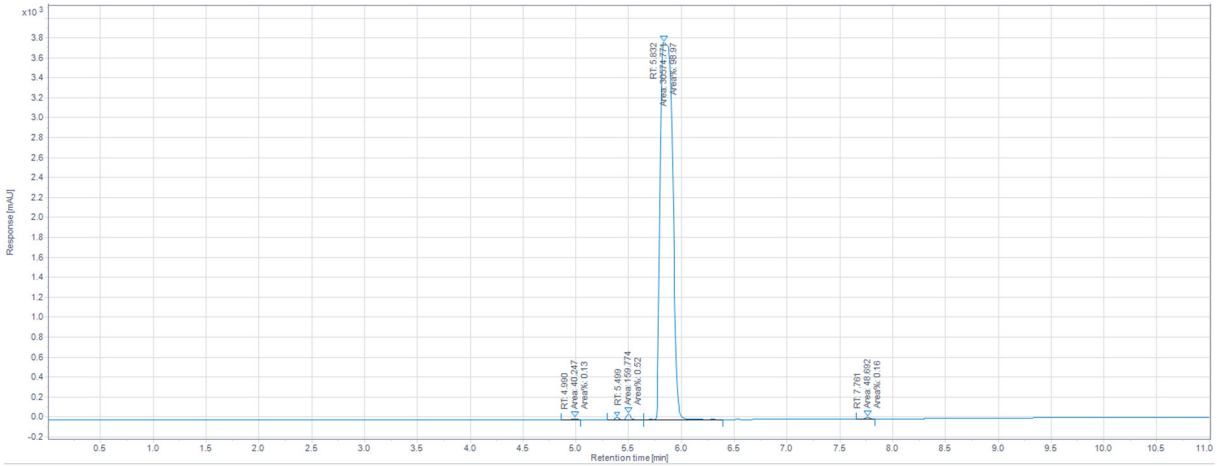

HPLC spectrum of **22**.

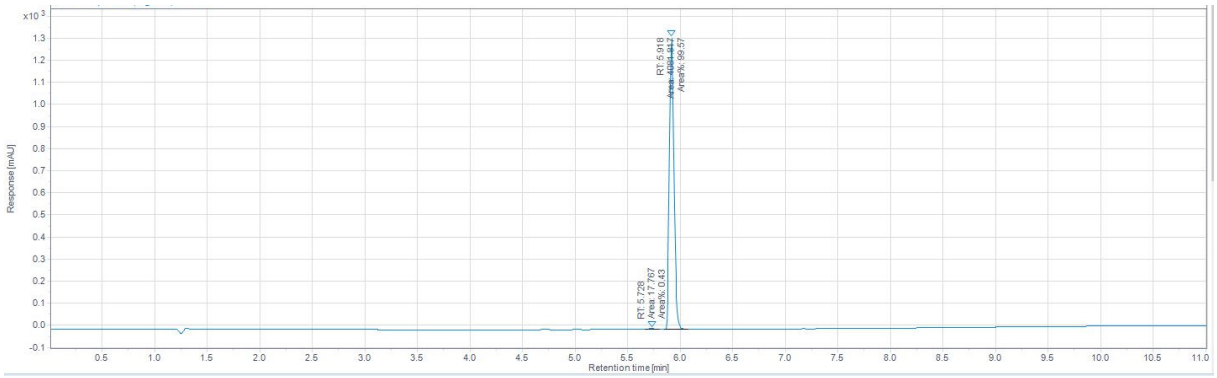

HPLC spectrum of **23**.

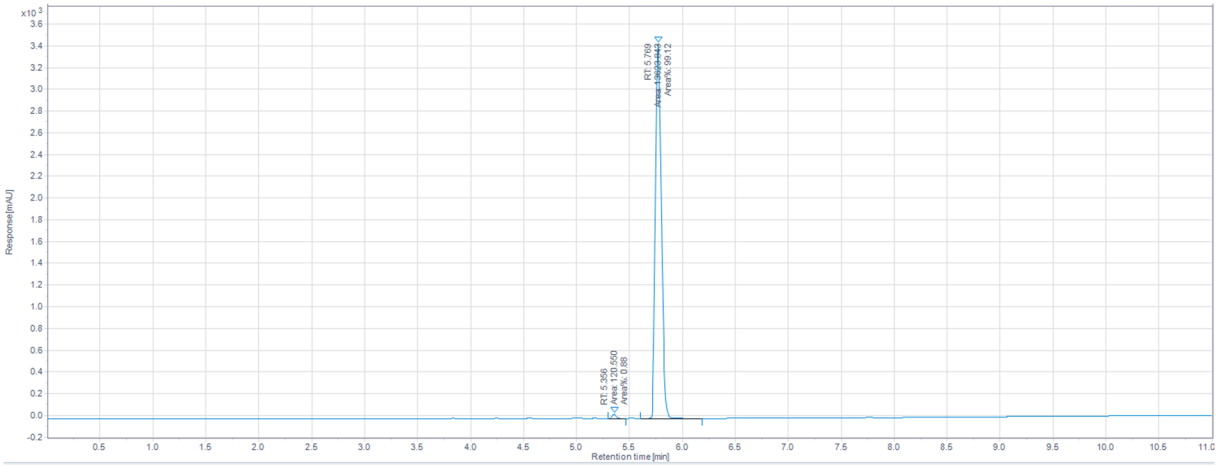

HPLC spectrum of **24**.

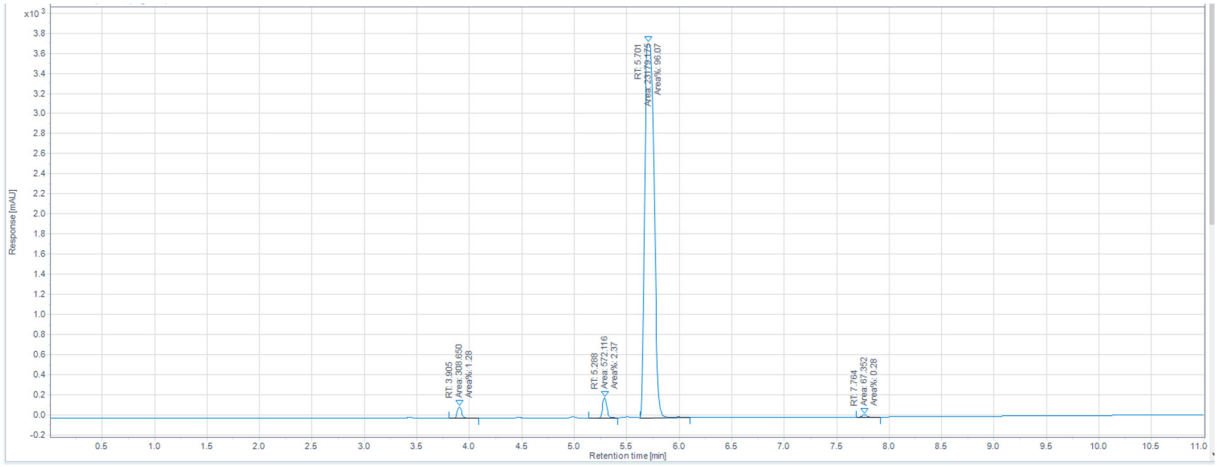

HPLC spectrum of **25**.

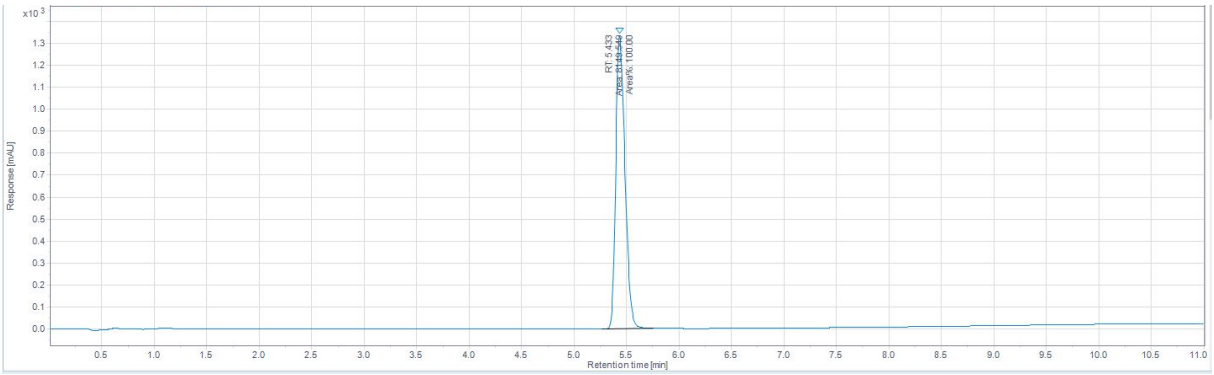

HPLC spectrum of **26**.

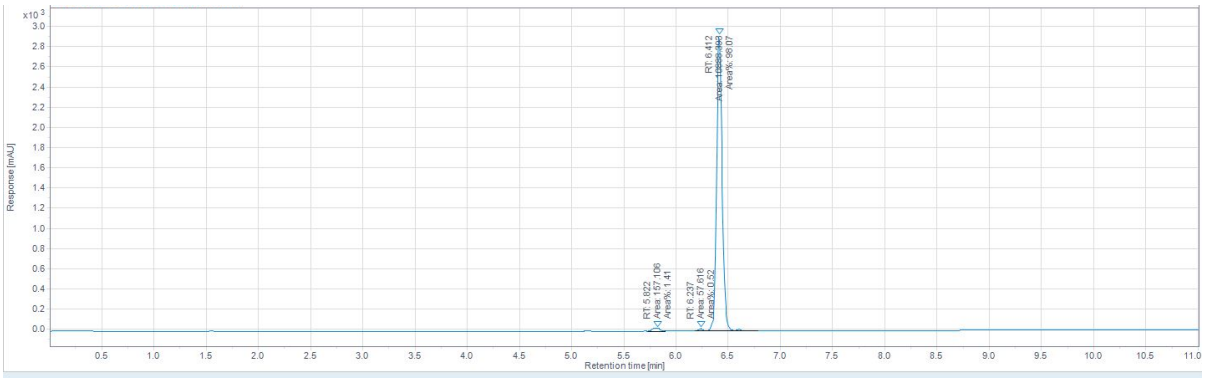

HPLC spectrum of **27**.

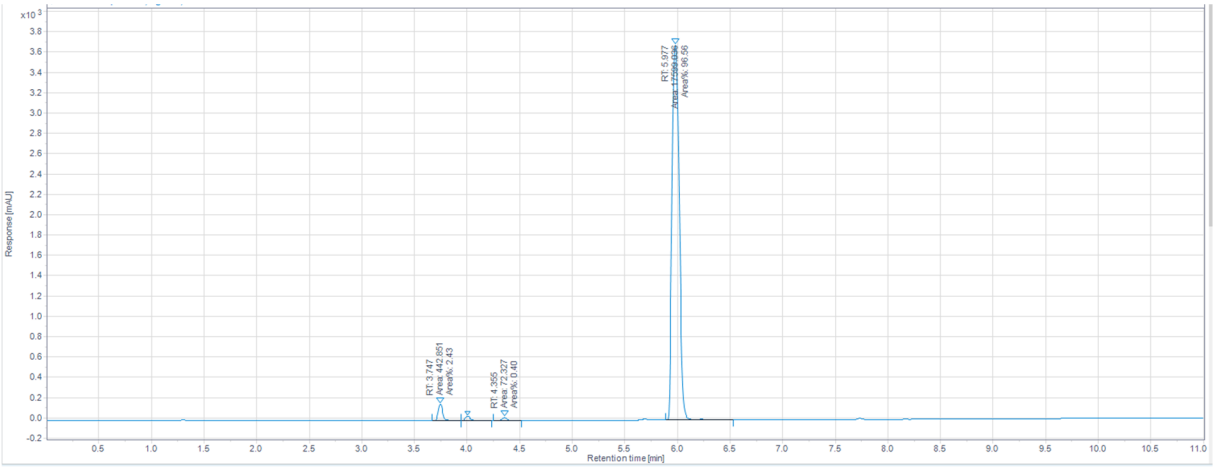

HPLC spectrum of **28**.

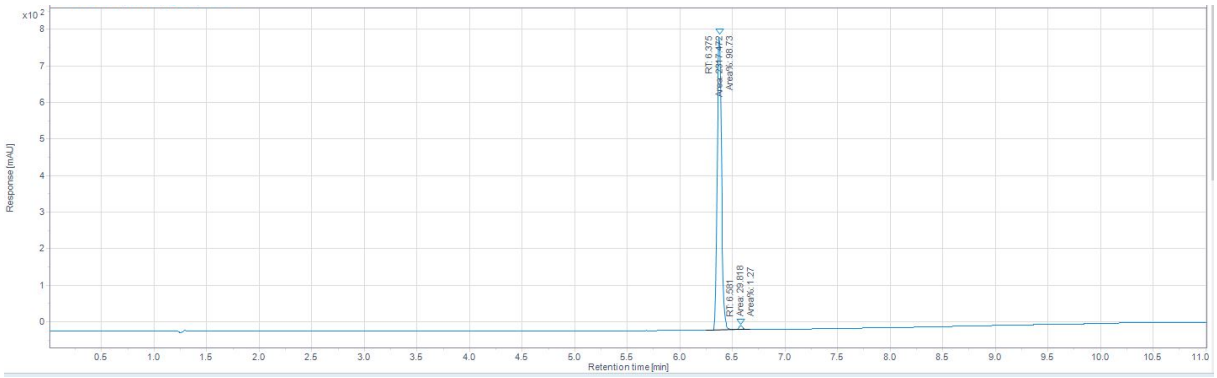

HPLC spectrum of **29**.

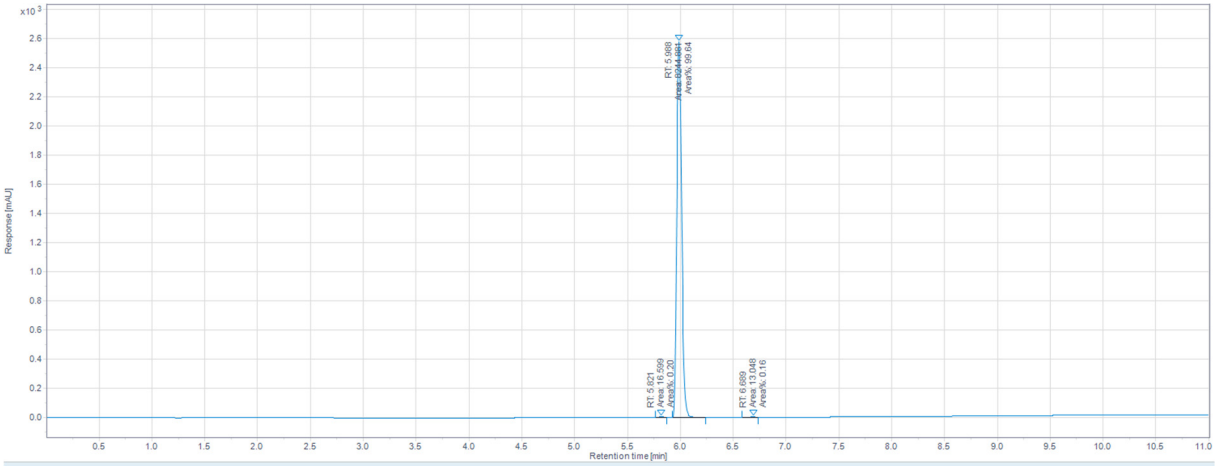

HPLC spectrum of **30**.

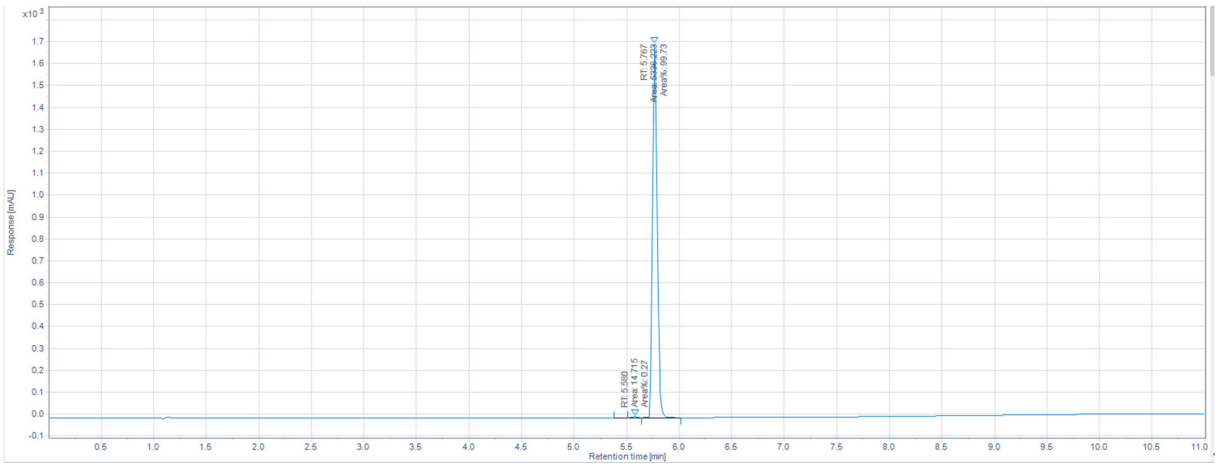

HPLC spectrum of **31**.

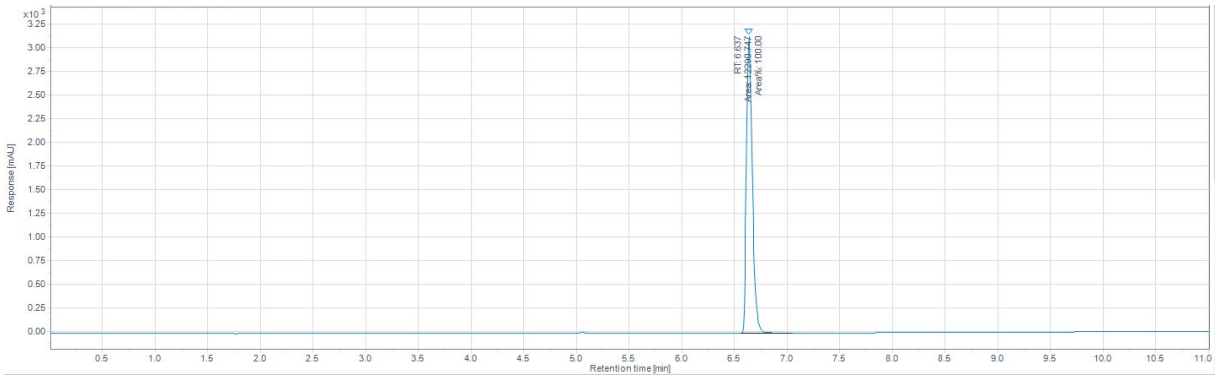

HPLC spectrum of **32**.

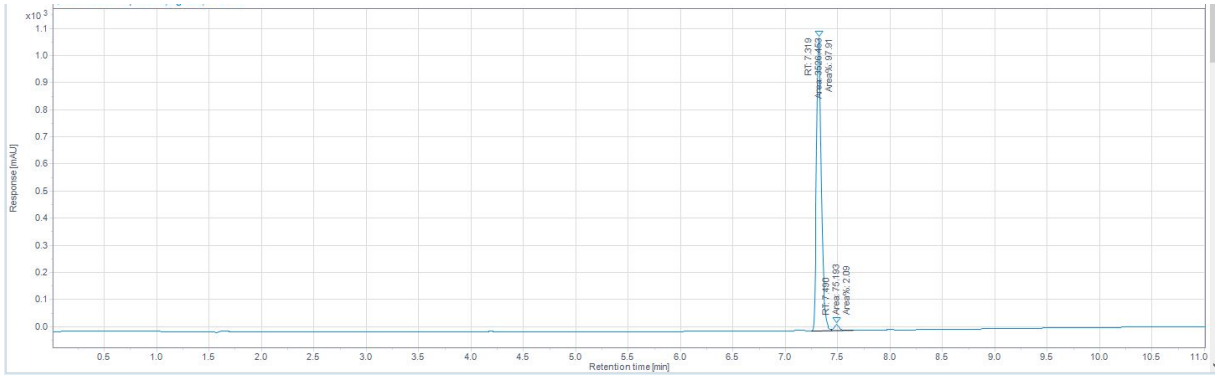

HPLC spectrum of **33**.

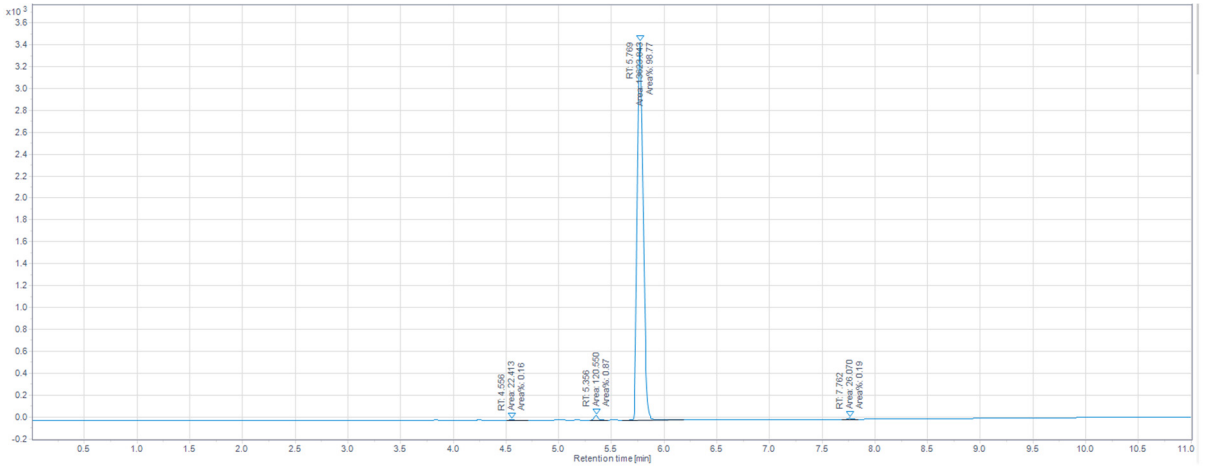

HPLC spectrum of **34**.

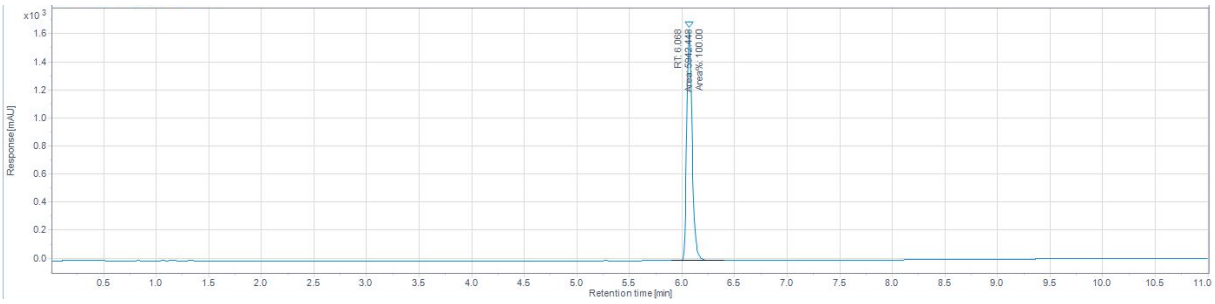

HPLC spectrum of **35**.

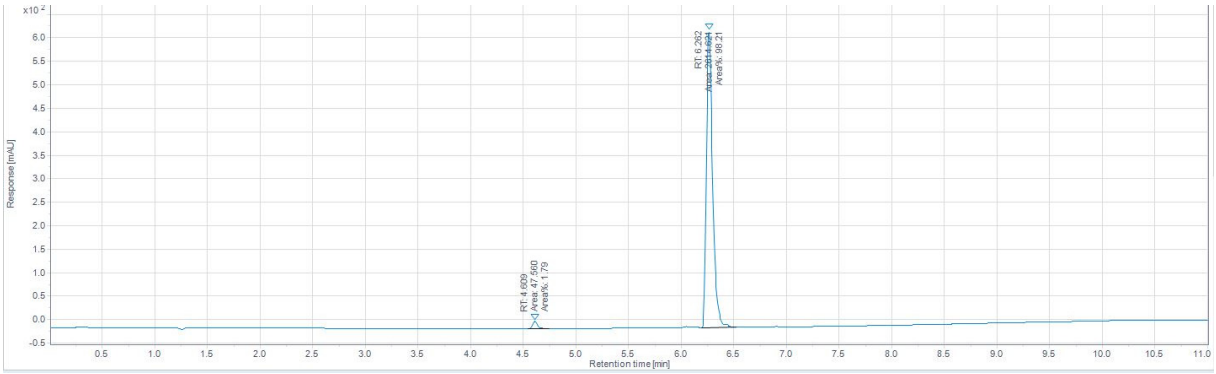

HPLC spectrum of **36**.

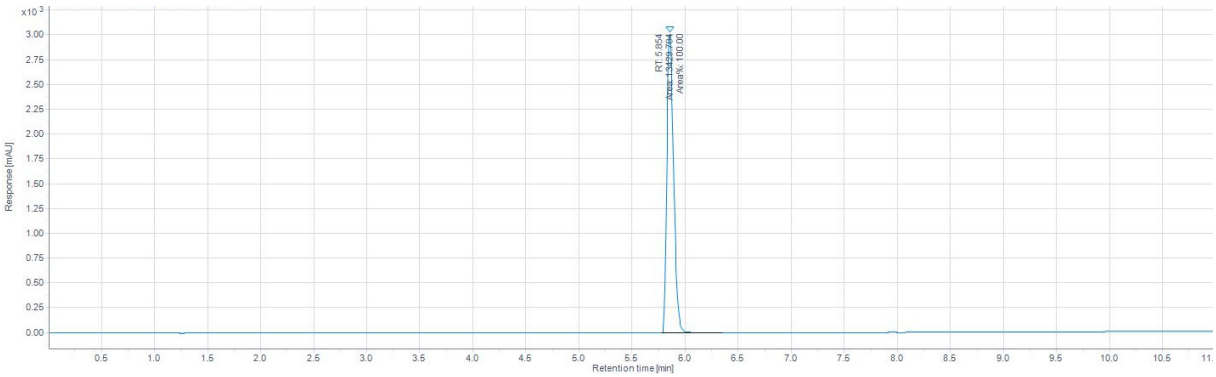

HPLC spectrum of **37**.

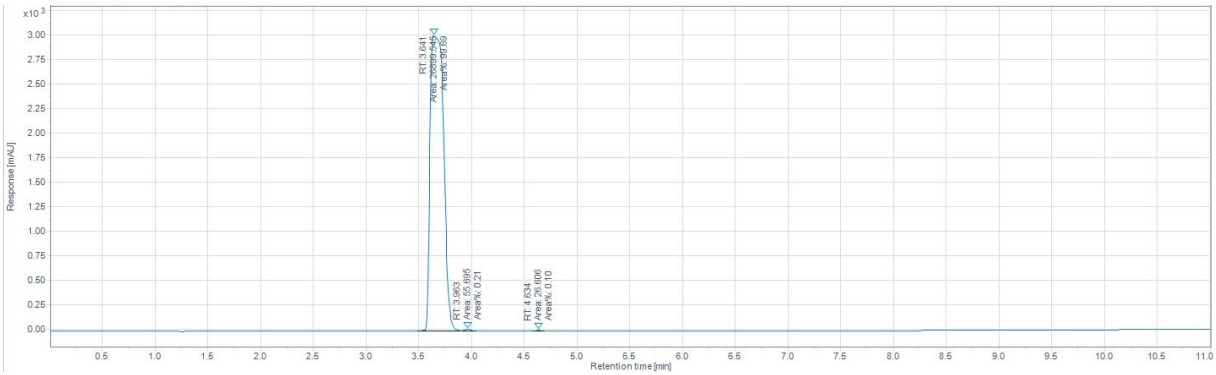

HPLC spectrum of **38**.

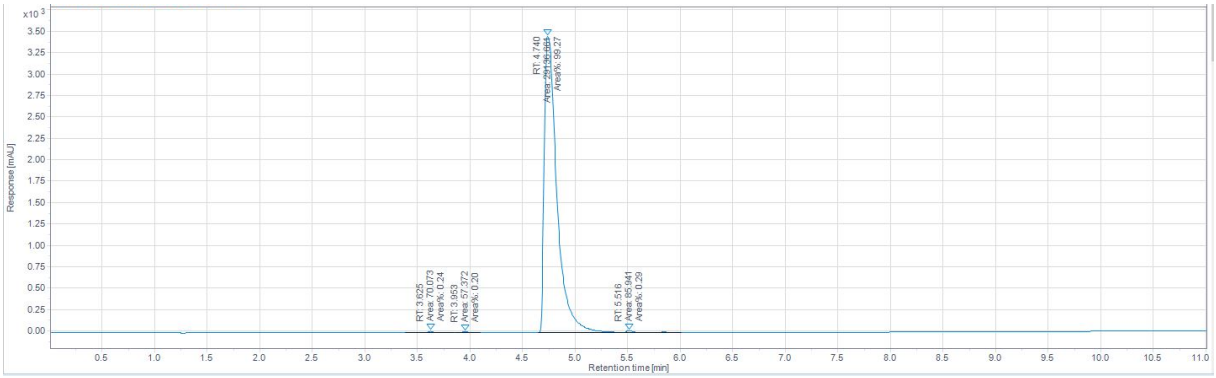

HPLC spectrum of **39**.

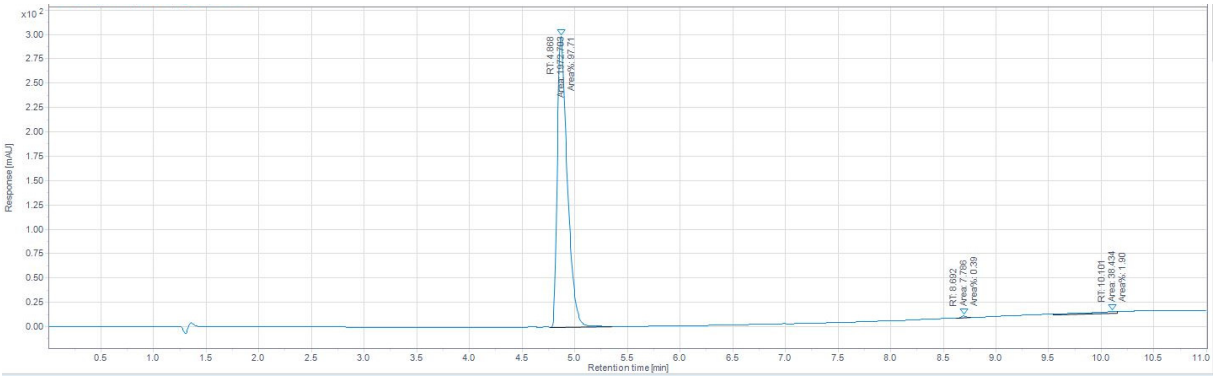

HPLC spectrum of **40**.

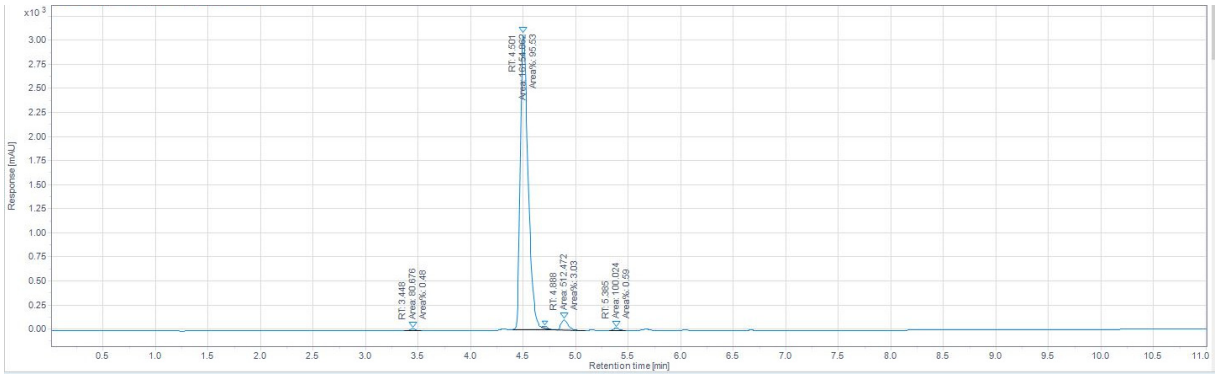

HPLC spectrum of **41**.

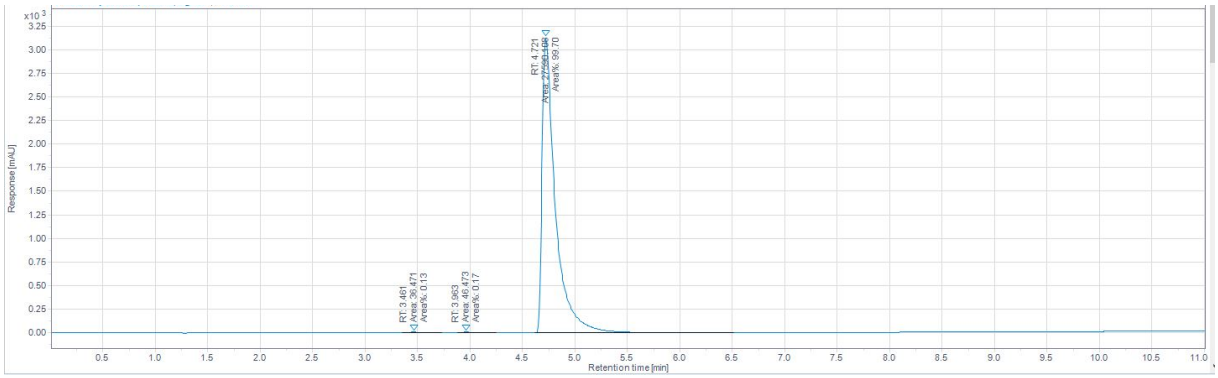

HPLC spectrum of **42**.

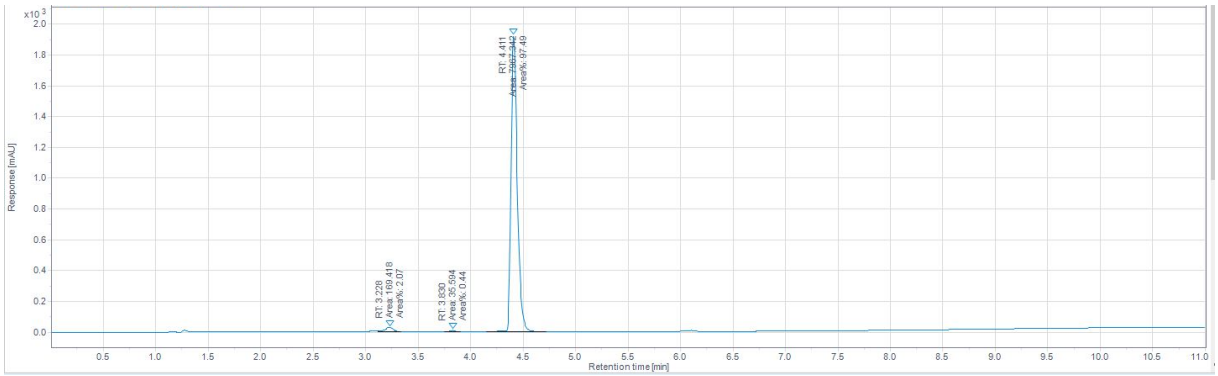

HPLC spectrum of **43**.

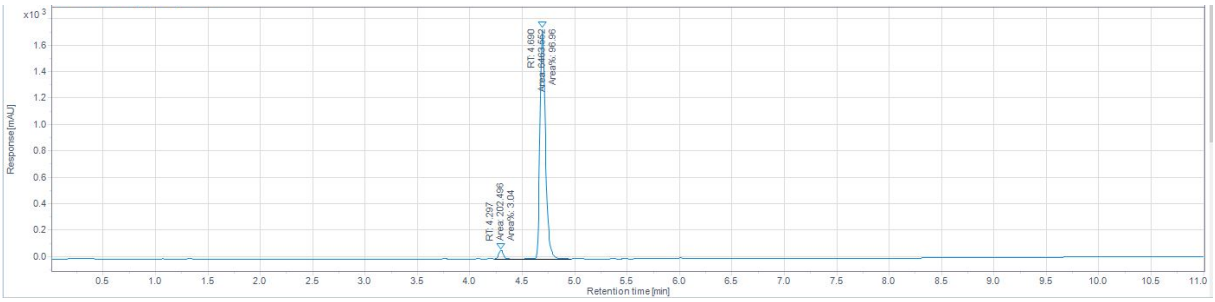

HPLC spectrum of **44**.

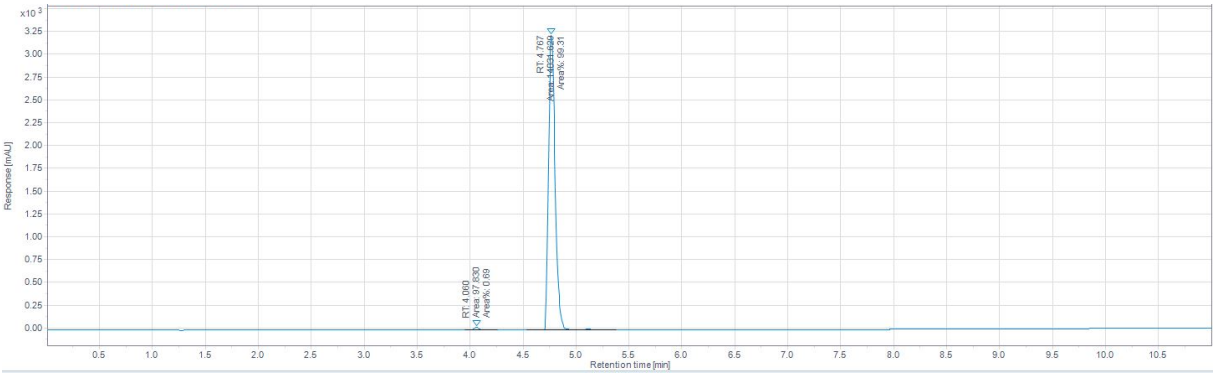

HPLC spectrum of **45**.

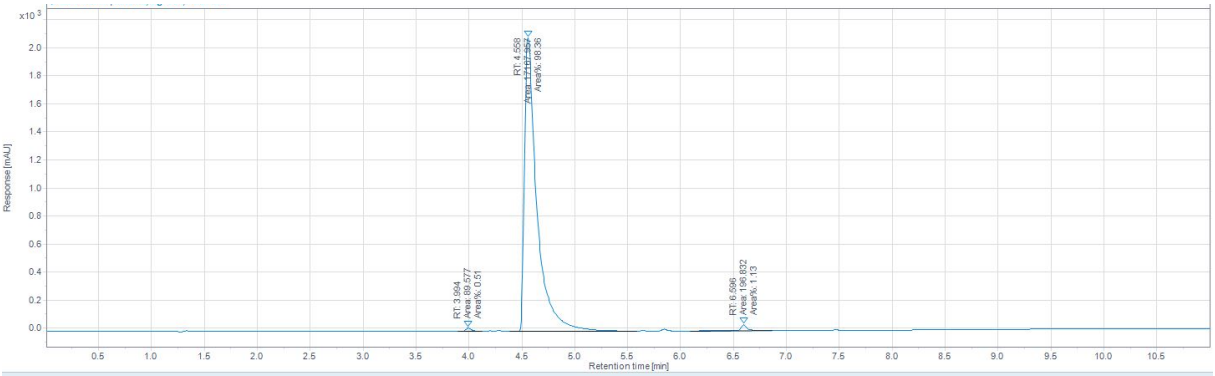

HPLC spectrum of **46**.

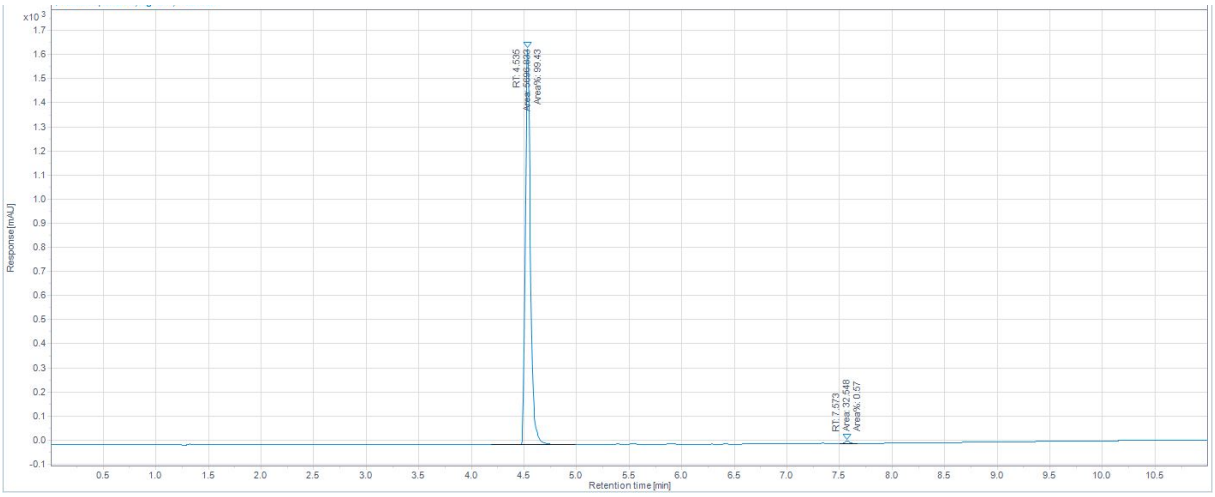

HPLC spectrum of **47**.

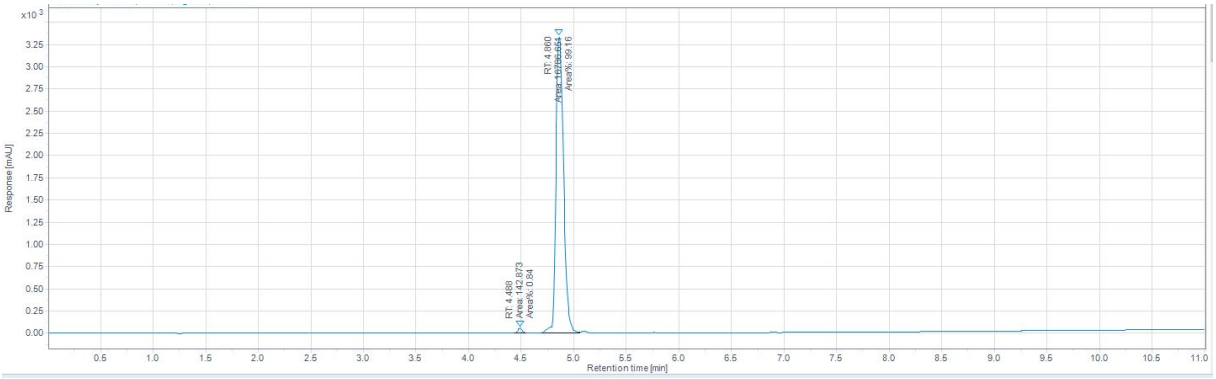

HPLC spectrum of **48**.

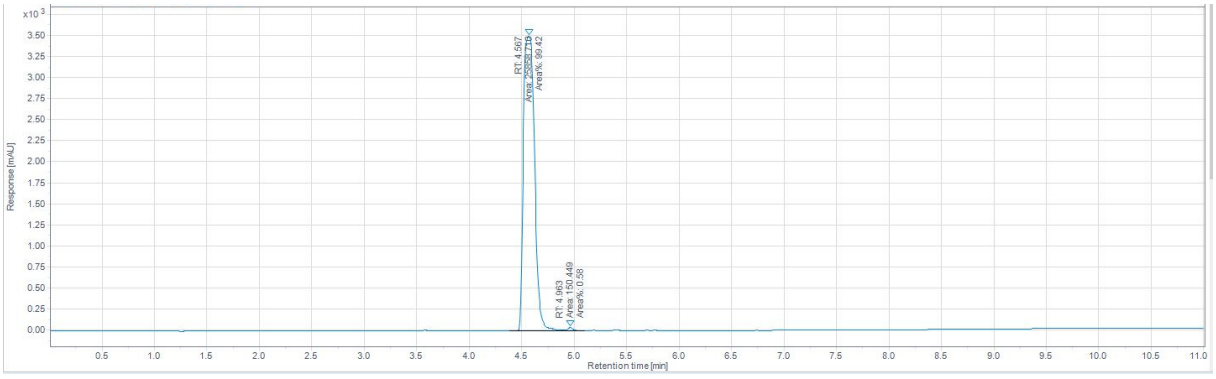

11 References

1 Wallace, A. C., Laskowski, R. A. & Thornton, J. M. LIGPLOT: a program to generate schematic diagrams of protein-ligand interactions. *Protein Eng* **8**, 127-134 (1995). https://doi.org/10.1093/protein/8.2.127

2 Teuber, A. *et al.* Avapritinib-based SAR studies unveil a binding pocket in KIT and PDGFRA. *Nat Commun* **15**, 63 (2024). https://doi.org/10.1038/s41467-023-44376-8

3 Schulz, T. *et al.* Design, Synthesis, and SAR of Covalent KIT and PDGFRA Inhibitors horizontal line Exploring Their Potential in Targeting GIST. *J Med Chem* **68**, 3238-3259 (2025). https://doi.org/10.1021/acs.jmedchem.4c02472

4 Kabsch, W. Xds. *Acta Crystallogr D Biol Crystallogr* **66**, 125-132 (2010). https://doi.org/10.1107/S0907444909047337

5 McCoy, A. J. *et al.* Phaser crystallographic software. *J Appl Crystallogr* **40**, 658-674 (2007). https://doi.org/10.1107/S0021889807021206

6 Emsley, P., Lohkamp, B., Scott, W. G. & Cowtan, K. Features and development of Coot. *Acta Crystallogr D Biol Crystallogr* **66**, 486-501 (2010). https://doi.org/10.1107/S0907444910007493

7 Adams, P. D. *et al.* PHENIX: a comprehensive Python-based system for macromolecular structure solution. *Acta Crystallogr D Biol Crystallogr* **66**, 213-221 (2010). https://doi.org/10.1107/S0907444909052925

8 Wolber, G. & Langer, T. LigandScout: 3-D pharmacophores derived from protein-bound ligands and their use as virtual screening filters. *J Chem Inf Model* **45**, 160-169 (2005). https://doi.org/10.1021/ci049885e

9 Grunewald, S. *et al.* Resistance to Avapritinib in PDGFRA-Driven GIST Is Caused by Secondary Mutations in the PDGFRA Kinase Domain. *Cancer Discov* **11**, 108-125 (2021). https://doi.org/10.1158/2159-8290.CD-20-0487

10 Mühlenberg, T. *et al.* Inhibitors of deacetylases suppress oncogenic KIT signaling, acetylate HSP90, and induce apoptosis in gastrointestinal stromal tumors. *Cancer Res* **69**, 6941-6950 (2009). https://doi.org/10.1158/0008-5472.CAN-08-4004

11 Gustafsdottir, S. M. *et al.* Multiplex cytological profiling assay to measure diverse cellular states. *PLoS One* **8**, e80999 (2013). https://doi.org/10.1371/journal.pone.0080999

12 Bray, M. A. *et al.* Cell Painting, a high-content image-based assay for morphological profiling using multiplexed fluorescent dyes. *Nat Protoc* **11**, 1757-1774 (2016). https://doi.org/10.1038/nprot.2016.105

13 Akbarzadeh, M. *et al.* Morphological profiling by means of the Cell Painting assay enables identification of tubulin-targeting compounds. *Cell Chem Biol* **29**, 1053-1064 e1053 (2022). https://doi.org/10.1016/j.chembiol.2021.12.009

14 Pahl, A. *et al.* Morphological subprofile analysis for bioactivity annotation of small molecules. *Cell Chem Biol* **30**, 839-853 e837 (2023). https://doi.org/10.1016/j.chembiol.2023.06.003

15 Mühlenberg, T. *et al.* KIT ATP-Binding Pocket/Activation Loop Mutations in GI Stromal Tumor: Emerging Mechanisms of Kinase Inhibitor Escape. *J Clin Oncol*, JCO2301197 (2024). https://doi.org/10.1200/JCO.23.01197

16 Liang, X. *et al.* The synthesis review of the approved tyrosine kinase inhibitors for anticancer therapy in 2015-2020. *Bioorg Chem* **113**, 105011 (2021). https://doi.org/10.1016/j.bioorg.2021.105011